UNCLASSIFIED

AD NUMBER	
AD103405	
CLASSIFICATION CHANGES	
TO:	**UNCLASSIFIED**
FROM:	**CONFIDENTIAL**
LIMITATION CHANGES	
TO: **Approved for public release; distribution is unlimited. Document partially illegible.**	
FROM: **Distribution authorized to U.S. Gov't. agencies and their contractors; Administrative/Operational Use; MAY 1956. Other requests shall be referred to Office of Naval Research, Washington, DC. Document partially illegible.**	
AUTHORITY	
CNO ltr, dtd Dec 15, 1988; cno ltr, Dec 15, 1988	

THIS PAGE IS UNCLASSIFIED

CONFIDENTIAL

AD 103405

Armed Services Technical Information Agency

Reproduced by

DOCUMENT SERVICE CENTER

KNOTT BUILDING, DAYTON, 2, OHIO

CONFIDENTIAL

U.S. NAVY
OFFICE OF NAVAL RESEARCH
WASHINGTON, D. C.

31 May 1956
Report No. 1106
(Final) Volume I
Copy No.

FC

RESEARCH, DEVELOPMENT, AND TESTING OF UNDERWATER PROPULSION DEVICES

★

Contract N6ori-10, Task Order I
Project NR 097 003

NOTICE: THIS DOCUMENT CONTAINS INFORMATION AFFECTING THE NATIONAL DEFENSE OF THE UNITED STATES WITHIN THE MEANING OF THE ESPIONAGE LAWS, TITLE 18, U.S.C., SECTIONS 793 and 794. THE TRANSMISSION OR THE REVELATION OF ITS CONTENTS IN ANY MANNER TO AN UNAUTHORIZED PERSON IS PROHIBITED BY LAW.

DISCLAIMER NOTICE

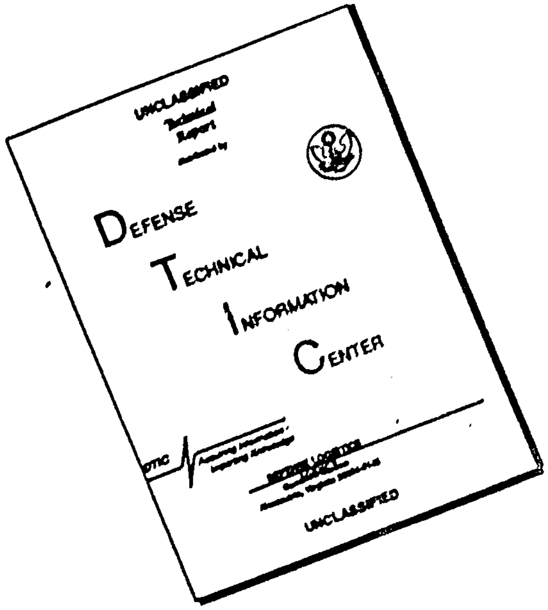

THIS DOCUMENT IS BEST QUALITY AVAILABLE. THE COPY FURNISHED TO DTIC CONTAINED A SIGNIFICANT NUMBER OF PAGES WHICH DO NOT REPRODUCE LEGIBLY.

United States Patent Office Secrecy Order

NOTICE

The Aerojet-General Corporation has filed patent applications in the U. S. Patent Office to cover inventions disclosed in this publication, and the Commissioner of Patents has issued a secrecy order thereon.

Compliance with the provisions of this secrecy order requires that those who receive a disclosure of the secret subject matter be informed of the existence of the secrecy order and of the penalties for the violation thereof.

The recipient of this report is accordingly advised that this publication includes information which is now under a secrecy order. It is requested that he notify all persons who will have access to this material of the secrecy order.

Each secrecy order provides that any person who has received a disclosure of the subject matter covered by the secrecy order is

> "in nowise to publish or disclose the invention or any material information with respect thereto, including hitherto unpublished details of the subject matter of said application, in any way to any person not cognizant of the invention prior to the date of the order, including any employee of the principals, but to keep the same secret except by written permission first obtained of the Commissioner of Patents."

Although the original secrecy order forbids disclosure of the material to persons not cognizant of the invention prior to the date of the order, a supplemental permit attached to each order does permit such disclosure to:

> "(a) Any officer or employee of any department, independent agency, or bureau of the Government of the United States.
>
> "(b) Any person designated specifically by the head of any department, independent agency or bureau of the Government of the United States, or by his duly authorized subordinate, as a proper individual to receive the disclosure of the above indicated application for use in the prosecution of the war.
>
> "The principals under the secrecy are further authorized to disclose the subject matter of this application to the minimum necessary number of persons of known loyalty and discretion, employed by or working with the principals or their licensees and whose duties involve cooperation in the development, manufacture or use of the subject matter by or for the Government of the United States, provided such persons are advised of the issuance of the secrecy order."

No other disclosures are authorized, without written permission from the Commissioner of Patents. Public Law No. 239, 77th Congress, provides that whoever shall "willfully publish or disclose or authorize or cause to be published or disclosed such invention, or any material information with respect thereto," which is under a secrecy order, "shall, upon conviction, be fined not more than $10,000 or imprisoned for not more than two years or both." In addition, Public Law No. 700, 76th Congress, provides that the invention in a patent may be held abandoned, if it be established that there has been a disclosure in violation of the secrecy order.

It must be understood that the requirements of the secrecy order of the Commissioner of Patents are in addition to the usual security regulations which are in force with respect to activities of the Aerojet-General Corporation. The usual security regulations must still be observed notwithstanding anything set forth in the secrecy order of the Commissioner of Patents.

31 May 1956

Report No. 1106
(Final)
Volume I

RESEARCH, DEVELOPMENT, AND TESTING OF UNDERWATER PROPULSION DEVICES

Contract N6ori-10
Task Order I
Project NR 097 003

Written by:

M. Bielecki
W. S. De Bear
H. M. Higgins
A. E. Lemke
R. Spies
J. A. Stubstad
R. M. Viney

No. of Pages: 146

Period Covered:

1 January 1946 through 29 February 1956

Approved by:

R M Viney

R. M. Viney
Project Engineer

C A Gongwer

C. A. Gongwer
Manager
Underwater Engine Division

AEROJET-GENERAL CORPORATION

Azusa, California

CONTENTS

CONTENTS (cont.)

CONTENTS (cont.)

CONTENTS (cont.)

CONTENTS (cont.)

Report No. 1106

CONTRACT FULFILLMENT STATEMENT

This final report is submitted in fulfillment of Contract N6ori-10, Task Order I, and covers the period 1 January 1946 through 29 February 1956.

I. OBJECTIVE

A. Contract N6ori-10 was negotiated between the Office of Research and Inventions, Navy Department, and the Aerojet Engineering Corporation, and the work commenced in January 1946. After the establishment of the Office of Naval Research, this contract came under the technical supervision of the Power Branch, Material Sciences Division. The original work statement under Contract N6ori-10, Task Order I, specified that the contractor shall perform research, development, and test work in the field of hydropulse propulsion devices. The primary devices to be considered were the Direct Hydropulse, the Inverted Hydropulse, and the Gaseous Hydropulse. An analysis of the Hydroturbojet was also to be made, so that performance could be compared with that of the hydropulse devices, and with other methods of underwater propulsion. To accomplish this task, the Contractor agreed to the following tasks:

1. Construct experimental models of the necessary components and assemblies, in order to accumulate design data.

2. Perform the necessary tests to obtain additional fundamental data on gas generation, reaction speeds, heat transfer, etc.

3. Determine performance characteristics such as dynamic thrust, external and internal drag, thermodynamic efficiency, diffuser efficiencies, and propulsive efficiency for the hydropulse motors.

4. Develop and operate the direct hydropulse with water-reactive chemicals superior to the sodium-potassium alloy. Primary emphasis was to be placed on the use of readily available hydrocarbon fuels for the gaseous hydropulse.

B. Subsequent to the early development work on the hydropulse motors, the contract was amended several times to authorize the investigation of other types of underwater propulsion devices and provide for the necessary associated equipment. This included the following endeavors:

1. Development of the molten-lithium-fueled hydroduct.

2. Development of Alclo as a propellant and its application to the hydroduct, hydroductor, steam generators, and submarine power plants.

3. Development of a solid-propellant, gas-turbine torpedo power plant.

4. Design and construction of a large high-speed rotating boom and circular water-channel test facility.

C. The detailed objectives of the various programs are more thoroughly described in Sections IV through XV.

II. SUMMARY

A. DIRECT HYDROPULSE

1. Direct hydropulse motors were designed, fabricated and tested using liquid NaK alloy, molten lithium, or ethyl aluminum sesquihydride as water-reactive fuels. Performance values were very similar for the NaK alloy and ethyl aluminum sesquihydride, while the molten lithium, with its higher heat of hydrolysis, gave the best performance.

2. Representative values of specific power were 40,000 $\frac{\text{ft lb/sec}}{\text{lb fuel/sec}}$ for NaK alloy, 50,000 for ethyl aluminum sesquihydride, and 388,000 for molten lithium. This performance value for the lithium hydropulse was obtained at a velocity of 57.5 knots; the specific impulse was 4000 $\frac{\text{lb thrust}}{\text{lb fuel/sec}}$. This corresponds to a specific fuel consumption of 5.1 $\frac{\text{lb fuel}}{\text{thrust hp/hr}}$.

3. The highest speed of operation on the 80-ft rotating boom for the molten-lithium hydropulse was 64 knots. Satisfactory designs were developed for the grid-reed entrance valves, fuel injectors, mounting struts, water ducts, and external streamlining of the motor for operation at these speeds. In addition, a satisfactory method for heating and handling the molten lithium at 450°F was developed.

B. INVERTED HYDROPULSE

The development of a solid sodium cartridge, inverted hydropulse was attempted and abandoned because controlled reaction of the solid sodium fuel could not be obtained.

C. GASEOUS HYDROPULSE

1. Extensive development of the steam hydropulse and the nitromethane hydropulse was not pursued, as the gasoline-air hydropulse proved to be a more feasible design.

2. A gasoline-air hydropulse was developed that was capable of propelling a 15-ft boat loaded with three people at a speed of 8.1 knots with fuel consumption at the rate of 3 gallons per hour. Maximum thrust was 180 lb, and the maximum specific impulse was 55,000 $\frac{\text{lb thrust}}{\text{lb fuel/sec}}$.

3. The use of transparent models and high-speed photographic techniques, coupled with a step-analysis of the hydropulse cycle, proved to be a very satisfactory method of obtaining experimental data and correlating this data with theoretical calculations.

4. Considerable effort was applied to the development of methods of pre-compression of the gasoline-air fuel mixture so that higher efficiencies could be obtained, but no completely satisfactory solution of this problem was obtained.

D. HYDROTURBOJET

Performance calculations that were made of the hydroturbojet cycle showed that at a nominal chamber pressure of 640 psia a specific impulse of $1500 \frac{\text{lb thrust}}{\text{lb fuel/sec}}$ could be obtained. Feasibility of this type of propulsion system was later confirmed by development of a hydroturbojet torpedo under Contract 9768.

E. HYDRODUCT AND HYDRODUCTOR

1. Vapor-phase hydroducts were designed and developed to operate on molten lithium or Alclo. The best performance obtained with the molten lithium hydroduct on the rotating boom was a thrust of 600 lb, and a specific impulse of $1235 \frac{\text{lb thrust}}{\text{lb fuel/sec}}$.

2. The Alclo propellant with its higher energy per unit volume was utilized in developing a free-running hydroduct test missile. The feasibility of this type of propulsion system was proved by free-running range tests of a 4.5-in.-dia Alclo hydroduct test missile. Specific impulse of this motor, obtained in the static test pit, was $325 \frac{\text{lb thrust}}{\text{lb fuel/sec}}$. Satisfactory motor designs were developed so that most of the metal parts were made of aluminum, despite the fact that the flame temperature of the burning Alclo was on the order of 7000°F.

3. Results of the full-scale steam-jet condenser studies of the hydroductor motor showed that performance of this motor at extreme depths (1000 ft) should be comparable to performance of the hydroduct at shallow depths. Satisfactory combustion chambers for the hydroductor configuration were developed and static-pit tests, under simulated free-running operating conditions, showed that adequate thrust should be obtained from this motor. Free-running range tests of the 4.5-in.-dia hydroductor test missile were not satisfactory and results indicate that the drag (associated with the condensing-water inlet scoops) is excessive for the thrust produced by the motor. Further study of this hydrodynamic problem is warranted.

F. HYDROFUELS

1. Ethyl aluminum sesquihydride and aluminum borohydride were synthesized for use as hydrofuels, but development was dropped in favor of the higher energy and more readily available metal-alloy hydrofuels.

2. A wide variety of metal-alloy hydrofuels were investigated with the aim of reducing the cost and obtaining an alloy with a low melting point. The best hydrofuel for use in the hydropulse was an alloy of 66.4% lithium, 16.6% aluminum, 7.0% sodium and 10.0% calcium. It had a melting point of 340°F and was 20% better than lithium on a weight basis, and 55% better on a volume basis. In addition to actual formulation of metal alloy hydrofuels, a great deal of basic information on melting points of various metal alloys was obtained.

3. A method of rapidly melting lithium by chemical means was developed. By using sealed steel heating tubes, molten lithium was available for use 10 sec after ignition of the heating charge.

4. The development of reaction chambers using a solid-lithium-and-water propellant system was investigated, but controlled stable operation of these motors could not be obtained.

G. ALCLO DEVELOPMENT PROGRAM

1. Alclo is a highly compressed mixture of potassium perchlorate and powdered aluminum. To improve the mechanical strength of the compacted grain and the combustion stability, a small percentage of lead powder was added. This propellant is very desirable for underwater applications because of its high energy per unit volume, and the fact that it produces no gaseous products of combustion. It has a specific gravity of 2.80, and when burned it releases heat at the rate of 2.17 kcal per gram of propellant.

2. Extensive investigations were made to determine the burning characteristics of Alclo with various additives, as well as determining the physical properties of the propellant and the effects of storage and environment. It was determined that Alclo was not adversely affected by temperatures within the range of -60 to +175°F. Alclo is not affected by thermal shock and the burning rate varies only slightly within the above temperature range.

3. Compaction techniques were developed for the production of Alclo grains. A 20-ton-capacity and a 400-ton-capacity hydraulic press were designed and fabricated, and these presses were capable of compacting grains from 1/4 to 4.75 in. in diameter. A satisfactory restriction was developed for the Alclo grain that consisted of three layers of glass tape impregnated with Selectron resin.

4. Extensive tests were made to determine the safety requirements for handling Alclo propellant and it was found that, in general, Alclo propellant should be treated like other propellant grains of the same size. There is essentially no explosive hazard with Alclo (unless it is in the powdered form) but the material will ignite if subjected to undue heat, friction, or impact.

5. Vertical steam generators were used extensively in determining the performance characteristics of the various Alclo grains. A large vertical steam generator was built to accommodate a 3.75-in.-dia Alclo grain, 4 ft long, and was capable of producing 5.3 lb/sec of saturated steam at 225 psia. The vertical steam generators operated very stably in all tests, and were a very satisfactory mechanism for obtaining performance values for the comparison of different propellant formulations.

6. Alclo was also used as the fuel for an experimental model of a closed-cycle submarine power plant. Methods were developed for satisfactorily burning the Alclo in the furnace and several hours of operation showed no damage to the refractory brick or the boiler tubes from the high heat concentrations. The products of combustion were removed by slagging the KCl within the furnace and picking up the Al_2O_3 powder in a dust collector. Burning of the propellant was sufficiently controlled so that the test unit was operated as a closed cycle.

H. SOLID-PROPELLANT GAS-TURBINE TORPEDO POWER PLANT

1. Two turbine-driven torpedo power plants were developed to operate from the gases produced by the burning of Aeroplex AN-2091AX propellant in a gas generator. One engine operated at the 28-hp level, while the other operated at the 80-hp level. Satisfactory operation was obtained for runs as long as 4 min.

2. A speed-control valve was developed for use with this power plant that maintained the turbine speed constant within ± 1.5%, while the back pressure was varied from 50 to 460 psi.

3. A design study was conducted to determine the feasibility of using this type of power plant in a full-scale torpedo. Using a torpedo 21 in. in dia and 123 in. long (half-length), a power plant developing 675 shaft hp can be installed which will drive the torpedo at 70 knots for 20,000 yd.

I. 80-FT ROTATING TEST BOOM AND CIRCULAR WATER-CHANNEL TEST FACILITIES

This large test facility was designed and constructed for dynamic testing of underwater propulsion devices, and for conducting high-speed hydrodynamic studies. Small-scale units can be tested at the 50 ft radius of the rotating boom at velocities up to 100 knots. Torpedoes 21 in. in dia by 105 in. long have been tested at the 40-ft radius at speeds above 50 knots. The facility is amply instrumented for conducting tests of this nature.

III. CONCLUSIONS AND RECOMMENDATIONS

A. The direct hydropulse proved to be a feasible type of underwater propulsion, but the operating economy and the complications attendant with the use of molten lithium made it undesirable in relation to conventional methods of torpedo propulsion. The gasoline-air hydropulse proved to be a very simple and uncomplicated device for underwater propulsion, but it was not as economical to operate as the conventional outboard motor.

B. Alclo propella is a very satisfactory source of heat energy, and is potentially applicable to a wide variety of underwater propulsion devices because of its high energy per unit volume and the fact that it does not produce any gaseous wake. The Alclo hydroduct was proved as a feasible free-running high-speed underwater missile with a powered range several times that of underwater rockets propelled by conventional solid propellants. The Alclo hydroductor development program has not been completed, but this device promises to have equal performance to the Alclo hydroduct, and to be relatively insensitive to depth. Alclo propellant in the form of powder, pellets, or small grains has proved a very satisfactory heat source for use in a wide variety of igniters for both liquid and solid propellants. The Alclo-fueled closed-cycle submarine power plant offers a very high performance as a chemical power plant for the long-range underwater propulsion of submarines. Alclo-powered vertical steam generators should be very useful for some test installations requiring high power inputs for short durations. The range of burning rates obtainable with Alclo propellant can probably be extended by the incorporation of other additives, or by the change in particle size of the constituents. This should be studied, as well as the burning of Alclo at higher pressures (up to 6000 psi), so that Alclo could be considered for additional applications. The development of igniters for application to various Alclo grains also warrants further extensive development work.

C. The solid-propellant, gas-turbine power plant for torpedo propulsion is one of the most promising engines for use in high-speed long-range torpedoes. It is considerably less complicated than other torpedo power plants, and in addition, has a long shelf life, is very safe to handle, and would be very reliable. Its only disadvantage is the fact that it has a gaseous exhaust.

D. The large ring-channel test facility has proved to be a very satisfactory and necessary facility for conducting development tests of underwater propulsion devices, and for the hydrodynamic testing programs. This facility is available for use by other agencies under Navy sponsorship.

IV. DIRECT HYDROPULSE

A. INTRODUCTION

1. The direct hydropulse is defined as an underwater propulsive device in which a hydrofuel is injected intermittently into the water in a submerged duct. Mechanical check valves are provided at the forward end of the duct. They open to allow the entrance of water during the low-pressure part of the cycle, and close during the high-pressure part of the cycle, causing the expulsion of water out the tailpipe. The hydrofuels principally used were sodium-potassium alloy and molten lithium. A schematic diagram of a direct hydropulse giving the nomenclature of the parts is shown in Figure 1.

2. The development of the direct hydropulse using liquid NaK alloy as the water-reactive propellant was initially sponsored by the Bureau of Aeronautics under Contract NOa(s) 5350, Task No. 3. Results of these initial investigations are reported in References 1 and 2. This program was augmented in 1946 when the Office of Naval Research became the sponsoring agency under the present contract. The primary objective of this program was to develop the direct hydropulse, in order to obtain the maximum efficiency and performance of all its components. The first hydropulse motors were tested using NaK alloy because of its desirable water-reactive characteristics, relatively low cost, and ease of handling in its liquid condition at normal temperatures. Successful performance with this fuel indicated the desirability of using higher-energy fuels, such as molten lithium and ethyl aluminum sesquihidride, so that much better motor performance could be obtained. As the molten lithium motors directly evolved from the best NaK alloy motors, the program of component development cannot be separated between the two types of motors. The different components and phases in the development of the most satisfactory motors are described in the following section.

B. DESIGN AND DEVELOPMENT PROGRAM

1. General Motor Configuration

A summary of the general configurations of the various hydropulse motors that were fabricated and tested is presented in sketch form in Figures 2 and 3. Photographs of some of these units are shown in Figures 4 through 13. The evaluation of the design of these various units is directly related to the program to obtain high speeds and better performance within the limitations of the needs of the individual motor components. The discussion regarding these components will illustrate some of the design changes that were made.

2. Entrance Valves

a. The entrance valves used in the early hydropulse models were of the grid and reed type similar to those used in the V-1 (Buzz-Bomb). The flow of water into the motor is unrestricted, but back-flow is prevented by the closure of the reeds against the sloping grids. These valves were assembled in several arrangements to best fit the configuration of the complete motor, or to reduce the frontal drag. Figure 4 shows a typical square-faced valve assembly in a twin-barrel unit. In order that the valve section could be faired into the body more readily, thus reducing frontal area and drag, several motors were fabricated with valves slanted at a 60° included angle, as shown in Figures 5 and 14.

b. In order to further streamline the complete hydropulse motor, and to provide a design that might be compatible with operation as a power plant for a torpedo, the four-barreled side-entrance hydropulse, Mk I, was designed and fabricated. The grid and reed valve arrangement in this unit is shown in Figures 6 and 15. The side-entrance hydropulse, Mk II, shown in Figures 7 and 16, was fabricated to provide better flow of ram water in the motor without increasing drag.

c. Several other configurations for the entrance valves were considered. A multi-ball valve and a conical-spring valve (see Reference 3) were fabricated and tested, but were abandoned because of high hydraulic losses and their slow closing action. Generally, the square-faced valve assembly was found most satisfactory from the standpoint of fabrication and durability. Modifications, such as the double-sided valve shown in Figure 17, were also tested. These grids provided an increase in the open area of the valve of about 7-1/2% for a valve of a given size, but little, if any, increase in efficiency resulted. Under the higher pressures developed in the molten-lithium motors, there was a distinct tendency for the grids to bend. This bending was minimized by shortening the fore and aft dimensions from the original 3-1/2 to 2-3/4 in., thus reducing their unsupported extension; and by turning the top grid upside down. A comparison between the shorter grid and the size previously used is shown in Figure 18.

d. The reeds are of blued Swedish spring-steel stock, or of heat-treated beryllium copper. The latter material provided better fatigue and corrosion resistance. In the early, relatively low-pressure motors, the copper reeds used were 0.017 in. thick. The thickness was increased to 0.018, 0.022, and finally to 0.025 in. as the motor pressures were increased. Pressures in excess of 500 psi are developed in the molten-lithium motors. This also made it necessary to increase the thickness of the valve-box sides from 3/4 to 1-1/16 in.

3. Injectors

a. The development of suitable injectors was probably the most important problem in obtaining the desired cyclic operation of the hydropulse. The injector must properly valve the correct amount of fuel intermittently into the motor at the right time in the cycle. A wide variety of injectors were designed and some of those fabricated and tested are shown in the charts of Figures 19 and 20. All of the injectors (except the self-cycling type described in paragraph 3,c, had pintle valves that were actuated by a hydraulic impulse from a Bosch Diesel jerk pump which was driven by a variable-speed motor. By varying the fuel-orifice size, the fuel-line pressure, the gas-dome closing pressure on top of the pintle, the duration and actuating time of the hydraulic impulse, and the speed of the Bosch pump, a wide variety of operating conditions could be tested. In the early phases of the program, water in a continuous stream (or in an interrupted stream to coincide with fuel injection) was supplied to provide better mixing and a more rapid reaction. Later designs provided fuel-injection patterns in the shape of fans, solid cones and hollow cones, with very finely divided fuel particles, and the injection of water was eliminated. This simplified the complete motor considerably. The Type 11 injector, with a spiral pintle providing a finely divided fuel spray (Figure 21) and the Type 15 injector with a "Sprayco" nozzle insert (Figure 22) proved to be two of the most satisfactory injectors for the NaK hydropulse motors.

b. Injectors for the molten lithium hydropulse had an additional design requirement in that they had to be heated to 500°F to insure free passage of the fuel. This was accomplished in all cases by heating the body of the injector with cartridge-type heaters in a manner similar to the Type 26 injector shown in Figure 23. The injector parts were made of stainless steel, and the fuel was separated from the actuating-oil system by stainless-steel bellows. O-rings could be used only in the top, cooled part of the injector to seal the area between the dome closing-gas pressure and the actuating oil. As with the NaK injectors, the best efficiency was obtained when the fuel is injected in the shortest possible time, and is introduced in the finest possible spray to insure a rapid and complete reaction. The Type 26 injector (Figure 26) was therefore built with a replaceable pintle tip and fuel orifice so that a variety of fuel spray characteristics could be tested. Reference 4 describes these tests and the pintle tip and orifice combinations are shown in Figure 24. The reinforced Sprayco vane shown in Sketch 10 of Figure 24 proved to be one of the most satisfactory configurations. Unit No. 25, when tested with this spray mechanism, produced performance figures of 5.3 to 6.0 lb of lithium per thrust hp-hr (see paragraph 4,c) with an injection reaction period of only 0.008 sec. With the increase in fuel pressure (up to 2200 psi) to obtain the desired fuel flow rate in a very short time, and the increased hydraulic hammer due to the sudden stoppage of the more rapidly moving lithium, mechanical failure of the bellows seal became frequent. The injector was therefore modified to eliminate the bellows. Lubrication of the pintle was needed when the bellows was eliminated, and it was accomplished by a constant, forced seepage of Silicone oil through the bearing surfaces, effectively preventing the entrance of any lithium. This system of lubrication completely eliminated all injector failures. This Type 27 injector is shown in Figures 8 and 25. A final modification was made in the shape of the pintle tip, to prevent sudden hammer-like pressure rises in the barrel. The pintle tip was rounded in such a manner (see Figure 26) that the injection rate was small at the start of opening of the pintle, increasing slowly, and then rapidly until the pintle was full open. The number of tests with this pintle tip was not sufficient to allow full evaluation of its merits. It should be noted, however, that this was the tip used in Run No. 36, the most efficient run ever made (fuel consumption was 5.1 pounds of lithium per thrust hp-hr).

c. Compact self-cycling injectors that eliminate the external actuating mechanism entirely were very desirable for torpedo applications of the hydropulse. Several designs were fabricated and tested (see Figures 19 and 20 for sketches, and Reference 5 for a complete description). NaK-alloy motors were operated successfully with self-cycling injectors, but development time was not available to incorporate them into the lithium motors. The self-cycling injector was not as amenable to testing under variable conditions as one that was externally actuated; therefore, they were not used in the lithium-motor development program. It was felt that knowledge of the desired injector characteristics obtained with the non-self-cycling injectors could be used in designing self-cycling injectors for actual hydropulse applications when the need was established.

4. Duct Development

a. Some changes were made in the design of the duct as soon as higher speeds and higher pressures were obtained with the motors. Generally, these changes were made to strengthen the motor and to increase the overall streamlining. The friction losses were reduced by using smoother materials, eliminating interior screw threads, and making the changes in the shape less abrupt.

b. Several units were built with an enlarged section in the duct between the valve housing and the transition. It was hoped that the fuel combustion would be better because of the larger quantity of water available for the reaction. Duct efficiencies for these motors were calculated to be between 60 and 65%, as compared with 75 to 80% for the standard duct shape. (Duct efficiency is defined as the actual thrust, divided by the thrust indicated by planimetering the pressure-time curves.)

c. The effect of barrel length is to change the optimum frequency of operation, with the longer barrel giving lower frequencies. Tests were made with barrels varying in length from 30 to 48 in., but a 48-in. barrel was used on the majority of the test units.

d. If the entrance diffusor was too long, excessive water-hammer pressures were developed when the reed valves closed. This was particularly evident in the side-entrance hydropulse, Mark II (Figure 7). When the diffusor was shortened from 9-1/2 to 3-1/2 in., the overall performance was increased 33%. Too short a diffusor also gave inferior performance (see Reference 6).

5. High-Speed Motor Construction

a. Operation of the hydropulse on the 80-ft boom at speeds greater than 25 knots introduced a number of problems. The first to be encountered was that of aeration. Previous motors were operated in a free-flooded condition; that is, with no watertight security in the space between the duct and the duct fairing. At speeds greater than 17 knots, sufficient vacuum was produced on portions of the fairing to cause air to be drawn down through the hollow strut and to be discharged under water. By welding or soldering all seams, the fairing of Unit 22-C was made sufficiently watertight to prevent this aeration; elimination of the aeration decreased the drag by approximately 40%.

b. Eliminating aeration altered the forces acting on the motor fairing, thereby reducing the "torsional divergence" speed (Reference 7) of the strut to 30 knots. As a result, when the test speed was increased to this amount, the strut became unstable and was bent severely. Subsequent motors were therefore built with shorter, thicker struts having calculated "speeds of divergence" well above the anticipated operating velocities.

c. The increase of operating speeds above 60 knots, and barrel pressures above 750 psi, required that almost the entire motor be rebuilt and strengthened. Motor fairings that were originally made of 20-gage stainless-steel sheet were replaced with 12 gage stock, well reinforced by back-up strips. The diffuser head was fabricated from 1-1/8-in.-thick steel plate, which was machined to shape and welded together in the proper form. It was closely fitted to the housing, and secured with an adequate number of large-diameter screws.

d. The increase in speed also required a continual improvement in streamlining to prevent external cavitation. Thinner, sharper mounting-strut fairings, more elongated diffuser heads, and housing of the injectors and the pressure pickups within the outside shell were necessary to accomplish this. Several tests were made with Unit 26 (see Figure 13), the motor having a fineness ratio of 5:1, and with the shape of the Mk 40 torpedo on a two-thirds scale. This motor was found to have 35% less drag than Unit 25 (see Figure 12) and to be capable of being towed at 65 knots without cavitation. In operation, however, cavitation was detected at the nose with each pulse, when the speed exceeded 62 knots. Figure 27 shows this motor in operation at 56.5 knots on the 80-ft rotating boom.

6. Special Design Considerations for Molten Lithium

a. Before molten lithium could be used as the fuel in a direct hydropulse, considerable experience had to be gained in its handling and control. Most of the problems were concerned with the proper materials to be used, and the method of heating the fuel system (the melting temperature of lithium is 370°F, but the fuel system was heated to 500°F to insure a free flow of fuel). Many techniques were developed in the molten-lithium gas-generator test program, and additional information was supplied from studies conducted by the Research Chemistry Group.

b. Stainless or chrome-molybdenum steels (SAE 4130) proved to be very compatible with the molten lithium, and were used in the majority of test motors, fuel lines, and fuel tanks.

c. Dowtherm-jacketed fuel tanks and lines were tried, but were found impractical because any leakage would allow the lithium and Dowtherm to react. Several methods of using electrical heaters were tried. The use of Calrod heaters inside of, or strapped to the outside of fuel lines proved to be impractical, but small cartridge heaters worked effectively to heat pressure-line valves, injectors, etc. The most effective method for heating the fuel tank and the sections of the fuel lines above water was with strip heaters. The strip heaters were bolted to the outside surface of the tank, and to steel plates which enclosed the fuel lines. The underwater portion of the fuel line, and that section above water which was in danger of being sprayed with water during a test run, were heated by Nichrome wire coils. The waterproofing of this electrical system presented a serious problem because of the high temperatures, vibration, and space limitations involved. The stainless-steel fuel lines were treated in the following manner (see Figure 28), and proved successful in many test runs.

(1) The fuel line was coated with silicone varnish.

(2) Three layers of 0.007-in.-thick silicone-impregnated glass tape were applied, together with three more coats of varnish. This provided electrical insulation.

(3) Nichrome heating wire was wrapped in a tight spiral along the fuel line.

(4) Three more layers of 0.007-in. silicone-impregnated glass tape were applied, along with three more coats of silicone varnish. This provided external electrical insulation, together with some external heat insulation.

(5) The final waterproof insulation was made of a piece of tubing 1/2-in. larger in diameter than the fuel line, and bent to the same shape as the fuel line. After flattening, so it would just fit over the fuel line, the tubing was split lengthwise, fitted over the fuel line, and silver-soldered in place. This construction gave an outside diameter only 5/16 in. greater than the diameter of the bare fuel line itself, thus allowing the best streamlining. A lithium system using this construction is shown in Figure 29.

d. Several other waterproofing materials, such as Glyptal, Geolite, and a 1/16-in.-thick bronze, metalized spray coating were tried, but proved too brittle or too sensitive to the high temperatures to be satisfactory.

C. TESTING PROCEDURES

1. <u>General Conditions</u>

a. Test units were secured to one end of the 80-ft rotating boom in such a manner that their center lines were about 19 in. below the surface of the water. Figure 11 shows this method of mounting. This same type of mounting was also used on the smaller 40-ft boom, as shown in Figure 30.

b. In the tests in the small ring channel, the hydropulse motor being tested provided the only power source for pushing the boom. In all tests in the large ring channel, the boom was brought up to the desired operating speed by means of the 250-hp electric drive-motor. (This system conserved the hydrofuel and created much more stable running conditions.) When the boom was up to speed, the hydropulse motor was started, and the throttle adjusted so that the desired thrust was delivered to the boom by the hydropulse. Figure 27 shows Unit 26 operating at a speed of 56.5 knots.

c. The frequency of actuation was controlled by a variable-speed motor driving a Bosch diesel pump. The hydraulic-oil impulses from this pump actuated the fuel-valving pintle.

d. In most runs a pressure pickup, in conjunction with an oscillograph, was used to measure and record the instantaneous pressure in the barrel. A reluctance-type pickup was used until the barrel pressures exceeded its limit of measurement; then a condenser-type pickup was used. In all cases, the pickup was inserted into the barrel near the transition section.

2. Data Recording

a. Running conditions established before the start of each test include the approximate operating velocity, the frequency of actuation, fuel pressure, and the gas-dome pressure (for pintle loading). The weight of fuel carried was also noted.

b. At regular intervals during the run, measurements were taken of the throttle setting, the speed of the unit through the water, the thrust being delivered to the boom, and the elapsed time. Continuous pressure-time recordings were made on the oscillograph during most runs. In some cases high-speed motion pictures were taken of the test motor in operation through the underwater observation windows.

3. Calculations

a. The gross thrust is the algebraic sum of two quantities, the average thrust indicated on the thrust-meter, and the average drag of the unit. The former is found by converting the microampere reading on the thrust-meter to pounds by means of a dead-weight calibration. This thrust may be either positive or negative, depending upon whether the operating unit is pushing the boom (positive) or is acting as a drag on it (negative). The average drag of the unit varies directly as the square of its velocity through the water; it therefore is determined easily by applying the experimentally found drag coefficient (C_D = pounds drag per inch of water-velocity head) for the unit in question. For tests with the molten lithium hydropulse on the small 40-ft boom, the speed had to be limited to 25 knots. To accomplish this, a controllable water drag was installed on the opposite boom end. The calibrated drag from this brake was then included to obtain the gross thrust.

b. The speed of the unit through the water is indicated on a tachometer calibrated in knots which measures the velocity of boom rotation, or by measuring the time per revolution of the boom and dividing this time by the path circumference. An allowance for drag or backflow in the water channel is then made. In no case has this correction exceeded one foot per second.

c. Because instantaneous fuel flow rates are unknown, calculations are based on an average flow rate. This rate is determined by dividing the quantity of fuel used by the total elapsed running time. Conditions during the run are held as steady as possible so that the overall fuel flow rate is representative.

D. ANALYSIS OF PERFORMANCE AND RESULTS OF INVESTIGATION

1. Specific impulse, specific power and specific fuel consumption are three measures of the general efficiency of a device such as the hydropulse. They are calculated from the experimental data in the following manner:

a. Specific impulse $(I_{sp}) = \frac{\text{gross thrust}}{\text{fuel flow rate}}$

$$= \frac{\text{lb thrust}}{\text{lb/sec}}$$

b. The specific power is a measure of overall efficiency, to the extent that it takes into account the power output.

$$\text{Specific Power} = I_{sp} \times \text{Velocity} = \frac{\text{lb thrust}}{\text{lb/sec}} \times \frac{\text{ft}}{\text{sec}}$$

$$= \frac{\text{ft lb/sec}}{\text{lb fuel/sec}}$$

c. The specific fuel consumption (W_f) is obtained from Specific Power by using the proper conversion factors,

$$W_f = \frac{1{,}980{,}000}{I_{sp} \times V} = \frac{\text{lb fuel}}{\text{thrust hp-hr}}$$

2. A summary of these quantities is tabulated for most of the molten-lithium test runs in Table 1, and is plotted for comparative purposes in Figure 31. Also shown in Figure 31 are performance points for the best NaK-alloy hydropulse test run. As noted in Table 1, the following performance values were obtained:

a. The highest Specific Power obtained was 388,000 $\frac{\text{ft-lb/sec}}{\text{lb fuel/sec}}$ at a velocity of 57.5 knots and a Specific Impulse of 4000 lb $\frac{\text{thrust}}{\text{lb/sec}}$. This corresponds to a specific fuel consumption (W_f) of 5.1 lb fuel/thrust hp-hr.

b. The highest thrust obtained was 1380 lb, at a speed of 61.0 knots. This thrust corresponds to a cross-sectional specific thrust of 110 psi based on barrel cross-section.

c. The highest speed attained was 64.0 knots. As explained previously, the operating speed was limited because of the cavitation resulting from an insufficiently streamlined motor profile.

3. As previously discussed, a great deal of effort was expended on injector design and development, for the purpose of increasing both the thrust and the fuel economy. The methods attempted, and the degree of success achieved, are indicated in Table 2. Pressure-time curves were obtained, and are shown for one specific test in Figure 32, and for various runs in Figure 33.

4. By combining experimental data with a step-by-step mathematical calculation, it was possible to determine the motions of the water and gas in the hydropulse. The pressure-time curve (Figure 32) taken at the motor throat provided the principal experimental data. From calculations, the following information could be determined, and some of the values obtained are:

a. Duct Efficiency - 90 to 95%

b. Propulsive Efficiency - 52%

c. Jet Efficiency - 65%

d. Pump Efficiency - 80%

e. Thermal Efficiency - 39%

f. The Thermodynamic Cycle

g. Optimum Cyclic Frequency

h. Confinement Parameter

The necessary calculations and a complete discussion of the analysis are given in References 4, 8, and 9.

5. Using ethyl aluminum sesquihydride for fuel, one motor attained an equilibrium speed of 22.4 knots at a specific impulse of 805 lb of fuel per lb thrust per sec. This figure is consistent with previous runs with this fuel, and is comparable to the better NaK alloy results. See Section IX,C for a further discussion of this fuel.

6. Acoustical measurements to determine the intensity and frequency of the underwater sound generated by the hydropulse were conducted by the Underwater Ordnance Division of the Naval Ordnance Test Station, with the assistance of the Naval Electronics Laboratory, San Diego, and are fully described in Reference 10. The important conclusions reached were as follows:

a. The sound output in the 20- to 60-kc range caused by the firing of the hydropulse was not sufficient to register above the general background noise resulting from the passage of the unit and its supporting strut through the water.

b. The peak intensity levels in the 0.05- to 20-kc band occurred at the point of closest approach of the unit to the hydrophones (10 ft) and were 135 decibels above the reference level of 0.0002 dyne per cm^2. This would correspond to about 85 decibels above 0.0002 dyne per cm^2 at 1000 yd in open water, if no allowance is made for augmentation of the measured noise by reflection from the sides of the pool.

V. INVERTED HYDROPULSE

A. INTRODUCTION

1. The inverted hydropulse is similar to the direct hydropulse (see Section IV) except that the fuel and water are injected into a high-temperature reaction chamber instead of directly into the duct. From this chamber, the high-pressure gases are suitably introduced into the duct in an intermittent or pulsating manner.

2. Two types of inverted hydropulse were considered. One had a solid-sodium cartridge, and the other was to use a separate lithium-water gas generator to supply the high-pressure gases.

B. DESIGN

1. The solid-sodium-cartridge hydropulse consisted of a conventional hydropulse duct surrounded by a concentric fuel jacket into which the solid sodium is placed (see Figures 34 and 35). An annular piston is placed behind the sodium, which forces the fuel through a perforated conical partition into the reaction chamber. A ring of holes connects the reaction chamber to the duct which allows the passage of gases. Pulsing action is obtained by the intermittent injection of water into the reaction chamber against the perforated cone. The sodium cartridge is kept against this cone by the gas-actuated piston in the rear. Additional data regarding this design will be found in Reference 3.

2. The lithium-water inverted hydropulse was to be similar in design to the nitromethane hydropulse described in Section VI,D. It was not fabricated and tested because tests with the nitromethane hydropulse showed that intermittent valving of hot gases into the duct from a steady reaction chamber was not practical.

C. RESULTS OF INVESTIGATION

Sporadic and uncontrolled reaction of the solid-sodium fuel proved this device to be an unfeasible design. Proper hydropulse action could not be obtained, and further investigations were not conducted on this type of hydropulse.

VI. GASEOUS HYDROPULSE

A. INTRODUCTION

A gaseous hydropulse is similar to the direct hydropulse in its type of water duct. However, water is not used as one of the reactants. The actuating gases are generated in a chamber adjacent to the duct, and may consist of compressed air, or be formed by the explosion products of gasoline and air, or by the chemical reaction between one of many other fuel combinations. A schematic diagram and the nomenclature of the gasoline-air hydropulse are shown in Figure 36.

B. COMPRESSED AIR HYDROPULSE

The compressed-air hydropulse shown in Figures 37 and 38 was fabricated and tested. The unit was mounted by a parallelogram type of suspension in a large water tank and air at 250 psi was admitted through a valve which was suitably designed for control of frequency and quantity. This motor was used principally to test various air admission sections. Development was discontinued so that more effort could be expended on the gasoline-air hydropulse. The performance of the compressed air hydropulse at various cyclic frequencies is shown in Figure 39.

C. STEAM HYDROPULSE

Operation of the hydropulse with steam was initiated by simply substituting a 1-1/4-in. steam-supply line for the 1-1/4-in. air-supply line on the compressed-air-actuated unit (see B above). Insulation was provided, and a superheater was used to raise the 250-psi saturated steam from the plant boilers to 650°F total temperature. Various steam-admission systems were tried (see Reference 11) but performance was very poor because a large interface area between the steam and water was present, which condensed much of the steam before it could expand.

D. NITROMETHANE HYDROPULSE

1. This motor was a gaseous hydropulse designed to use the high-temperature gases produced from a nitromethane gas generator. The gas generator was designed on the assumption that it could be sufficiently well insulated to deliver gases at a temperature near 3500°F, and at 250 psi pressure. This insulation problem was quite severe, as evidenced by measuring

the heat loss from a gas generator submerged in a measured quantity of water. This test showed that 85% of the heat was being lost to the water through the chamber and manifold walls. This reduced the gas temperature to about 650°F. Molybdenum inside liners and asbestos outside insulation raised the available gas temperature to 1500°F.

2. The nitromethane gaseous hydropulse used for stationary tank testing is shown in Figures 40 and 41. The hot gases produced from decomposition of nitromethane are led around the motor throat for full-circle admission. The gas-pulse valving is accomplished by a sleeve (Figure 41) which fits inside the barrel and seats around its forward edge in a circular seat ground in the casing. It is given axial motion by hydraulic pressure pulses on the little pistons which push on lugs attached to the sleeve.

3. It was difficult to secure satisfactory operation. Overpressures were obtained in the gas generator if the valving operation in the hydropulse was not at the proper rate, and the gas generator would die out if gas was valved at too high a rate.

E. GASOLINE-AIR HYDROPULSE

1. Description of Cycle

The principal parts of a typical gasoline-air hydropulse are shown in Figure 36. The operation of this motor is as follows:

The propulsive force is supplied by expanding gases which result from the combustion of the fuel-air mixture in the combustion chamber. The expanding gases open the combustion-chamber exhaust valve, causing the water inlet valve to close, displacing the water to the rear and out through the tailpipe. The continuing displacement of this water mass under its own momentum, and the sudden cooling of the gases by the great surface area of the expanded bubble, bring the pressure of the gas below ambient. A new charge of fuel and air is drawn through the carburetor and poppet valve into the combustion chamber. At the same time, water at ambient pressure (or at ram pressure if the engine has forward velocity) rushes through the reed check valve at the front end of the motor and refills the duct. The movement of this incoming water mass closes the combustion-chamber exhaust valve, or, if spring-loaded, the valve closes before the water arrives. The mixture is then ignited by an intermittent spark of a controlled frequency. For motors of the sizes tested, this frequency lies between 5 and 8 cycles per sec.

2. Design and Development Program

a. General Motor Configuration

The general motor configuration was determined by experience gained from the development of the direct hydropulse and the need for improving specific components of the gasoline-air hydropulse. As shown in Figures 42 through 55, a wide variety of design configurations were fabricated and tested. The most promising features of each were incorporated into subsequent designs, the best of which are represented by Figures 52 and 54.

b. Water-Entrance Valves

(1) Generally each unit had a standard reed-type water-entrance valve at the forward end of the duct. This assembly was very similar to that described in Section IV for the direct hydropulse, with the exception that the Swedish steel or beryllium copper reeds were 0.012 to 0.016 in. thick.

(2) Several other types of water-entrance valves were tried, in order to increase the open area of the valve and to decrease the pressure drop through the valve. The valve shown in Figure 51 contained 74 leaf-spring check valves covering slots 3/8 x 2 in. In all cases, the standard grid-reed-type valve proved superior to the other types because of its low pressure-drop and endurance.

c. Duct and Casing Development

(1) As shown in the figures cited above, a multitude of shapes were tested in an effort to obtain better scavenging, and to increase the overall performance. Little success was had along this line in the early part of the program, as each new unit tested presented a new problem of water-spray dilution and the quenching of the combustion gases, resulting in limited performance. A comprehensive study of the water behavior in the various sections of the motor was made with the aid of the transparent plastic model shown in Figure 45. High-speed motion pictures were taken of this unit in operation, and this data aided materially in determining the necessary approach on the new designs. Reproductions of these movies are shown in Reference 3.

(2) As a result of the above studies, the inner combustion chamber was eliminated from the duct design, and the induction pipe was enlarged to become the combustion chamber. This decreased the internal drag within the duct. Increased performance was also obtained by admitting the combustion gases tangentially to the duct just behind the reed-valve assembly. The performance was further improved by placing a rubber-coated-canvas flap valve over the entrance of the combustion chamber into the water duct, as shown in Figures 46 and 56. High-speed motion pictures were also taken of this motor in operation.

(3) A large number of changes in the geometry of the water duct were made (keeping the standard 4-in.-dia tailpipe) in an effort to increase the quantity of water pumped per cycle, and thereby increasing the thrust augmentation. Figure 57 shows the approximate best

dimensions for motors with 6-, 7-, and 8-in. casings in conjunction with a 4-in. barrel. A casing shape similar to the design shown in Figure 49 proved to be very satisfactory, and was usually made in a 7 to 8 in. size. For some motors, the shape had to be modified to accomodate the combustion-chamber exhaust-valve arrangement, but the cross-sectional area of the casing approximately equalled that of an 8-in.-dia casing.

(4) Sprays of water, drawn from the water external to the duct, were used to chill the gas bubble when the pressure of the bubble drops below ambient. They were incorporated to further increase the vacuum to aid in scavenging, and had the effect of increasing thrust by approximately 10%. The leaf-spring check valves used to seal the water-spray holes are shown in Figure 58. A study of number and location of holes for the sprays showed that about 20 1/8-in.-dia holes was the minimum number for maximum improvement, and that they should be located in the upper half of the transition between casing and tailpipe.

d. Combustion-Chamber Development

(1) One of the greatest sources of trouble in the early development of this motor was the rapid chilling of the combustion process, and the wetting of the spark plug by water splash into the combustion chamber and up the induction pipe. Numerous baffles, etc., were tried and the problem was finally eliminated by the combustion-chamber exhaust valve mentioned in paragraph 2,c, above.

(2) Studies and tests were made to determine the optimum combustion-chamber shape and volume. After many trials, a chamber with an elliptical cross section whose major axis is placed at right angles to the axis of the motor was found to be the best of those tested (see Figure 49). In this type of exhaust port, the expanding gases are permitted to act in piston-like fashion across a greater area of the casing water.

(3) Quite a bit of effort was expended in trying to achieve some pre-compression of the fuel-air charge before ignition, but no appreciable success was attained. The study of high-speed motion pictures of the operating clear-plastic models proved to be an efficient method of analyzing the combustion process, and was used on the various designs.

e. Combustion-Chamber Exhaust Valve

(1) The introduction of the flap valve to separate the combustion chamber from the casing was beneficial in several ways in addition to the ones previously mentioned. It was found that the cyclic frequency could be increased on many of the models, and the motor performance was increased radically in other cases, but the durability of the valve was very poor.

(2) Because of the importance of the combustion-chamber exhaust valve, a large portion of time was devoted to its development. A variety of materials were tested for both the flexible and rigid types of valve. Flexible materials included neoprene on nylon fabric, rubber on nylon fabric, and canvas, all cut in varying shapes. Rigid valves were made of steel, aluminum or magnesium, and were of different types. The metal exhaust valve, which has been provided in the GAH-97, proved to be an improvement over valves of the flexible type. This exhaust valve is shown exposed in Figure 59. The valve is hinged and sealed at its forward edge, and swings shut into a recess 5/8 in. deep, the sides of which are scraped to fit very closely to the curved edges of the valve. A leaf spring holds it shut except during combustion and expansion. The expulsion of this valve from its recess by the high-pressure gas, causes it to travel down to the vertical position under its own momentum. The water in the casing shears smoothly off the sharp edge of the valve during this action, somewhat similar to the manner in which a sharp-edged orifice generates a smooth surface on the water jet issuing from it. This action generates a smooth-walled bubble for the gas to expand in without excessive loss of heat.

(3) Subsequent testing showed that a motor having a rubber exhaust valve produced a slightly higher specific impulse than a motor with a rigid or metal valve. However, the higher thrust produced by the metal valve, plus inherent advantages such as durability, smooth-bubble formation, and reduced maintenance made it the more promising valve.

f. Induction of the Fuel-Air Charge

(1) Carburetors of the automotive type were used to obtain the proper fuel-air mixture. Removal of the choke, accelerator pump, and reduction in main venturi size were the usual modifications made; however, units will run on stock carburetors. For some of the high-thrust motors, the diameter of the float-chamber filling jet had to be increased.

(2) The standard induction head and fuel-heater assembly, as shown in Figure 52, was generally used.

(3) A feather-valve type of induction head was developed (Figure 60) to replace the poppet valve. Its resemblance to an air-compressor valve is apparent, as it also uses thin steel strips over slots in a plate. The purpose of this valve is to induct the charge in such a uniformly distributed manner as to produce a relatively distinct surface of separation between the new charge and the burned gases, hence improving the volumetric efficiency beyond that possible with the poppet-valve arrangement and preventing flow in the opposite direction during the pressure phase of the cycle.

g. Fuels

(1) The standard fuel was 60 to 70 octane gasoline. Several additives were tested to see whether they increased the burning rate of the fuel, but regular gasoline was found to be superior to any of the other fuels tested.

(2) Some of the other fuels tested were a saturated solution of acetylene in acetone, an 0.8% solution of white phosphorus in Union 76 gasoline, high-test aviation gasoline (100 octane), and a 60% solution of white phosphorus in carbon disulphide.

h. Ignition Systems

(1) For the majority of tests in the static test tanks and on the boat, an electropneumatic time-delay relay, in series with a vibrator, high-tension coil, and spark plug, energized by storage batteries or dry cells, was used to produce a regular spark at any frequency from 5 to 8 cps.

(2) Other devices tested but found impractical were:

(a) A continuous spark furnished by a Ford spark coil.

(b) Ignition by means of a hot spot in the combustion chamber.

(3) A turbo-magnetic ignition system (Figure 61) was developed to eliminate the use of batteries and other bulky items. The power to drive the turbine is obtained from a pulsating jet of water bled from the motor casing. The turbine is geared to a one-point magneto assembly. Speed control of this system is obtained by means of a centrifugal friction governor attached to the water turbine. This system was later redesigned for lightness for use with the GAH-106, aluminum boat model, and the governor design modified to produce a steady running condition. This turbo-magneto is shown in Figure 51, in back of the carburetor. Time did not permit the complete development and testing of this component.

i. Streamlined Models

(1) The streamlined units pictured in Figures 48, 50, 51 and 52 were developed for boat and field tests. They were mounted on various types of outboard brackets which could be quickly fastened to the stern of a standard 15-foot work boat.

(2) These motors were tested on the rotating-booms, as well as on the 15-foot boat, to determine the effect of forward speed on the operation of the unit and to determine overall performance.

j. Compressed-Air Models

(1) Subsequent to the completion of the development program described in the above paragraphs, the program was resumed with the objective of increasing the chamber pressure, thrust, and power output of the motor by precompression of the fuel-air charge and by increasing the cyclic rate. Two concurrent programs were undertaken, one aimed at securing the necessary degree of precompression, the other at testing a hydropulse motor under the supercharged conditions of intake air at 100 psig. A complete summary of the results of these programs is given in Reference 12.

(2) The motors shown in Figures 53, 54, and 55 were fabricated and tested as part of this program. The preliminary design calculations indicated that the following performance should be obtained when using intake air supercharged to 100 psig.

(a) Maximum chamber pressure - 700 psi

(b) Thrust from a 4-in.-dia tail-pipe unit - 1000 lb

(c) Specific Fuel consumption - $\frac{0.5 \text{ lb fuel}}{\text{indicated hp hr}}$

(d) Speed - 60 knots

(e) Indicated horsepower - 500

(f) Indicated horsepower of compressor needed - 100

(3) The desired performance was not obtained. One of the primary development problems was the production of large quantities of fuel-vapor without the benefit of the high temperatures existing during compression in a reciprocating engine. This was partially accomplished by the development of a plenum chamber equipped with an air-atomizing fuel injector and a fan turbulator (see Reference 13). Another unresolved problem was the lag in ignition of the compressed air-fuel mixture. During the early combustion phase, the mixture would expand so that the full power potential of the motor could not be realized. Further development time was not available to pursue this program.

3. Method of Testing

a. Static Tests

(1) Most of the models were tested in the static test tanks on parallelogram thrust stands equipped with coil extension springs to resist the thrust. (Figures 62 and 63.)

(2) The Lucite models were mounted in the open for easy photography with the water entrance valve in one horizontal steel tank and the end of the tailpipe in another. Thrust was measured by jet impingement on a flat plate.

b. Dynamic Tests

Some of the streamlined models were tested on the 40-ft rotating boom but most of the dynamic tests were made with the 15-ft work boat. Open-water testing took place on the Morris Dam Reservoir as well as the testings in the Ring Channel such as shown in Figure 64.

c. Data Recorded

(1) Thrust, fuel flow rate, and frequency were measured during all of the tests.

(2) Pressure-time measurements were made of a great many of the test motors. This was accomplished with a diaphragm-reluctance type of pressure pickup and measurements were recorded on an oscillograph.

4. Analysis of Performance and Results of Investigation

The following performance figures were obtained during this development program:

a. Thrust measurements were made statically, and varied from 45 lb for the early models to a peak of 180 lb for the GAH-97 (Figure 62).

b. Specific Impulse (I_{sp}) was calculated from the measured thrust and fuel flow rates. I_{sp} values of 11,600 $\frac{\text{lb thrust}}{\text{lb fuel/sec}}$ were obtained on some of the early models. This was increased to a maximum of about 55,000 $\frac{\text{lb thrust}}{\text{lb fuel/sec}}$ on some of the best models. A theoretical maximum value that could be obtained under the operating conditions of the standard gasoline-air hydropulse is 114,000 (see Reference 6).

c. The pressure-time curves of the hydropulse cycle and the pressure-volume data obtained from the high-speed motion pictures were used extensively to determine performance values and indicate design improvements to be made. The step-by-step integration method described in Reference 8 was calculated for all of the Lucite models tested, and for several of the steel models. From these calculations, the following representative data were obtained:

(1) Duct Efficiency - 90 to 96%

(2) Indicated Horsepower - 15.9

(3) Work per cycle (GAH-97) - 1625 ft lb

(4) Indicated Thermal Efficiency - 13.1%

In addition, bubble temperatures and the complete pressure-volume data were obtained. The analysis made in Reference 5 of the heat lost to the water (lack of spray control) proved invaluable in determining design corrections necessary for increased performance. A typical pressure-time oscillograph record is shown in Figure 65 with the corresponding calculated pressure-volume diagram in Figure 66. The sequence of events in the hydropulse cycle, as determined from the high-speed motion pictures, is shown in Figure 67.

d. As a measure of overall performance, the various gasoline-air hydropulse models were dynamically tested in a 15-ft work boat. The GAH-106 as shown in Figure 52 propelled the 15-ft boat loaded with three people (approximately 500 lb) at a speed of 8.1 knots, with fuel consumption at the rate of 3 gal/hr.

e. The gasoline-air hydropulse possesses several advantages which make it attractive for the propulsion of small boats or assault craft. These advantages are, low initial cost, simplicity, ease of maintenance, and lack of lubrication requirements. However, the consumption of gasoline is about 50% greater than that of a gasoline engine-propeller combination, and, because of the relatively high exit-jet velocity, the propulsive efficiency of the hydropulse is lower than that of a propeller, except at high forward speeds. With supercharging, the efficiency of the motor should compare favorably with that of conventional engines. Improved efficiency and high cross-sectional thrust, plus the advantages mentioned above, should make this motor especially attractive.

VII. HYDROTURBOJET

A. DESCRIPTION OF THE CYCLE

1. The hydroturbojet is a bipropellant rocket motor, best suited to propulsion of an underwater missile. One propellant is a water-reactive chemical, and the other is water, normally obtained from the medium

through which the missile travels. An example of a typical water-reactive propellant is molten lithium, and in Figure 68 a system employing it may be seen arranged within a torpedo envelope. In this system, the lithium is heated to a liquid state before injection into the combustion chamber. In the combustion chamber it reacts with water, producing hydrogen, lithium hydroxide, and heat. The heat of the reaction evaporates the excess water, about 90% of the total water supplied, into steam of approximately 80% quality. The products from the chamber, consisting largely of wet steam, are expanded rearward through the nozzle. For each pound of lithium about 24 lb of water are supplied to the main combustion chamber, of which 2.6 lb of water take part in the reaction. The exhaust velocity is in the order of 2000 ft per sec. Propellant supply to the combustion chamber may be accomplished by pumps or other means, and if pumped, a small gas-turbine driven by reaction products is normally employed to operate the pumps.

2. The cycle may be broken down into the following four parts:

a. The pump cycle, to raise the propellant pressures to the combustion-chamber pressure.

b. The combustion chamber, where the chemical reaction takes place at constant pressure.

c. The nozzle expansion, where the reaction products are accelerated by an expansion process to provide thrust.

d. The turbine expansion, where work is derived to operate the propellant-feed pumps.

B. ANALYSIS

1. Because no prior reference material was available on the subject of hydroturbojet cycle characteristics, it was necessary to derive the equations for the specific impulse and thrust for this cycle. Before proceeding, a detailed analysis of the general cycle was made. Four distinct cases were apparent.

Case 1 - where all mass is in vaporized or gaseous state after reaction

Case 2 - where some excess water is in droplet form after reaction

Case 3 - where there are gas or vapor bubbles in the excess water

Case 4 - where there may be any combination of these cases.

A working knowledge of the effect of pressure ratio, mixing ratio, machine efficiencies, heat of reaction of the propellant, and velocity was desired for all of these cases. However, the calculations completed under this contract consider the first two cases only, as the necessary information was not available to study the two-phase systems of Cases 3 and 4.

2. In deriving the equations and for evaluating the system variables, the use of lithium and aluminum borohydride were assumed as two typical water-reactive propellants which showed promise of future application. Inasmuch as the complete equation derivations are quite lengthy and are fully expanded in the partial reports on this contract, they have been omitted from this final report, and only their end-products are presented in graphical form. Figures 69 through 72 represent a summary of the cycle characteristics as determined under this contract. Nomenclature appearing in these figures is identified as follows:

I_{sp} = specific impulse = $\frac{\text{lb thrust}}{\text{lb of fuel/sec}}$

β = mixture ratio = $\frac{\text{mass fuel}}{\text{mass fuel plus mass water}}$

h_m = heat available, per unit mass of reaction products, for use in an isentropic expansion

$\frac{1}{\sigma}$ = pressure ratio

P_1 = pressure, inlet condition, absolute

u_o = velocity, ambient condition

u_3 = velocity, nozzle inlet condition

J = conversion factor, heat-to-work

g = gravity constant

Attention is drawn to References 3, 11, and 14 in which more detailed information is available. Also of interest is Reference 15 which reports generally on the subject of hydrofuels for torpedo propulsion.

C. DISCUSSION OF RESULTS

1. The performance calculations show that the hydroturbojet, using lithium-water propellants and operating with a nominal chamber pressure of 640 psia, at zero forward speed, can develop a specific impulse as high as 1500 $\frac{\text{lb thrust}}{\text{lb of fuel/sec}}$, which will decrease no more than 2% at a forward

velocity of 100 ft/sec. The aluminum borohydride-water propellant would provide, under similar operating conditions, a specific impulse of 900 to 1100. The performance quoted will occur at chamber temperatures below 850°F, and may improve at higher temperatures. For the lithium-water reaction the accuracy of the specific impulse data is expected to be within ± 5%, while for the aluminum borohydride-water combination, the error may be somewhat greater, due to lack of precise knowledge of the heat of hydrolysis of aluminum borohydride.

2. In making these calculations, it was considered that the lithium was melted by heat from the combustion chamber and so this heat was not considered in the calculations. In the case of a short-duration device, it might be possible to supply the heat required to melt the lithium from an external source, and thus increase the performance.

3. The curves for I_{sp} vs β shown in Figures 71 and 72, indicate that there will be two points of optimum operation, one at a low value of β, and one at a value of β near the stoichiometric ratio. The optimum high β value probably could not be used, due to the very high temperatures involved.

4. Subsequent to the completion of this analytical study, a lithium hydroturbojet was developed and fabricated by the Aerojet-General Corporation under Contract NOrd 9768. This unit, housed in a Mark-40-type torpedo envelope, was designed to provide 2000 lb thrust for a duration of 46 sec, and to propel the torpedo at 80 knots over a 2000-yd range. The development was completed through the captive-cable testing stage. The highest speed developed on the captive cable was 57 knots, where the duration was limited to 15 seconds. A complete discussion of the design and development of this propulsion system can be found in the Final Report on Contract NOrd 9768, Reference 16, and the semiannual progress reports, References 17 through 21. Figure 73 shows the graphical results of cable run No. 15 for this torpedo running on submerged cables. In general, the calculated performance for this propulsion system was approximately 10% higher than that obtained in tests.

5. During the Mk 40 development, molten sodium was also tested at full prototype thrust levels. Actual specific impulse obtained was 250, equivalent to 13.07 pounds per shaft horsepower-hour. A graph of I_{sp} vs β for sodium is shown in Figure 74.

D. CONCLUSIONS AND RECOMMENDATIONS

1. The hydroturbojet cycle was clearly established as a feasible propulsion system of unusually high specific impulse, especially applicable to high-thrust, short-duration requirements.

2. Practical experience gained in developing and operating the 2000-lb lithium-water Mk 40 torpedo motor requires the mentioning of several points deserving careful consideration before the cycle can be judged on a competitive basis with other systems, as follows:

a. System Complexity

The development-phase design of the hydroturbojet was not overly complicated, if compared to that of present 3-liquid torpedo propellant systems. The production design would have simplified service procedures that could be adequately handled by trained fleet personnel.

b. Reliability

The system is capable of acceptable reliability in the hands of trained personnel.

c. Range

Duration is severely limited in comparison to other systems, primarily because of the space problems imposed by the low density of the water-reactive propellants.

d. Safety

Risks are somewhat greater and accident-prevention measures need to be more elaborate with a propellant such as molten lithium in the proximity of water.

e. Precision

Experience revealed that very accurate control of mixture ratios of reactants was required for optimum performance. In the auxiliary turbine, variance in mixture ratio above the optimum β value of 0.08 produced excessive heat and erosion, while ratios below 0.08 caused rapid contamination with lithium hydroxide. Performance efficiency of the main combustion chamber dropped when values of β exceeded 0.04 and the chamber was subject to hydroxide deposits on β values less than 0.04.

f. Logistics

The expense and availability of water-reactive propellants of sufficient quality, particularly in a time of national emergency, should be considered.

3. Further research and development to overcome some of the objectionable features of this cycle should be considered. However, as a more immediate approach to the need for a high-performance torpedo-propulsion

system that is simple, safe, reliable, and capable of long-range, attention is directed to Section XIII and to Reference 22 which sets forth the advantages of a solid propellant* turbine-drive system for torpedo propulsion. With this recently developed propellant, a power plant can be designed to provide 2500 lb of thrust for a duration of 8 min; i.e., sufficient power to drive a 21-in.-dia, 10-ft torpedo for 20,000 yd at 70 knots.

VIII. AEROJET HYDRODUCT

A. HISTORY OF DEVELOPMENT

1. The Aerojet Hydroduct is a simple high-speed underwater propulsive device utilizing free water (i.e., water that is not carried in the vehicle) to obtain a high specific impulse. In its operation, it is the underwater counterpart to the aerodynamic ramjet. This motor is also referred to as a vapor-phase hydroduct, as distinguished from the hydroduct described in Reference 23, which operates with a bubbly-water mixture. The compressibility effects in the gas-water mixture do not permit the development of the high jet velocities that can be obtained with a vapor exhaust.

2. The hydroduct receives free water through an opening in the nose section. This water is led through suitably designed passages to a combustion chamber where energy is added from some type of fuel. This energy is utilized in converting the water to steam, which in turn is expelled through a suitably designed nozzle to obtain the necessary forward thrust. Schematic diagrams of the two types of hydroducts studied at Aerojet-General are shown in Figures 75 and 76.

3. Work was initially started on a hydroduct utilizing the exothermic reaction between lithium and water to provide the energy needed by the system. After considerable study and development on this system, the program emphasis was shifted to the development of the Alclo Hydroduct because of its greater performance potential. A detailed description of the development of these two motors is given in the following sections.

B. MOLTEN-LITHIUM HYDRODUCT

1. Introduction

a. The molten-lithium hydroduct is designed to operate on the continuous injection of molten lithium into water which is flowing through the duct. Free water is diffused in the nose of the hydroduct to a stagnation cross-section, where nearly full ram-pressure is developed. The fuel is injected at this cross-section, and the heat released by the chemical reaction flashes all, or nearly all, of the water to steam at the pressure of the stagnation region. Thrust is produced by the expansion of the steam and reaction products to ambient pressure.

---

*Aerojet-General type AN-2091AX ammonium nitrate propellant.

b. The designed mixture ratio of approximately 20:1 (water to lithium by weight) is nearly seven times the stoichiometric ratio, so that the exhaust is made up of a mass of steam mixed with the solid particles of lithium hydroxide and a small amount of hydrogen.

c. The preliminary calculations of the performance of the lithium hydroduct operating at 100 knots on the 80-ft rotating boom (Reference 5) showed that the following values could be obtained:

(1) Drag of test model - 290 lb

(2) Chamber Pressure - 158 psia

(3) Ram Pressure - 192 psi

(4) Pressure Ratio, P_c/P_e - 9.88

(5) Specific Impulse - 1140 lb thrust/lb/sec

(6) Mass flow, lithium - 0.254 lb/sec

(7) Mass flow, water - 4.37 lb/sec

On the basis of these figures, the hydroduct motor components were designed. The following sections describe the specific details of the development program.

2. Design and Development Program

a. Duct Design

(1) The hydroduct is inherently a high-speed device, inasmuch as the combustion pressure, which must be high to obtain good thermodynamic efficiency, is a function of the square of its forward speed.

(2) The external form of the hydroduct (Figure 77) was determined from an analytic extrapolation of the Mark 40 torpedo minimum-pressure coefficient to avoid cavitation at 100 knots. By increasing the length-to-diameter ratio of the Mark 40 torpedo shape from 5:1 to 10:1, the minimum pressure coefficient was reduced from -0.17 to -0.085. The Mark 40 torpedo shape was based on the Lyon Form A configuration (see Reference 24).

(3) External diffusion of the inlet water to the nose of the hydroduct has been provided to minimize the amount of the relatively inefficient internal diffusion. This design also tends to equalize the external and internal pressures at the nose-entry lip, thus preventing separation of the flow at the diffuser lip.

(4) The results of static tests of the hydroduct motor showed that increased performance could be obtained at mixture ratios of 28:1, instead of the original design ratio of 20:1, and that higher fuel flow rates could be used to provide more thrust. The nose-inlet diameter and diffuser proportions were therefore enlarged to accommodate this increased water flow without an increase in pressure drop through the injector.

b. Fuel Injection

(1) Previous test data obtained on the molten-lithium gas generator and hydroturbojet programs showed that the best injector arrangement for the combustion of molten-lithium and water is an axial intersection of a convergent cone of water with a divergent cone of highly atomized lithium. This arrangement was used in the hydroduct injector, and is illustrated in Figures 75, 78, and 79.

(2) For theoretical maximum efficiency of injection, the transverse momentum components of the lithium and water sprays should be equal. With more than a 20:1 weight ratio of water to lithium this was not practical, because of the relatively high required velocity of the lithium spray. If the velocity of the lithium spray is high in relation to the water spray, poor combustion results, because the lithium spray tends to break through the water spray without reacting. Better results are obtained when the lithium and water velocities are approximately equal. This was not possible because the pressure drop through the water injector had to be limited to not more than 50 psi, in order to allow a sufficiently high chamber pressure to be developed (maximum ram pressure available is 192 psig at 100 knots). The combustion vibration that occurred because of the injector design was satisfactorily suppressed by the insertion of turbulence-producing baffles in the combustion chamber downstream from the intersection of the lithium and water sprays. These "turbulators" assisted in obtaining a more intimate mixing of the lithium and water, but they were also subjected to severe thermal shock and erosion. Molybdenum, SAE 4130 steel, and Timken turbine alloy were tested as materials for the turbulators. The SAE 4130 steel turbulators with a thickness of 1 to 1-1/8 in. proved to have adequate thermal capacity and erosion resistance, and were used in the subsequent tests of the motor.

c. Suspension Strut

(1) To drive the hydroduct through the water at 100 knots, the strut had to be sufficiently rigid to resist failure from torsional divergence and flutter, yet be within a reasonable size to avoid prohibitive aeration and feathering at the surface.

(2) The strut resulting from these design considerations (Figures 78, 80, and 81) has a fineness ratio of 40:1 at the water surface, to avoid wave-formation, aeration, and to minimize form drag. It is made of solid steel, with a maximum thickness of 3/4-in. To eliminate dynamic effects of the water, the strut was designed with its section median line approaching the curvature of the 50-ft turning cycle.

(3) The calculated speed of torsional divergence of the strut is 185 knots. Since the center of gravity of the hydroduct is forward of the elastic axis of the strut, the critical flutter speed is above the speed of divergence. The estimated drag of the strut alone is 261 lb at 100 knots.

(4) The strut was hollowed out in one section to accommodate the fuel and instrumentation lines, thereby maintaining the cleanness of line required for achieving high speeds through the water.

d. Fuel-Heating System

(1) To insure free-flow of the lithium through the fuel line and injector, all parts of this system were heated to a temperature above the 367°F melting point of the lithium.

(2) The experience obtained in the hydropulse work in heating the lithium-conveying system was utilized in designing the hydroduct heating system. This system, which must be encompassed in an extremely small space in the hydroduct, consists of a continuous helix of Nichrome wire wrapped around the fuel line and injector. Glass tape, impregnated with Silicone varnish, was used as electrical insulation for the Nichrome wire. Because of the internal space limitations of the hydroduct, the amount of insulation was kept at a minimum, and particular care was exercised to prevent grounding of the Nichrome heating coil to the hydroduct assembly.

(3) O-ring seals at all the joints insured complete watertightness of the space into which the fuel line and fuel injector fit. Figure 78 is an assembly drawing of the hydroduct showing the installation of the injector and fuel line.

(4) Investigation of the stoppage of the lithium flow in some of the tests showed that the supposedly pure lithium contained solid lithium nitride impurities. Repurifying the fuel, and the provision of a strainer in the tank outlet, eliminated this problem.

e. Tail Plug

The blunt exit of the exhaust nozzle was fitted with a faired tail plug to reduce the drag of the hydroduct to a minimum, while the unit was being accelerated to the 100-knot operating speed. An ejection mechanism, incorporated in the faired plug and actuated pneumatically by pressure in the chamber, ejects the plug an instant before firing. An assembly drawing of the tail-plug ejector is shown in Figure 82. A seal is provided at the face of the water injector which seals off the forward end of the chamber to permit pneumatic pressurization of the chamber through the chamber-pressure tap.

f. Critical-Pressure Exhaust Nozzle

All tests during the latter part of the program were made with the critical-pressure exhaust nozzle. A description and analysis of this nozzle is presented in Section XV,C.

3. <u>Testing Procedures</u>

a. Static Tests

(1) The hydroduct was set up on the thrust stand and operated as a rocket motor using molten lithium and water. The test setup is shown in Figure 83. Pressurized water tanks supplied water to the nose of the hydroduct, at ram pressure, through a flexible hose connection. Molten lithium was forced by helium pressure from an electrically heated fuel tank through an electrically heated fuel line and injector.

(2) Water from an independent source was run over the external surface of the hydroduct to simulate the heat-transfer conditions of an underwater run.

(3) Recording instruments measured chamber pressure, ram pressure, water flow, thrust, and temperatures of the fuel and of the fuel system.

b. Drag Tests

(1) The hydroduct suspension strut was mounted on the 10-ft-boom extension arm and towed through the water at speeds up to 98.5 knots. The submergence was measured and the angle of attack checked before and after the run by swinging the strut across a dial indicator fastened to the bridge. The gross drag of the strut-and-extension arm assembly was measured by means of the reluctance-type pickup on the boom thrust-suspension system.

(2) The mounting strut was then removed, and the extension arm with the diagonal strut brace in position was driven through the same speed range. A fairing block was fitted to the end of the extension arm to close up the end of the extension arm fairing. The net drag of the strut was the difference between these drag measurements.

(3) The hydroduct was assembled on the suspension strut with the nose plugged and the tail-plug fairing installed. The depth of submergence was measured and the angle of attack of the strut was checked. The gross drag of the assembly was recorded at intermediate speeds up to 98.5 knots. The net drag of the hydroduct was the difference between these drag measurements and the previously obtained strut drag measurements. The hydroduct in position for drag testing is shown in Figure 81.

c. Dynamic Tests

(1) The hydroduct chamber was pressurized to 200 psi and the hydroduct brought up to speed by the boom-drive motor. Upon reaching operating speed, the tail plug was ejected by tripping open the 400-psi solenoid valve. This valve was operated by a momentary-contact switch in order to make certain that the valve is closed after ejection of the tail plug. Upon ejection of the tail plug, the fuel line-valve was opened and the hydroduct was fired.

(2) Underwater motion pictures were taken at 3000 frames per sec to show expansion of the exhaust jet and the flow patterns around the hydroduct body.

4. Results of Investigation

a. Various fuel-water mixture ratios were tested in the static-motor setup in order to determine optimum performance conditions. Some of the results of these tests are shown in Table 3.

b. Results of the dynamic tests are shown in Table 4. The highest thrust obtained was 600 lb, and the best specific impulse was 1235 lb thrust/lb fuel/sec.

c. The results of the drag tests, made to determine the net drag of the hydroduct, are shown in Figure 84. The hydroduct drag coefficient, based on frontal area and determined from data at 98.5 knots, was computed to be 0.081.

C. ALCLO HYDRODUCT

1. Introduction

a. The development of the molten-lithium hydroduct proved that this type of propulsion motor was entirely feasible. Adequate thrust could be produced by this ramjet type of motor so that it would have a high sustained operating speed. The development of Alclo (see Section X) gave additional promise to the hydroduct, in that some of the major disadvantages of molten lithium could be eliminated. The particular advantages of the Alclo propellant were:

(1) The propellant is inexpensive and its constituents are readily available.

(2) The power plant would be ready for use at any time without heating or pressurization of the fuel.

(3) The high energy per unit volume of Alclo will permit speeds and ranges of a missile of a given displacement to equal or exceed those obtainable with any other known type of underwater propulsion system.

(4) The reaction products of Alclo are solids, and the vehicle therefore will have no gaseous wake.

b. The Alclo hydroduct, as shown schematically in Figure 76, operates on the expansion of steam generated by heat released by the burning Alclo. The Alclo, which contains fuel and oxidizer in stoichiometric proportions, does not react with the water. It is end-burning, the heat released being transferred to the free water which flows continuously through the duct.

c. During the early development program of the Alclo Hydroduct motor, it became apparent that the motor would have adequate performance to power a free-running missile. Design studies performed under Contract N1235-73462 for the Naval Ordnance Test Station (Reference 25), also showed that stable equilibrium velocities could be obtained with a prototype Alclo Hydroduct missile. Therefore, the major design and development effort was placed upon the attainment of motor configurations suitable for incorporation into a free-running test missile that could be range-fired to completely prove this power plant.

2. Design and Development Program

a. Alclo Motor

(1) Investigations of combustion-chamber stability, methods of water injection, optimum water-to-propellant ratio, variation of burning rate with chamber pressure, and the effect of solids in the exhaust were conducted. For the purpose of establishing the parameters governing the design of a combustion chamber fueled with Alclo, several experimental motors were designed and fabricated for static testing on a thrust stand in a test pit. The motors were designed for operation as rocket motors, with simulated ram-water being injected into the motor from a pressurized water tank. The 2-in.-dia Alclo grain, formed at a pressure of 80,000 psi and encased in a copper restrictor, was used in these motors. A drawing of the 2-in.-dia Alclo motor is shown in Figure 85.

(2) As the testing proceeded, it was noted that the copper melted from the restrictor, acted as a binder to hold the mass of the reaction products together, and thus clogged the water injector and the exhaust nozzle. Various methods of cooling the restrictor to keep it intact and prevent it from melting were tested, but proved unsatisfactory. A thin-walled steel jacket was substituted for the copper as one modification, and the grain was pressed directly into the combustion chamber in another modification. Both

were unsatisfactory. Efforts were therefore directed towards development of a restrictor that would be consumed, as the burning progressed down the grain, with the evolution of as little gas as possible and the complete burning of the restriction material. Various tape and bonding materials were tried and the selectron-fiber glass-tape combination proved to be the best. This method of restricting the Alclo grain is completely described in Section X.

(3) Early tests with the 2-in.-dia Alclo grain provided a great deal of data on the performance of the motor, but the design of the test motor was not well suited for incorporation into a test missile. The principal modification necessary was in the method of water injection. In the design of the Alclo hydroduct test missile, water enters the nose of the missile and it can be carried aft in a tube running through the center of the grain, or it may be led around the outside of the grain. The cored type of grain was tested in the motor designed for a 3-in.-dia Alclo grain (Figure 86). It was not possible to maintain a proper restriction around the center tube through the grain, and this design was abandoned in favor of the solid grain.

(4) Improvements were being continually made in the pressing techniques, so that larger Alclo grains could be made on the 400-ton-press equipment. A 3.75-in.-dia grain was the largest size that could be made without subjecting the press equipment to its maximum rated capacity, so this size grain was adopted for use in the free-running test missile. The test missile used to accommodate this grain had a maximum diameter of 4.5 in. All efforts were then directed towards completing the development of the best motor configuration. Static motors were subjected to exhaustive testing so that optimum performance could be obtained in the hydroduct test missile. The final design is shown in the assembly drawing of the static-test motor in Figure 87, and the test setup is shown in Figure 88. Some of the tests conducted were as follows:

(a) A series of area-ratio tests (area of burning face/area of nozzle throat) were made over a range of water-to-propellant ratios from 1.5 to 6.0 to determine the variation in chamber pressure and the proper area ratio for operation of the hydroduct test vehicle. An area ratio of 6.75 was established as the proper design point so that the chamber pressure would be 300 psia. The results of these tests are plotted in Figure 89.

(b) Investigation of the mixing of the water, flame, and hot reaction products was made by varying the size and spacing of the turbulator rings which were arranged in series in the combustion chamber. The effect on the chamber pressure of the ratio of the clear opening of the rings to the area of the grain was determined.

(c) Control of the water-injection pressure drop through the motor was effected by proper sizing of the water ports and of the annular water passage between the restriction and the chamber wall. The effect on the motor performance of the water velocity through the annular water passage was determined, and satisfactory performance was obtained when the pressure drop through this passage was 10 psi.

(d) To obtain a rapid rise to the operating chamber pressure when starting the motor, water-injection-delay tests were carried out. This was done by delaying the start of injection of the water by a predetermined fraction of a second after ignition.

(e) To keep the chamber of the hydroduct test vehicle watertight when submerged at launching, a burst diaphragm was fitted in the water intake forward of the injector, and a closure was placed in the exhaust nozzle downstream of the throat. For the water-inlet closure, thin sheet aluminum was tested and found satisfactory.

(f) For sealing the exhaust nozzle of the test vehicle, several shapes and materials were tested, each of which was cemented into the nozzle exit. The sealed nozzle was hydrostatically tested successfully to a simulated depth of 140 ft. The closures were blown out without excessive rise in chamber pressure. A 1/16-in.-thick Lucite dome, mounted with the convex side outward, was selected as the best closure because of strength considerations, and because no water need be displaced for full expansion of the steam. A nozzle closure at the throat initially restricts full expansion.

(g) An aluminum combustion chamber and nozzle section were fabricated, and withstood erosion satisfactorily when tested over a range of water-to-propellant ratios from 1.5 to 6.0; this established that aluminum was suitable for use in the construction of the hydroduct test vehicle, thus materially reducing its weight.

(h) Various types of igniters were tested, including the ones shown on Figures 85 and 86. The igniter shown in Figure 87 contained 0.2 gm Alclo powder and 6 Alclo pills and it was used on the most of the static tests and the early free-running missile tests. It was later replaced by the Mark II stand-off igniter shown in Figure 90 to provide more rapid ignition of the grain.

(5) In an effort to obtain better mixing of the water with the flame and hot reaction products, a motor was designed with spray injectors located aft of the grain, as shown in Figure 91. The water was brought aft from the nose through an annular passage formed by the double-wall chamber to a ring of injectors spaced around the inside of the chamber. A small flow of water is bypassed along the grain to ensure proper cooling

of the restriction. To accommodate a given size of grain, the outside diameter of the double-wall chamber motor must be greater than that of the single-wall motor. The drag of a hydroduct designed with a double-wall motor would therefore be greater than that of a hydroduct using a single-wall motor. Test results with this motor showed improved performance but the increase in performance was not adequate to compensate for the increased drag of the larger missile.

b. Free-Running Test Missile

(1) To demonstrate the practicability of a high-speed hydroduct fueled with Alclo, and to compare its performance with that of underwater missiles propelled by conventional rockets, a 4.5-in.-dia Alclo hydroduct was designed for free-running operation. A drawing and a photograph of the missile are shown in Figures 92 and 93. The missile is powered by a 3.75-in.-dia Alclo grain, and its calculated performance is shown in Figure 94. The missile was designed for launching at 200 ft/sec at a 50-ft depth.

(2) The body form of the missile has a fineness ratio of 10.5:1, which will permit cavitation-free operation at shallow depth. The missile is stabilized, and made to revolve slowly by three tail fins which are canted at an angle to the axis of the missile.

(3) The missile was launched underwater by a rocket booster which brought the missile to operating speed at the end of the 20-ft launcher.

3. Test Procedures

a. Static Tests

(1) The Alclo motor was mounted on a thrust stand in the static test pit, and was operated as a rocket motor with water supplied to the injector at ram pressure from a pressurized water tank. A 4.5-in.-dia motor set up for static testing is shown in Figure 88.

(2) The thrust, chamber pressure, ram pressure, and water flow rates were recorded on a multichannel oscillograph using reluctance-type pressure pickups.

(3) The proper sequence of igniting the grain and injecting the water, which is necessary in a booster-launched hydroduct missile, was effected with a firing-sequence control circuit using a system of relays.

b. Dynamic Tests

(1) Free-running tests were carried out at the underwater test range of the Naval Ordnance Test Station at San Clemente Island, where the launching depth could be varied and underwater pictures taken of the missile in operation.

(2) Additional ballistic tests were conducted on the Morris Dam Torpedo Range, under Contract Nonr 1002(00).

4. Results of Investigation

a. The free-running range firings of the Alclo Hydroduct test missile proved that this type of propulsion system was entirely feasible, and that very satisfactory ballistic performance could be obtained. Complete results of the range-firing programs are given in References 26 through 32.

b. Studies made of prototype hydroduct missiles have been reported in References 25 and 33.

c. An underwater rocket such as the Hydroduct, powered by Alclo propellant, has several times the powered range of an underwater rocket of comparable size powered by conventional solid propellants.

IX. HYDROFUELS

A. INTRODUCTION

1. Laboratory work on new fuels was directed toward the preparation and study of high-energy compounds, most of which were water-reactive. A byproduct of this investigation was the discovery of solutions suitable for use as rocket fuels. The materials of particular interest were ethyl aluminum sesquihydride, aluminum borohydride, and lithium. Ethyl aluminum sesquihydride served only as an interim fuel to provide experience in the handling of air- and water-reactive materials in anticipation of extensive use of aluminum borohydride. Lithium was given primary consideration because of its use in hydropulse-motor tests. In addition to the studies on preparative reactions, considerable effort was expended to determine suitable materials for handling these materials, with particular emphasis being placed upon lithium problems.

2. To augment the laboratory studies, reaction tests were made with rocket motors using both solid and liquid lithium. Additional data were obtained on lithium handling techniques, the reaction of lithium-water and other fuel combinations, compatible materials, and the design of reaction chambers and injectors.

3. In order to provide a readily available supply of molten lithium for injection into the motor, methods of rapidly melting lithium by chemical means were investigated.

4. Because of the limited availability and cost of lithium as a hydrofuel, considerable effort was expended to develop an alloy as an effective substitute. The goal of the development was a hydrofuel that

would have a low melting point, preferably below the boiling point of water, a high energy-density, a high availability, low cost, a high degree of fluidity when molten to facilitate injection, stability in air, and non-corrosive with regard to equipment.

B. ETHYL ALUMINUM SESQUIHYDRIDE

1. Ethyl aluminum sesquihydride was considered for use in the hydropulse because it had a theoretical gas-producing capacity of 933 cc/gm, compared to that of the NaK alloy of 350 cc/g. It was considered only as a temporary substitute for aluminum borohydride, which has a theoretical hydrolytic gas yield of 3700 cc/g.

2. Ethyl aluminum sesquihydride was prepared by the method indicated in the reactions

$$2\ Al + 3\ C_2H_5Cl \longrightarrow (C_2H_5)_3Al_2Cl_3 \quad (1)$$

$$3\ LiH + (C_2H_5)_3Al_2Cl_3 \longrightarrow 3\ LiCl + (C_2H_5)_3\ Al_2H_3 \quad (2)$$

The procedure for preparing this material is illustrated in Figures 95 and 96. The entire process is described in detail in References 3, 6, 14, and 34.

3. A total of over 40 lb of ethyl aluminum sesquihydride was prepared, and several tests were made in the direct hydropulse motor. These tests proved that this fuel was slightly better than the NaK alloy, but the performance was not sufficiently better to warrant continued production for hydropulse use.

C. ALUMINUM BOROHYDRIDE

1. Aluminum borohydride, because of its theoretical hydrolytic gas yield of 3760 cc/g, represented one of the best water-reactive liquid fuels for use in the hydropulse. Its preparation and handling were considered too difficult and costly to justify an attempt at preparation of sufficient quantities for motor tests, but it was considered necessary to prepare small quantities in order to conduct stability tests with various lubricants, shaft packings, and motor construction materials, as well as the shock and thermal-stability measurements.

2. The method chosen from the multitude of available reactions for the preparation of aluminum borohydride involved these equations

$$H_3BO_3 + 3\ CH_3OH \longrightarrow (CH_3O)_3B + 3\ H_2O \quad (3)$$

$$(CH_3O)_3\ B + 4\ NaH \longrightarrow NaBH_4 + 3\ CH_3ONa \quad (4)$$

$$AlCl_3 + 3\ NaBH_4 \longrightarrow 3NaCl + Al(BH_4)_3 \quad (5)$$

As shown in the above reactions, the preparation of trimethyl borate and sodium borohydride was prerequisite to that of aluminum borohydride, and considerable effort was expended on the proper preparation of these materials. The apparatus used to conduct the reactions shown above is schematically presented in Figures 97, 98, and 99. A complete description of the method of preparation is described in References 3, 5, and 6. Aluminum borohydride was found to be insensitive to shock from a No. 8 detonating cap in a sand-stemmed Trauzl block, and also insensitive to very rapidly applied pressure. Further details of these tests, and of the results of stability tests with various materials, are given in the previous references. Further work with this material was conducted under Contract N7onr-462, Task Order III, and reported in References 35, 36, and 37.

D. REACTION EXPERIMENTS WITH MOLTEN-LITHIUM-AND-WATER SYSTEM

1. This work was originally begun as a result of calculations showing that the reaction of this fuel yielded a higher energy per pound than most other water-reactive chemicals (lithium has seven times the heat of reaction of NaK alloy). It was planned to use lithium in the hydropulse and the hydroturbojet and considerable data had to be obtained on handling techniques, design of reaction chambers and injectors, and performance of experimental motors.

2. Reaction tests were made with simple rocket motors, one of which is shown in Figure 100. Water was supplied from a pressurized tank through flexible tubing and flow was regulated by a volume-control valve. A Dowtherm heating system was used in the first tests, but was replaced by an all-electric system in the interests of safety and simplicity.

3. Some of the best results of this program are shown in Figure 101. References 3 and 6 provide additional descriptions of this test program. Further work of this type was done on the developmental phases of the hydropulse and the hydroduct, presented in Sections IV and VIII of this report, and under Contract NOrd 9768, References 16 through 21.

E. REACTION EXPERIMENTS WITH SOLID LITHIUM-AND-WATER SYSTEM

1. One of the primary disadvantages of the molten-lithium fuel systems was the need for extensive heating equipment and the time required to raise the temperature of the fuel system to the proper level. In an effort to eliminate this problem and to provide a fuel system that would be immediately available, experiments were conducted with solid-lithium motors. The test motors consisted of a de Laval nozzle and a cylindrical section operated as a conventional rocket motor. Two methods of injection were used. Either the water was injected against solid lithium packed in one end of the reaction chamber, or both propellants were injected, as in a conventional bipropellant motor, except that, in this program, one propellant was a liquid and the other a solid.

2. Some of the motors that were fabricated and tested are described as follows:

a. A "contra-flow" motor is shown in Figure 102. In this motor, the injection water was directed at the lithium face, opposing the flow of the reaction products. The reaction became very unstable as burning progressed down the lithium grain.

b. An "extrusion" motor is shown in Figure 103. Solid lithium was extruded under hydraulic pressure into the reaction chamber, where water was sprayed against it. Stable operation was achieved, but considerable energy was required to extrude the lithium.

c. A "traveling-injector" motor, shown in Figure 104, was tested. In this design, the water was injected into the chamber in the form of a hollow conical spray at the end of a hollow tube. The tube traveled along the center line of the motor through a hole drilled in the lithium. In the motor shown, the injector was rigidly coupled to an actuating piston fitted in a cylinder. One side was pressurized with gas, the other side of the cylinder contained oil which flowed through a flow-control valve and a rotometer. Thus, the injector velocity, and hence, the rate of reaction of the lithium, could be accurately controlled. The movement of the piston operated a cam mechanism which, by means of micro switches and electric valves, turned on the water flow when the injector was at a predetermined point with respect to the face of the solid fuel. Another type of traveling injector motor is shown in Figure 105. These motors operated in a more stable manner than the contra-flow and extrusion motors, but were still subject to fairly wide variations in chamber pressure.

d. A "direct-flow" motor (Figure 106) was tested, in which the solid-lithium charge was in the form of a hollow cylinder. Since the water injector was located at the end opposite the nozzle, the reaction products passed through the hole in the lithium slug into the forward chamber, where considerably more water was added before the gases were expelled through the nozzle. This motor did not operate in a stable manner because the lithium melted rapidly as the hot reaction passed through the hollow lithium grain.

e. The 4% decrease in volume upon solidification of molten lithium precluded casting the lithium into the motor, so that all of these motors were loaded by tamping preformed pieces of lithium into the motor section. Injection of water against an ounce or two of sodium rammed against the lithium face was the most satisfactory method of starting the lithium-and-water reaction.

3. All of the motors tested were fairly small (about 50 lb of thrust), and the auxiliary equipment necessary to obtain moderately stable operation was considered unduly complicated. Development of this type of motor was therefore abandoned. Complete details of the tests and further description of the motors can be found in References 3, 5, and 6.

F. LOW-MELTING-POINT WATER-REACTIVE ALLOYS

1. Using molten lithium as fuel, underwater motors which far surpassed the performance of any previous underwater motors were developed. Unfortunately, the limited availability and high cost of lithium preclude its use where large quantities of fuel are required, as in ship propulsion. Moreover, lithium has a low specific gravity (0.534) which makes it bulky to store, and although its melting point is not so high as to make it impossible to handle, still, if its melting point were lower, the design and maintenance of lithium-fueled motors would be greatly simplified. Consequently a substitute metal-alloy hydrofuel was sought.

The search for a substitute metal-alloy hydrofuel was directed toward two objectives, to discover (1) a suitable hydrofuel which contains little or no lithium, and (2) a hydrofuel which has a lower melting point or a higher energy-density ratio than lithium.

2. The various alloy hydrofuels were prepared by melting the weighed constituents in a pot under a blanket of helium, agitating vigorously to assure uniformity, and then pouring into a split mold to cast a billet 1 in. in dia by 4 to 6 in. in length. The components of the melter are shown in Figure 107.

3. Testing of the hydrofuels was accomplished in the following manner:

a. The various alloy samples were tested in a single-shot hydropulse mounted in a test pit. The duct of the single-shot hydropulse (shown in Figure 108) was identical to that of the regular hydropulse with two exceptions. It had a blind forward end instead of a grid-and-reed valve bank, and it was equipped with a burst diaphragm of 0.005-in.-thick aluminum foil to block off the barrel exit.

b. For testing of the hydrofuels, a sample weighing approximately 5 g was placed in a special impinging-jet injector, which was then secured in place on the transition section in the usual manner. The barrel was completely filled with water through a tube-fitting near the barrel exit. The injector was then heated by means of a torch (not shown in the figure) until its temperature was 30 to 100°F above the melting point of the alloy. When this temperature was reached, the fuel was pressurized to 1500 psi by helium gas and the molten hydrofuel was sprayed into the water in the barrel. The resulting reaction ruptured the diaphragm and expelled the water from the barrel in a manner similar to that experienced in the usual hydropulse. A pressure-time oscillograph record of the reaction, as shown in Figure 109, was obtained for measuring the work done by the fuel. A test using lithium for a fuel is shown in Figure 110, and one using an alloy of magnesium and lithium is shown in Figure 111.

c. In all cases, the following data were recorded:

(1) Alloy composition, percent by weight

(2) Melting point, °F*

(3) Specific gravity

(4) Injection temperature, °F

(5) Injection pressure (always 1500 psi)

(6) Weight of fuel injected, g

(7) Barrel pressure during the explosion (oscillograph recording)

(8) Effect of air on the alloy

(9) Effect of water at room temperature on the alloy

(10) Physical properties, such as hardness, ductility, machinability, etc.

d. Data obtained with lithium as the hydrofuel were used as a standard, and were compared with data from all other fuels tested. A rough qualitative comparison was obtainable immediately by observing how far the water was thrown by the explosion.

4. As the basis for consideration of substitute hydrofuels for lithium, only those metals having a positive heat of reaction with water were considered. In addition, emphasis was placed on the metals that are readily available and low in cost. Therefore, the principal metals considered were aluminum, magnesium, silicon, calcium, manganese, sodium, zinc, and potassium (arranged in order of their decreasing fuel values). Table 5 lists all the metals and their heats of hydrolysis (taken directly from Reference 38).

*The melting point of an alloy was determined by melting a sample in an atmosphere of helium, inserting a thermocouple, and then permitting the alloy to cool slowly while taking readings of temperature vs time. A plateau in the cooling curve was taken as the melting point. The alloy was stirred frequently before it solidified to detect any indications of "mushiness." The melting points reported should be considered as preliminary experimental data because time did not permit the complete verification of the existence of the various alloys indicated by this method.

a. Results of the tests of aluminum-base alloys are summarized in Table 6.

(1) Pure molten aluminum at 1500°F undergoes no reaction when sprayed into water.

(2) Aluminum with a small amount of mercury (less than 9% but exact quantity unknown) reacts when sprayed at 1378°F into water, but the reaction does not occur at an explosive rate.

(3) Alloys high in aluminum content are not as a class freely mobile when molten, and consequently are unsuitable because of injection difficulties. This is true of all alloys containing magnesium, calcium, sodium, or lithium, in which aluminum is the major constituent.

(4) Except for alloys high in lithium, aluminum alloys are hard and brittle. A number of them cracked during cooling, and others shattered like glass when dropped.

b. Results of the tests of magnesium-base alloys are summarized in Table 7.

(1) There is a partial reaction when magnesium at 1500°F is sprayed into water. For complete reaction, magnesium and its alloys require an igniter, such as lithium or sodium.

(2) Sodium alone does not alloy with magnesium or magnesium alloys in sufficient quantity to serve as an igniter. It is therefore necessary to use lithium as the principal igniter. The exact quantity required is not known, but probably is about 10%. In general, the lower the temperature of injection, the greater the quantity of igniter required.

(3) Alloys high in magnesium are soft and ductile as a group. Magnesium alloys containing appreciable quantities of aluminum are hard and brittle until lithium is added.

(4) A number of the magnesium alloys react explosively when sprayed into water, and could be used as fuels. The melting points of all alloys tested, however, were still too high to permit their ready use.

(5) The best magnesium-base alloy tested was one consisting of 1.0 Mg/Zn (one part of magnesium to one part of zinc) to which

was added 12 wt% of lithium. This alloy, with a melting point of 730°F, is only 37% as good as lithium on a weight basis, but is 26% better than lithium on a volume basis.*

c. The results of the tests of calcium-base alloys are summarized in Table 8.

(1) Calcium-aluminum, calcium-magnesium, and calcium-zinc alloys are hard and brittle unless large amounts of lithium are added. The alloys, for the most part, are also viscous when molten.

(2) Calcium-base alloys, like aluminum- and magnesium-base alloys, require lithium as an igniter. Neither sodium nor potassium can be made to alloy in sufficient quantity to be effective. The quantity of lithium required varies, but ranges upwards from 5%.

d. Calcium-magnesium-zinc alloys containing 5% of lithium as an igniter have the lowest melting points of any of the low-lithium-content alloys investigated. A summary of the composition and melting points of these alloys is presented in Table 9. The improvement in the melting point was obtained at the expense of substituting low-fuel-value zinc for high-fuel-value magnesium and calcium. While no tests were made, it is certain that the high-zinc fuel will have a much poorer performance than the low-zinc alloy No. 28. Because 470° is still too high a melting point to permit the use of this alloy in existing equipment, a really satisfactory substitute for lithium still remains to be found.

e. The results of the tests of the lithium-calcium alloys are summarized in Table 10.

(1) Calcium, up to a concentration of 50%, lowers the melting point of lithium appreciably, as shown in Table 10 and Figure 112.

---

*It should be noted that all references to the comparison of the performance of a hydrofuel are based upon the test method using the single-shot hydropulse. In the hydropulse, thrust is obtained by the expansion of the gas generated pushing a slug of water out the tailpipe. It is important that a sufficient amount of gas be generated by the reaction, and it is advantageous for the heat of the reaction to be used to expand the gas bubble rather than to heat the slug of water. Subsequent tests made under Contract NOrd 12650 of some of the metal-alloy hydrofuels in a typical rocket-thrust motor showed that these hydrofuels do not perform as well as lithium on either a weight or volume basis. This is explained by the fact that performance of the thrust motor is a function of the total heat released by the reaction rather than any particular partition of the energy released.

(2) Lithium-calcium alloys, at the low injection temperatures permissible with their use, require the addition of sodium as an igniter (potassium does not alloy). The minimum quantity of sodium required was not determined, but was approximately 5%.

(3) The addition of sodium to lithium-calcium alloys lowers the melting point. As an example, an alloy of $\frac{1.5}{1}\frac{Li}{Ca}$ has a melting point of 295°F. With the addition of 5% of sodium, the melting point is reduced to 285°F. Approximately 5% sodium is the maximum that will alloy.

(4) Zinc added to the lithium-calcium-sodium alloy lowers the melting point still further, but reduces the performance of the fuel.

(5) The addition of magnesium to lithium-calcium-sodium alloy raises the melting point.

(6) The addition of 5% of silicon to the alloy has no effect on its melting point; the addition of larger quantities produces an increase in the melting point.

(7) The best lithium-calcium-sodium alloy produced consists of $\frac{1.5}{1}\frac{Li}{Ca}$ + 5% sodium + 10% aluminum. It has a melting point of 286°F, which is 73°F below the melting point of lithium. On a weight basis it is only 87% as good as lithium, but is 30% better on a volume basis.

f. The results of the tests of the lithium-aluminum alloys are summarized in Table 11.

(1) Aluminum is a desirable alloying agent because it greatly increases the energy per unit volume of a fuel. When added to lithium, however, it increases the melting point considerably.

(2) The addition of sodium to lithium-aluminum alloys, as reported by the Naval Ordnance Test Station in Pasadena, lowers the melting point of the alloy to approximately that of lithium. The resulting alloys, however, are mushy when molten and are not suitable for injection.

(3) The addition of silicon to the lithium-aluminum-sodium alloy results in no improvement.

(4) The addition of 10% of calcium lowers the melting point and produces an alloy which melts sharply to a mobile fluid.

(5) The addition of calcium and silicon raised the melting point materially.

(6) The best lithium-aluminum alloy produced consists of $\frac{4.0}{1}\frac{Li}{Al}$ + 7% sodium + 10% calcium; it melts at 343°F, is 20% better than lithium on a weight basis, and 55% better on a volume basis.

g. The results of the tests of the lithium-silicon alloys are summarized in Table 12.

(1) At least 10% of silicon can be alloyed with lithium without producing the slightest effect on the melting point of the lithium.

(2) The performance of silicon alloys is slightly better than that of lithium on a volume basis, and about the same as lithium on a weight basis.

h. It was found that the addition of either calcium, strontium, or barium to the lithium lowered the melting point of lithium markedly. The melting-point curves of lithium-calcium, lithium-strontium, and lithium-barium alloys are shown in Figures 112, 113, and 114. Lithium-calcium and lithium-barium alloys have definite melting points, whereas many of the lithium-strontium alloys melt over a wide temperature range. Calcium, strontium, and barium, when added in combination to lithium, produced alloys having lower melting points than when they were added singly. Table 13 gives the data for the ternary alloy of lithium-calcium-strontium, and Table 14 the data for the ternary alloy of lithium-calcium-barium. The alloy with the lowest melting point (51% Li, 7% Ca, 42% Ba) was tested in the single-shot hydropulse. Injected at 276°F, its performance was equal to that of lithium on a weight basis, and 66% better on a volume basis.

i. In the hope of lowering the melting point still further the quaternary alloys of lithium-calcium-strontium-barium were studied. These data are summarized in Table 15. Additional discussion of the results of these alloy investigations can be found in References 39 through 42.

5. Because of the lack of phase diagrams for most of the metals considered, considerable work was done on obtaining this fundamental information. Alloys were made and enough data taken to determine the general melting-point curves of the following metals.

a. Lithium-Zinc (Figure 115)

b. Magnesium-Strontium (Figure 116)

c. Magnesium-Barium (Figure 117)

d. Aluminum-Strontium (Figure 118)

e. Aluminum-Barium (Figure 119)

f. Strontium-Calcium (Figure 120)

g. Barium-Calcium (Figure 121)

h. Zinc-Strontium (Figure 122)

i. Zinc-Barium (Figure 123)

6. In addition to the various stainless steels, nickel steels, and 4130 steel commonly used for construction where the handling of lithium is involved, the following materials have been found to be satisfactory for this purpose: soft nickel; Haynes Stellite Star J; Haynes Stellite 31; Inconel X; Hastelloy grades B and C; Colmonoy No. 6, Norbide (boron carbide); Kennametal, Grades K-6, K-3H, K-136, and K-151-A; molybdenum; titanium; and beryllium. The composition of these materials is shown in Table 16. Vanadium and aluminum oxide (in the form of sapphire) also resist lithium, but have not been used as materials of construction. Nitrided Nitralloy is not resistant to lithium.

7. Further development of hydrofuels was conducted under Contract NOrd 12650, and reported in Reference 15. Particular emphasis was placed on the lithium-calcium-barium and lithium-calcium-barium-zinc alloys.

G. INSTANTANEOUS LITHIUM MELTING

1. Because lithium and most metal hydrofuels are solids at normal temperatures, and liquids are required for convenient fuel injection in motors; the problem was to melt the hydrofuel simply and rapidly. Three methods of melting lithium by chemical heat were considered and are shown schematically in Figure 124.

2. To confirm published data, the heat of fusion of pure lithium was experimentally determined and found to be 100 ± 5 cal/g. Using accepted values of specific heats, and assuming an initial temperature of 80°F and a final temperature of 450°F (90°F above the melting point), the total heat required to melt lithium is 324 Btu/lb.

3. The initial experimental work on this program was reported in Reference 42. Subsequent work was conducted under Contract NOrd 12650 and reported in Reference 15. The method utilizing a dispersed, powdered oxidizer, thoroughly mixed with powdered lithium and then compressed into a solid body, and the method of utilizing Alclo charges placed in a solid block of lithium, were abandoned in favor of a sealed-tube melting system. In this system, the chemicals which produce heat by a Thermitic type of reaction are confined in a sealed steel tube around which the lithium is cast. The lithium is therefore free of contamination.

4. Two compositions for use in the sealed, steel heating tubes were developed. One composition consisted of 37.4% commercial Thermit, 6.5% Dixie clay, 10.4% No. 120 atomized aluminum, and 45.7% 200-mesh black copper oxide. The other consisted of 2.8% potassium perchlorate, 12.3% Dixie clay, 17.0% No. 120 atomized aluminum, and 67.9% 200-mesh black copper oxide. All the ingredients were dried, mixed, and pressed in 3/4-in.-dia steel tubes at a pressure of 67,000 psi.

a. The first composition melted 3.5 lb of lithium in 40 sec, at the end of which time the lithium was utilized in a rocket thrust chamber. This composition could be burned only in a vertical position.

b. The second composition melted 3.5 lb of lithium in 50 sec, but, because of the horizontal position of the heating tubes, lithium was available for the rocket thrust chamber after only 10 sec.

X. ALCLO DEVELOPMENT PROGRAM

A. ALCLO STUDIES

1. Introduction

a. A compressed mixture of potassium perchlorate and powdered aluminum known as Alclo was investigated as a propellant for underwater missiles. When the Alclo-powder mixture is compressed under pressures of 40,000 psi and greater, it bonds together, and when ignited, will sustain controlled surface burning. It reacts according to the equation

$$8Al + 3KClO_4 \longrightarrow \underset{\text{(solid)}}{4Al_2O_3} + \underset{\text{(solid)}}{3KCl} + 2.49\ \frac{kcal}{g}\ \text{of propellant}$$

Alclo is very desirable for underwater applications because of its high energy-density (high energy per unit volume), and because it produces no gaseous products of combustion. Thus, the use of Alclo makes possible high-speed, depth-insensitive missiles which will leave no telltale gaseous wake.

b. Development work centered around adapting Alclo propellant for the propulsion of hydroduct and hydroductor-powered missiles. Its use in the hydroduct is as depicted in Figure 76. The compacted propellant was contained in a cartridge during early development work, and ignition was accomplished by means of an electric squib. The cartridge not only provided for ease of storing, handling, and loading, but also restricted the burning of the propellant to the end face of the grain. Later it was found desirable to restrict the grain with a glass fabric and polyester resin. Water under ram pressure is sprayed into the reaction chamber in such quantity as is required to produce wet steam. The pressure of the steam is maintained at approximately 250 psi by means of a supersonic exhaust nozzle.

c. When it was demonstrated that 87% Alclo + 13% lead was a stable-burning and usable propellant, design studies were made on several Alclo-powered propulsion systems. The desirability of fitting the propellant burning characteristics to the missile rather than making compromises in the hydrodynamic design was apparent. Therefore, considerable effort was expended to obtain Alclo-additive mixtures with a variety of burning rate-vs-pressure characteristics, with particular emphasis on increasing the range to much higher burning rates.

d. In order to design and develop Alclo-fueled steam generators, it was necessary to determine other burning characteristics; such as the effect of grain temperature or the burning rate, the effect of the material used as a restriction, the effect of age, high-temperature storage, moisture, thermal shock, and mechanical shock on the performance of the propellant. Considerable work was done to determine the effect on the burning rate caused by variations in the ingredients due to specification tolerances.

e. Many of the physical properties of Alclo were measured. Considerable work was done on improving the methods of preparation of Alclo grains in order to obtain acceptable physical characteristics for the propellant.

f. Efforts were made to improve the energy-density of Alclo, through the use of aluminum-rich mixtures, and tests were made using small-scale, Alclo-fueled steam generators to check the theoretical calculations.

g. Considerable attention was directed toward evaluating the hazards associated with the preparation, handling, and ultimate use of Alclo. Many of the explosive and sensitivity characteristics were determined.

2. <u>Burning Characteristics</u>

a. Burning Rate vs Pressure for Various Mixtures

(1) Design calculations for the hydroduct and hydroductor showed, theoretically, the burning rate which would be required

at the design operating pressure to give the desired mass flow of propellant. Work was therefore directed toward establishing the burning rate-vs-pressure characteristics of Alclo.

(2) Burning-rate tests were made by burning slender charges or strands (suitably restricted) in a Crawford bomb and later in vertical steam generators. These procedures are described in Reference 39. Burning rates were also checked in runs with the standard hydroduct test motors.

(3) The test results were plotted on logarithmic graph paper, making it possible to derive a numerical equation for the relationship of burning rate vs pressure. For restricted burning with a given propellant combination, the burning rate can be approximated by the following empirical relation

$$r = Cp^n$$

The burning rate (or velocity of propellant consumption) is designated by r (in./sec), the chamber pressure is p (psia), and C and n are constants. For most restricted burning propellants, n has values between 0.4 and 0.85. The constant C varies with the initial propellant temperature.

(4) In the burning-rate-vs-pressure equation ($r = Cp^n$), the value of exponent n is an indicator of the stability of burning to be expected from the particular mixture. Values of 1.0 and greater indicate complete instability while a value of 0 shows that the burning rate is completely insensitive to pressure. Propellants whose exponent lies between 0 and 0.8 are considered suitable for use in gas generators. A very important fact was revealed by the initial burning-rate tests on stoichiometric Alclo which showed that, up to 100 psia, n has a value of 0.27, and burning is very stable; but above 100 psia, n increases to 1.08 and therefore the burning is unstable.

(5) Because it was suspected that the burning-rate instability was being caused by breaking up of the propellant during burning, additives were used which promoted better bonding, thereby increasing the mechanical strength of the propellant. The characteristics of the additives which make them suitable for this use are, the ability to become plastic under the 80,000-psi forming pressure, and flow into any small remaining voids, and to form no noncondensable gases.

(6) A total of 40 different additives or combinations of additives was investigated. The mixtures which are considered suitable for use in combustion chambers are presented in Table 17. In order to quickly present an idea of the magnitude of the burning rates involved, the burning rate at 150 psia is also shown for each mixture. Values for stoichiometric Alclo are included in the table for purposes of comparison.

(7) The Alclo mixture containing 12.8% powdered lead was chosen as the most suitable for hydroduct application, not only because it gave adequate heat-release rates, but because there was no loss of energy-density value due to the addition of the lead. This was called the "standard" mixture. A plot of burning rate vs pressure for this propellant is included as Figure 125.

(8) The tests of additives which were performed were not designed primarily for studying the effects of combination of additives; therefore conclusive data are lacking. However, if interpolation and extrapolation of the data can be permitted when direct comparisons are not available, some useful summaries can be made. In several cases, it has been noticed that when two additives are used, the combined effect favors the additive which causes the greatest burning rate. Examples of this are shown in the lead-and-carbon black, and the lead-and-nickel oxide mixtures. One exception was seen in some less reliable data on the lead-graphite combination. Here the lower-burning-rate inducing graphite was favored. When two additives of approximately equal effectiveness are used, the combined effect is approximately equal to either one used alone. Examples of this are the lead-and-ferric oxide, and lead-and-ammonium dichromate systems. There are indications that in some combinations, the rate-pressure slope of one additive will be dominant. This has been noticed, particularly in combinations containing ferric oxide. Alclo with ferric oxide additive alone has a rate-pressure slope of 0.34. Two different proportions of Alclo, lead, and ferric oxide have slopes of 0.33 and 0.39, respectively. Thus, it is suggested that certain additives might be used to produce a rate-pressure curve of nearly constant slope regardless of the other additives which might be present. In four cases it was possible to compare varying amounts of a single additive. In all cases, the greater the percentage of additive used, the greater the resultant effect. The usual maximum percentage tried was 10%. With lead, however, as much as 30% was used.

(9) Additional details concerning the use of additives can be found in References 39, 41, 42, 43, 44, and 45.

b. Burning Rate vs Propellant Temperature

(1) The effect of propellant temperature on the burning rate was investigated. The samples used for these tests were 3/4-in.-dia copper-jacketed charges fitted with a Thermit-electric igniter. Each sample was equipped with two thermocouples, one on the copper jacket and the other in the propellant. Each sample was wound with a helical coil of Nichrome wire for heating. In the tests, the temperature of the sample was brought up slowly, held at the desired value for 2 min to insure equilibrium conditions, and then ignited at atmospheric pressure. Timing was done manually.

(2) In the range of temperatures from -10 to +350°F the effect of temperature on the burning rate was found to be very slight; less than a 2.5% increase in rate per 100°F increase in temperature. However, as the decomposition temperature of the $KClO_4$ is approached (750°F), the rate of burning is greatly affected (approximately 10% per 100°F).

(3) The vertical steam generator was used to make additional temperature-sensitivity tests in order that the sensitivity could be measured over a range of pressures at any given temperature between the freezing point and the boiling point of water. Runs were made at two temperature conditions, +32 and +212°F. For the cold runs, the entire chamber was packed in ice, and ice water was contained in the chamber. The propellant was conditioned in this manner for 5 min before firing. For the hot runs, a torch was played on the chamber until the water boiled. The propellant was conditioned for 7 min at this temperature before firing. These tests showed that in the range of temperature from +32 to +212°F, the effect of temperature on the burning rate of Alclo is negligible. These results corroborate the conclusions reached in the above.

(4) Further details can be found in References 41, 42, and 43.

c. Burning Rate vs Particle Size and Shape

(1) In order to test the effect of particle size of the oxidizer on the burning rate, tests were made on a mixture of standard proportions (31.4% Al, 55.8% $KClO_4$, 12.8% Pb), in which the average particle size of the $KClO_4$ was 7 microns instead of the standard 43. The burning rate proved to be almost identical with that of the standard mixture throughout the pressure range investigated (15 to 300 psia).

(2) To test the effect of various grades of aluminum on the burning characteristics of Alclo, four other grades of Alcoa aluminum powder were selected. Their descriptions are tabulated below, together with data for Grade 606, which is used in the standard Alclo grains:

Alcoa No.	Mesh Designation and Type	Data on Av. Mesh Size	Grease, %	Atmospheric Burning Rate in./sec
606	100-mesh unpolished-flake powder (low grease)	90% through 325 mesh	0.5	0.52
408	325-mesh polished-flake powder	98.5% min through 325 mesh	3.06	0.43
422	400-mesh polished flake powder	100% through 325 mesh 98% through 400 mesh	4.03	0.56
522	325-mesh polished-flake powder (low grease)	97% through 325 mesh; less than 0.2% on 100 mesh	0.76	0.63
101	100-mesh granular powder	80% through 325		0.052

Using the standard formulation (31.4% Al, 55.8% $KClO_4$, 12.8% Pb), the burning rates were checked at atmospheric pressure. From the data obtained, it appears that the burning rate increases not only with a decreasing particle size of the aluminum, but with decreasing grease content. Although the particle-size description of the atomized aluminum does not differ greatly from that of the flake aluminum, replacing the flake with the atomized aluminum reduces the burning rate by a factor of 10.

(3) Alclo mixtures containing Grade No. 552 and 101 aluminum indicated promise, and burning rates for these two mixtures were determined over a wide range of pressures. These data, together with that for the standard mixture, are presented as Figure 126.

(4) Using the standard formulation, as in the above tests, mixtures were made and tested in which the aluminum content was comprised of No. 606 and 552 in varying proportions, from 100% of one to 100% of the other. Similar tests were made on propellant grains containing mixtures of No. 606 and 101 aluminum. In both instances, a plot of the data showed that the resulting burning rate at any pressure varied linearly with the proportion of each type of aluminum (between the extremes). Thus, it can be seen that the burning rate of Alclo at any given pressure can be varied throughout the range indicated in Figure 126, solely by varying the proportions of the grades of aluminum in the mixture.

(5) The particle-size distribution of five batches of lead powder which varied widely were measured using the Micromerograph. Alclo grains were formulated using these different batches, holding all other factors essentially constant. The burning rates obtained with each were compared with the "standard" burning rate vs pressure curve in order to obtain a relative performance factor. A plot of geometric mean particle size of lead vs the performance factor is shown in Figure 127. Performance factor is defined as the ratio of the burning rate using the standard 6-micron lead powder to the burning rate of the mixture in question, all at atmospheric pressure. It is seen that variation of the particle-size distribution of the lead powder is an effective way of adjusting the burning rate of Alclo within the limits indicated.

(6) The burning rate is affected by the particle shape as well as by the particle size; that is, the specific surface (surface area/volume) of the constituents is usually the controlling factor. Further details and analyses concerning the effect of particle size and shape on the burning rate of Alclo can be found in References 13, 42, 44, and 45.

d. Burning Rate vs Propellant Density

Figure 128 is a plot of the burning rate, and specific gravity vs forming pressure. From these, the weight rate of burning (g/sec) was calculated and plotted. It is evident that the burning rate of Alclo decreases with increasing density. It is evident that in order to obtain a uniform rate of burning, it is necessary to have a uniform specific gravity throughout the grain. It is practically impossible to form an absolutely uniformly compacted grain because of the friction between the die wall and the powder during the pressing operation. Therefore, there will always be a density gradient in the compact, since it is more dense at the top or plunger end and less dense at the bottom (see paragraphs X,A,3,a and X,A,4,a,(4) for additional information). The greater the length-to-diameter ratio (L/D) of the compact, the greater the difference in densities from end to end. The density gradient will be less as the diameter of the compact is increased (with constant L/D), because the ratio of die-wall area to propellant-face area (S/A_p) is inversely proportional to the diameter. Therefore, for the greatest uniformity the compact should be short in length and large in diameter.

e. The Effect of Storage and Environment

(1) It was considered important to determine the effect of storage conditions on the performance of a propellant. Therefore, a series of tests was inaugurated to study the effect of long-term storage, as well as the effect of temperature shock, on Alclo.

(2) Stored grains were tested using a standard hydroduct test motor and standard running conditions. Their performance was compared to data obtained in the original control tests for the same batches of Alclo. The burning rate-vs-pressure characteristic of the propellant was used as the primary indicator of performance, while the specific impulse, being a less sensitive indicator, was secondary.

(3) An Alclo propellant grain which had been stored at ambient temperature (40 to 90°F) for a period of 16 months was tested. The specific impulse obtained was 329 lb-sec/lb, which may be compared to control values of 319 and 349. The burning rate obtained for the stored grain was 3% higher than the average for the control runs. This is considered to be within the experimental error of the control tests. It was concluded that storage for a period of 16 months at normal temperatures causes little or no deterioration of Alclo propellant.

(4) Three hydroduct propellant grains were stored at a temperature of 180°F for 59 days. Tests made in the standard combustion chamber showed that the performance (specific impulse and burning rate) of these grains was normal, and showed no signs of deterioration as the result of the long storage at high temperature. The equivalent age at 80°F of these grains, calculated on the assumption that a rise in temperature of 10°C doubles the speed of a chemical change, was 7.28 years.

(5) Two grains which had been stored at a temperature of 180°F for 9-1/2 months were tested, as above; both grains proved to be normal with respect to specific impulse, but the burning rates had suffered a 7% decrease due to the storage. The equivalent age at 80°F of these grains was calculated (using the above assumption) to be 36 years. Assuming that this method of comparing storage time is fairly reliable, the effect of normal storage would be to decrease the burning rate by only 0.2% per year.

(6) An Alclo propellant grain which had been stored at 180°F for a period of 15 months was tested, as above; the specific impulse was 335, which is considered normal. The burning rate with this grain was 12% less than that obtained in the control tests. The equivalent 80°F storage effect for this grain was calculated to be 0.21% per year, which is in good agreement with the above rate for 9-1/2 months.

(7) A series of tests was conducted to study the effect of temperature shock on standard 3.75-in.-dia Alclo grains. For these tests, six grains (three pairs) were selected and provided with hydroduct missile-type baseplates and standard igniters. One of each pair was left in normal storage and the remaining three grains were put through a temperature-cycling program in which they were changed alternately from a cold box (-10°F) to a hot box (+140°F) every 24 hr, until five complete cycles

were made. The six grains were tested in a standard combustion chamber, and the data for the temperature-cycled grains were compared with those of corresponding grains which remained in normal storage. The performance of the temperature-cycled grains was normal in every respect; there were no indications of any adverse characteristics in burning or performance.

(8) For details of these and other environmental tests, see References 12, 13, 39, 42, 44, and 45.

3. Preparation of Alclo Propellant Grains

a. Compaction Techniques

(1) Consideration was given to the problem of getting the Alclo into a proper form for use; it would be quite desirable to have it castable. This could be done by the addition of a suitable binder (sodium silicate is one), but like the loose powder, the result is of too low a specific gravity to be of practical use where space is at a premium. It was found by experiment that when the mixture was compacted at pressures of 40,000 psi and greater, it bonded together to form a solid.

(2) A 20-ton-capacity hydraulic press was designed and built to compact 3/4-in.-dia jacketed grains for propellant-development work. This press features remote control to eliminate all operational hazards. Ample "daylight-opening" (distance between platen and bed) and stroke was provided to enable the compaction of a 6.25-in.-long grain with a permanently mounted plunger of given length. Figure 129 shows the press with a charge of powder in the die cavity ready to begin a press. Figure 130 shows the 4-split die and die holder with the two end caps.

(3) A 400-ton capacity hydraulic press was designed and built to compact Alclo grains in sizes up to 4.75-in.-diameter. Extensive planning was done on the 400-ton press design to eliminate all hazards in its operation. The press features a hydraulic-operated, remotely controlled system for the insertion of the plungers. With this system, the operator pours the propellant mixture into the cavity and then leaves the building. The remainder of the pressing operation is completed by remote control before he again enters the building to pour in more powder. Figure 131 shows a view of the press with a plunger being inserted. The control panel is shown in Figure 132. A detailed description of the remote operation of the 400-ton press can be found in Reference 41.

(4) When propellant grains were to be compacted, it was found necessary to obtain the desired length by successive compactions of incremental amounts of powder. The length of each increment varied from about two diameters on the 3/4-in.-dia size to about 0.37 diameters on the 3.75-in.-dia size. This type of compaction presented no problems when the

metal jacketed grains, such as the 3/4-in.-dia and the 2-in.-dia, were being made. The interfaces in the 3.75-in.-dia grains were made sound by a flat serrated plunger end which approximated a RMS microinch roughness number of 500. The interface integrity was even more improved by allowing the grain to remain confined in the split dies for several hours after pressing and before removal. This also produced a smoother performing grain.

(5) The 3/4, 2, and 3-in.-dia grains were compacted with a forming pressure of 80,000 psi. The forming pressure was reduced to 45,000 psi on the 3.75-in.-dia grains without any appreciable change in density. This can be explained by the fact that as the ratio of length-to-diameter of the compact was decreased, and as the pressing area was increased with relation to the length of the compact, the die wall exerted correspondingly less friction, which allowed a higher net force on the compact.

(6) The compaction of Alclo powder does not follow the law of hydrostatics, that is to say, the density of an incremental compact is not uniform throughout. Theoretically a density maximum exists in the upper portion of the cylindrical compact near the die wall, while in the lower portion a zone at maximum density exists in the center. The latter, however, is usually considerably less marked than the density maxima next to the plunger. This subject is dealt with further in paragraph X,A,4,a,(4) of this report, and in Reference 42.

(7) High-quality compacting is difficult to obtain when using flake powder (as shown below), but it was found that the flake aluminum was the only grade that would produce the desired high burning rate. The following are the conditions that had to be met:

(a) Flake-type powder has a low apparent density, containing approximately 4 parts air to 1 part of powder by volume. The compaction must be done slowly to allow all the air to escape from the die fill. In order to minimize the possibility of entrapping air, the pressing procedure was as follows:

Close	3-1/2 min
Dwell	1 min at 20,000 psi
Dwell	3 min at 45,000 psi
Decompression	0.1 min from 45,000 to 0 psi

(b) The flake-type aluminum powder is very hard, being cold worked in a ball mill from the atomized condition. This decreases the plastic deformability of the powder and makes it necessary to use higher forming pressures.

(c) Die fill is a critical problem because of relatively high interparticle friction displayed by this powder, which has an immense surface-to-surface contact area. This condition resists mutual sliding and rotation of the particles in the powder mass as the compaction load is applied. It was therefore found necessary to exercise extreme care in making an even die fill.

(d) Aluminum powder has a high adhesive affinity for iron surfaces. This caused excessive cold-welding of the powder to the die wall during compression, which increased die-wall friction considerably. To minimize this effect, a molybdenum disulfide grease was rubbed into the die walls. Grains of more uniform density resulted.

(8) Figure 133 is a view of a portion of the room for the 400-ton press. The split die is shown with one section removed, revealing the completed Alclo grain. The six incremental pressings can be seen.

b. Application of Restriction, Base Plate, and Igniter

(1) After compaction it was necessary to prepare the Alclo grain for the desired end-burning characteristics, for mounting in the hydroduct or hydroductor missile, to impart the mechanical strength to the grain to withstand launching accelerations, and to provide a suitable igniter.

(2) A 3-layer laminate of glass tape and Selectron resin was applied to the grains to form the restriction. Reinforcing wires anchored at one end to the base plate were placed between the laminations (see Figure 134). This bound the grain assembly into a unit of suitably high strength, and provided the necessary means for attaching it to the test missile.

(3) The igniter assembly consisted of an aluminum cup closed at the open end by 1/8-in.-mesh screen and moisture-resistant paper. A plastic bubble surrounded the aluminum cup to help direct the ignition flame at the face of the grain, and to provide a moisture seal for the grain. This complete assembly is shown in Figure 90. Four of the grain support wires were extended in length above the grain face. These were then formed to hold the igniter container in place. During most of the development period, this igniter assembly contained a DuPont S-67 squib, 1 g of loose (not compacted) Alclo powder, and eight "aspirin-size" Alclo pellets. More recently, a DuPont S-75 squib, 1 g of "Starting Thermit," and eight Alclo pellets have been used.

(4) A completed grain (with injector baseplate, restriction, and igniter) ready for testing in the Alclo hydroduct motor is shown in Figure 135. Additional information concerning Alclo grain processing can be found in References 46 and 47.

c. Quality Control

(1) In order to eliminate propellant variation as a source of non-uniformity in motor tests, it was found necessary to impose rigid controls on the quality of the ingredients which went into the propellant, and to standardize and control the various handling and processing techniques. This subject is treated in References 13, 45, and 46.

(2) Quality Control of the Aluminum Powder

(a) The aluminum powder used was manufactured by the Aluminum Co. of America, and has the following catalogue description:

Grade and Classification	Mesh Designation and Type	Average Mesh-Size Data	Average Leafing Value	Remarks
Standard unpolished No. 606	100 mesh unpolished powder (low grease)	Less than 0.2% on 100 mesh, 90% through 325 mesh	Non-leafing	For pyrotechnics, and as a chemical reagent where a powder of high purity and low grease is required.

(b) A material specification (AMS C-88a) was written which established the minimum standards for purchase of the aluminum powder used in Alclo. In general, it conforms to the Joint Army-Navy Specification, JAN-A-289, for Type A, Class A powders. In addition, certain other requirements are listed.

(c) Each shipment must be accompanied by a certified copy of its physical analysis and chemical composition. A typical report reads as follows.

Physical Analysis

Through 100-mesh sieve	99.8%
Through 325-mesh sieve	82.0%

Chemical Composition

Material volatile at 105°C	0.5%
Oil and grease	1.5%
Iron	0.6%
Other metals	0.2%
Oxide	3.0%
Free metallic aluminum (by difference)	94.2%

(3) Quality Control of the Lead Powder

(a) The lead powder used was manufactured by Western Lead Products Company, Los Angeles, California.

(b) A material specification (AMS C-131a) was written which established the minimum standards for purchase of the lead powder used in Alclo. Each shipment must conform to the following properties:

> The lead powder shall have been manufactured from lead metal containing not less than 99.9% metallic lead.
>
> Other metallic impurities shall not exceed 1.0%
>
> Grit and other extraneous materials shall not exceed 1.0%
>
> Particle size distribution shall be obtained using a micromerograph Analyzer and shall be 50 wt% less than 20 microns.

(4) Quality Control of Potassium Perchlorate

(a) The potassium perchlorate was obtained from the Western Electrochemical Corporation in the crystalline form, in accordance with Aerojet Material Specification AMS-Cld, and is 99.5 ± 0.5% pure. This material was ground at Aerojet in accordance with Specification APS-C 1.45, to obtain uniformity of particle size as listed below:

Through 200-mesh	94 ± 4%
Through 250-mesh	91 ± 5%
Through 270-mesh	89 ± 5%
Through 325-mesh	78 ± 7%

The potassium perchlorate used in Alclo propellant was identical with that used in the production batches of asphalt-base and resin-base propellants at Aerojet.

(b) The potassium perchlorate was stored under humidity-controlled conditions, and discarded if not used within a certain specified time.

(5) Accuracy of Formulation

All constituents were weighed on a torsion balance. Weights were accurate to within ± 0.05%.

(6) Blending of Propellant Powder

(a) A double-cylinder blender was used which divides and screens the powder once each revolution. One half-hour was established as a standard mixing time.

(b) The powder was packaged from the double-cylinder blender by remote control.

(7) Process Control

(a) Desiccants and air-tight containers were used where there was a possibility of absorption of moisture by the raw materials, the mixed powder, or the completed grains.

(b) After the restriction was applied to the cylindrical surface of the grain, the exposed ends were coated with a film of strippable lacquer to protect the propellant from moisture while in temporary storage awaiting further processing and use.

(8) Batch-Testing

(a) As an overall control on the uniformity of the propellant, the practice of testing a certain percentage of the grains being produced was initiated. This testing was done in a standard hydroduct test motor in the static-test pit. The performance (specific impulse and burning rate) of the propellant was compared with that of the accepted standard. This provided a continuous check on the quality of the propellant being produced.

(b) An additional check was made on the grains used in range tests of a free-running missile. A grain made from the same batch was tested in the standard missile test motor in the static-test pit, and the performance was checked as above.

4. Physical Properties of Alclo

A summary of the important properties of Alclo are presented in Table 18.

a. Mechanical Strength

(1) An independent metals-testing laboratory made shear and compression tests on Alclo. For the shear tests the samples were

loaded in double shear with the line of shear perpendicular to the axis of pressing. (This is the direction of least strength for Alclo.) The results are as follows:

Mixture	Shear Strength, psi
87% Alclo and 13% lead	122
Stoichicmetric Alclo	74

(2) In the compression tests, the samples were loaded in the axial direction. The results are as follows:

Mixture	Compressive Strength, psi
Stoichiometric Alclo	4650
87% Alclo and 13% lead	5530

(3) The shape of the particles has a great influence on the strength of the resulting compact. Flakes, such as the aluminum used in Alclo, are poor from the standpoint of powder metallurgy, as described previously. Several Alclo mixtures were made and tested which contained atomized aluminum, and it was clearly evident that the physical strength of the compact was an improvement over that exhibited by standard Alclo.

(4) The hardness vs forming pressure was mentioned previously in paragraph X,A,2,d. The strength increases with increasing hardness. Hardness tests were made on several different sizes of propellant grains, and the hardness number was correlated with the specific gravity and burning rate. The Alclo grains were sawed in half longitudinally, set in plaster of paris, sanded smooth, and tested on a Rockwell superficial hardness tester. Enough hardness measurements were made over the face of each sample to permit a construction of lines of equal hardness (or density). One such "contour map" is shown in Figure 136 (the asymetry of which, incidentally, reflects an uneven die fill). The average hardness across the plane at several sections was calculated (giving consideration to the area represented by each point) and plotted along the length of the grain. The hardness distribution is greatly affected by the shape of the plunger end. A more complete report on this work is included in Reference 42.

(5) Work was done to determine the ability of an Alclo grain to resist the strains imparted during the rapid acceleration encountered during the booster phase of the free-running missiles. In the complete grain assembly, the restriction, with its steel reinforcing wires, is designed to assume nearly all of this load. Although the acceleration during the booster phase of the missile is 60 g, to check the safety factor two Alclo grains were accelerated to 300 g, the limit of the available test equipment. Actually, the program consisted of imposing an instantaneous peak

acceleration of 300 g, twice, then 10 successive peaks of 150 g on each grain. They were then inspected for apparent failures, and tested in the standard test motor. Both of these grains performed normally in every respect.

b. Thermal Conductivity

The thermal conductivity of Alclo was measured and found to be 3.7 Btu/hr ft^2 -(°F/ft), or less than one-half that for stainless steel.

c. Coefficient of Thermal Expansion

(1) The coefficient of thermal expansion of Alclo was measured. The expansion was found to be greater in the direction of the pressing of the sample than in a direction normal to the pressing. It was also noticed that Alclo + 13% lead has a greater expansion coefficient than the stoichiometric mixture of Alclo.

(2) These results, along with the coefficients for steel, aluminum, and copper are shown below.

Material		Temp Range, °F	Linear Expansion per Unit Length per °F
Stoichiometric Alclo	(axially)	60 - 400	5.85×10^{-5}
	(radially)	60 - 400	2.75×10^{-5}
87% Alclo + 13% Pb	(axially)	60 - 400	8.45×10^{-5}
	(radially)	60 - 400	3.15×10^{-5}
Steel		-	0.63×10^{-5}
Aluminum		-	1.24×10^{-5}
Copper		-	0.89×10^{-5}

d. Electrical Resistivity

The resistivity of a sample of Alclo was measured. Measured values varied over wide ranges, as is common with materials of this type. A value of 720×10^{-6} ohms/cir-mil-ft was taken to be the average electrical resistivity of Alclo.

e. Porosity Tests

Porosity tests of Alclo showed that the standard lead-containing mixture was less than one-third as porous as stoichiometric Alclo. In these tests helium gas was forced through compressed cylindrical samples in an axial direction, and the volume of gas passed in a given time was measured. A coefficient which is a measure of porosity to gas flow was computed. The samples were contained in copper jackets so that losses resulting from radial flow of the helium would be eliminated. The results are as follows:

Mixture	Porosity, $\frac{in.^3}{hr\text{-}in.^2 (\Delta P/in.)}$
Stoichiometric Alclo	0.0286
87% Alclo and 13% lead	0.0086

f. Flame Temperature

The theoretical flame temperature for Alclo was calculated to be 7150°F, using thermochemical data. No actual measurements of flame temperature were made, but bomb-calorimeter tests substantiated the theoretical heat of reaction of 2.17 kcal/g for the Alclo + 13% lead mixture.

5. Hazard Evaluation

It is well recognized that mixed powders of fuels and oxidizers such as aluminum and potassium perchlorate must be handled with care. When this mixture is loose before compaction, it may be ignited by a spark or a static charge of the magnitude that might be stored in the human body. It was therefore standard practice for personnel working with such mixtures to wear conductive safety shoes. The benches, floors, machinery, and other equipment were all connected to a common ground by means of an electrical conductor. Operations involving impact or friction were avoided where possible, and efforts were made to conduct all mechanical operations by remote control. A series of tests was made to determine the hazards involved in the handling and use of Alclo as a propellant. With the limited time and equipment available, as many of the standard Bureau of Mines tests as possible were made. Other tests of a more informal nature were performed for the purpose of providing first-hand knowledge to interested personnel of the "do's" and don'ts" in the everyday handling and use of Alclo. This work is described in References 41, 43, and 45.

a. Impact Sensitivity

(1) The impact sensitivity of Alclo was measured using standard Bureau of Mines practices. The sensitivity of Alclo was found to be in line with those for many presently used rocket propellants and for TNT. A list is presented below for comparison.

Material	Height of drop to cause explosion, cm
Alclo	35 (partial)
Nitroglycerin, drop on filter paper	8 to 10 (complete)
Nitroglycerin, blasting gelatin	12 (complete)
Nitroglycerin, Guhr dynamite	5 (complete)
Composition B	37 (complete)
TNT	35 (complete)
RDX	17 (complete)
Aeroplex AN-525 (NH_4ClO_4 base)	20 to 25 (partial)
Aeroplex AK-14 ($KClO_4$ base)	30 (partial)

(2) It is important to note that with Alclo (and with the Aeroplex propellants) the amount of material consumed in the detonation is some function of the severity of the impact. The explosion is one of very low order and does not propagate well. It is this feature which makes the handling of Alclo much safer than the impact test data alone would indicate.

b. Friction Sensitivity

Tests made at the Naval Ordnance Test Station, Inyokern, California, indicated that the friction sensitivity is the greatest single source of hazard associated with Alclo. It's friction sensitivity (measured by means of a standard pendulum with a steel shoe and a 4° impact angle) lay between that of PETN and RDX, with the value being closer to PETN.

c. Vacuum Stability

The Naval Ordnance Test Station reported that the vacuum stability of Alclo was found to be 0.21 cc/g in 48 hr at 100°C, which is entirely acceptable.

d. Autoignition Temperature of Alclo

(1) The autoignition temperature was investigated. It was found that the ignition temperature of the Alclo + 13% lead mixture was 850°F, compared with 1050°F for stoichiometric Alclo.

(2) Two methods were used in obtaining the above values. In the first, small samples of Alclo were inserted into an electric furnace which had reached the desired equilibrium temperature. If it did not ignite within one minute the sample was removed and another piece tried. Usually three samples were tried at each temperature, and then, the furnace temperature was raised in steps of 25°F until ignition was secured. Then the temperature was lowered in steps of 25°F until the samples no longer ignited. The autoignition temperature was taken to be the average of the temperatures going up and down. The second method involved the same procedures, except that a bath of molten metal was used.

e. Detonation Velocity

Eight attempts were made to measure the detonation velocity of compressed Alclo sticks using the D'Autriche method. Although numerous schemes for agravating the explosion conditions by confinement of the stick and its initiator were tried, in no case was it found possible to cause a detonation to progress through a stick of Alclo.

f. Explosive Power

(1) From a safety standpoint, it is imperative that the explosive power of a material as well as its sensitivity be known. For Alclo, this property was determined at Aerojet using the standard Trauzl lead-block test. The 10-g samples were sand-tamped into the hole in a lead block, and detonated by means of a No. 8 electric cap. The average increase in volume of the holes due to the explosion of Alclo was 25 cc. These values, as well as values for some high explosives, are tabulated below for comparison. The explosive value for uncompressed (powder) Alclo was also measured and is included in the tabulation.

Material	Expansion produced by 10-g sample, cc
Alclo	25
Alclo powder	125
Nitroglycerin	550
Blasting Gelatin	580
TNT	285

(2) The Trauzl test is essentially a measure of brisance or disruptive power and, for explosives of similar velocities of detonation, it supplies a basis for the comparison of their total energies. Alclo has a higher heat of reaction than any high explosive known to the author (2.49 kcal/gm for Alclo, 1.58 kcal/gm for nitroglycerin) but its Trauzl expansion is low. Because the detonation velocity of Alclo could not be sufficiently low to account for this incongruity, it was concluded that the small disruptive power of Alclo is a result of the absence of permanent gaseous products of reaction.

g. Handling

A review of the hazards data above indicates that sticks or grains of compressed Alclo propellant must be treated like other propellant grains of the same size. The hazards of handling Alclo are much less than those for cannon powder, black powder, or high explosives because of its small disruptive power. There is essentially no explosion hazard with Alclo (unless it is in the powder form). The material will ignite if subjected to undue heat, friction, or impact, and the main concern would be with the fire which ensues.

6. Miscellaneous Experiments

a. Aluminum-Rich Alclo

(1) An aluminum-rich mixture of Alclo was investigated as a possible energy source, for applications where a small quantity of non-condensable gas is not detrimental to the operation. Some of the devices in which this mixture might be used advantageously are the hydroduct, turbine starters, and all other gas generators in which free water is available and the working gas is discharged to the surrounding media without first being condensed.

(2) In the aluminum-rich mixtures, the Al and $KClO_4$ react in a stoichiometric ratio, melting and dispersing the excess aluminum present, which in turn reacts with the free water, giving off additional heat and some gaseous hydrogen. Because of the aluminum-and-free-water reaction, aluminum-rich mixtures produce more energy (for a given weight or volume) than the stoichiometric mixture, as may be seen from the following tabulation:

Mixture	Heat of Combustion kcal/g	Theoretical sp gr g/cc	Actual sp gr (80,000 psi) g/cc	Energy Density kcal/cc
100% Alclo (stoich.)	2.49	2.58	2.45	6.1
87% Alclo, 13% Pb	2.17	2.87	2.80	6.1
75% Alclo, 25% Al + Free H_2O	2.78	2.61	2.43	6.8
50% Alclo, 50% Al + Free H_2O	3.08	2.64	2.46	7.6
100% Aluminum Powder + Free H_2O	3.68	2.70	2.48	9.1

(3) Alclo mixtures containing excess aluminum in the amounts of 25, 35, 50, and 65% were tested in the vertical steam generators, and their theoretical heats of combustion were verified, thus proving that the aluminum reacts with the available water. These and other experiments are described in References 40 and 44.

b. Alclo-Aluminum-Water Paste

(1) The possibility of using Alclo in a bipropellant rocket system was investigated. Enough water was added to the Alclo to form a paste which could be extruded or pumped. This paste could be injected into a combustion chamber along with some additional water, and the heat of the Alclo reaction would convert the available water into steam.

(2) Such a paste has several advantages over solid or molten propellants. The paste may be easily pumped and injected into the combustion chamber; no heating is required before use; and there is little danger involved in its handling.

(3) Several proportions of Al, $KClO_4$ and water were tried. The burning was steady, but slow (at atmospheric pressure). The greater the percentage of $KClO_4$, the greater was the rate of burning. This work is further described in Reference 40.

B. VERTICAL STEAM GENERATOR

1. Introduction

a. Alclo is considered to have promise in a compact power package. Calculations have shown that the specific impulse of an Alclo-and-water system varies with the changing water-to-propellant ratio (W_w/W_p). With W_w/W_p of 0.6, the specific impulse was calculated to be 200 lb-sec/lb (based on water and propellant). If it can be assumed that as much as one-fourth of the sensible heat of the solids can be extracted in the exhaust nozzle, then this already high specific impulse would be increased by 25%. The specific gravity of this propellant and water combination is 1.67, which is about equal to the best solid- or liquid-propellant combination in use today.

b. When weight and space are not critical, and free water is available, greater propellant economy can be obtained by operating at the optimum W_w/W_p of 4.0, where the specific impulse by actual test was shown to be 325 lb-sec/lb based on the weight of Alclo only (see Figure 89). A substantial additional increase in performance of the steam generator can be obtained by using Alclo which is rich in aluminum (or magnesium), as shown in paragraph A,7,a, of this section.

2. Vertical Steam Generator, Mk I and Mk II

a. In order to test the burning rate characteristics of Alclo in a simple setup which would produce results directly applicable to the operation of the hydroduct (i.e., burning the propellant under pressure in a combustion chamber and producing steam), the vertical steam generator, Mk I (VSG Mk I) and the later VSG Mk II, were designed and operated. The VSG Mk II is shown in Figure 7. The Alclo charge was mounted axially in a reaction chamber which also contained water. With the ignition and subsequent burning of the Alclo, the heat of reaction converts the water into steam instantly, and the steam is then exhausted to the atmosphere through a nozzle. A perforated metal sleeve, which stabilizes the surface of the water, was provided in the chamber. A turbulator was included near the top of the chamber to promote complete mixing of the hot reaction products with the water. All the water necessary for steaming, as well as the Alclo charge, is contained in the combustion chamber. The unit is always run in the vertical position so that the water surface remains stable and decreases at a rate equal to the burning rate of the propellant. The water-to-propellant ratio is fixed by the geometry of the chamber in relation to the size of the propellant charge.

b. A total of more than 350 runs were made in these steam generators for the purpose of obtaining burning-rate vs pressure data on the various Alclo compositions, and to check the operational stability and efficiency of the vertical steam generator. Some of this work is described in Reference 40.

3. Vertical Steam Generator Mk III

a. A large unit was designed and built which had a power output and duration of sufficient magnitude to do useful and measurable work. A more comprehensive investigation of the problem of steam generators was accomplished with this unit. The unit, called the vertical steam generator Mark III, had a cylindrical tank, 12 in. in dia and 5 ft long, with a general configuration similar to the preceding vertical steam generator models. A standard 4-in.-pipe tee was flanged to the top of the chamber, to permit easy coupling of the exhaust steam line to the generator. A layout drawing of this unit is shown in Figure 138.

b. This steam generator was designed to accomodate a 3.75-in.-dia Alclo charge, 4 ft long and will produce 5.3 lb/sec of saturated steam at 225 psia. The 12.12-in. ID of the chamber establishes the maximum water-to-propellant ratio as 3.42. Ratios less than this design figure were obtained easily by including spacing rods or tubes in the water annulus, in order to decrease the water volume and exposed surface.

c. Because the heavy metal parts of the vertical steamer are heated to the steam temperature during the first part of a run, the operating conditions were not steady during this period of operation. In order to obtain more precise average operating data, short grains were mounted on a pedestal to position them high in the chamber, and to minimize the weight of metal that must be heated. In later tests, better data were obtained by using longer propellant charges.

d. The propellant grains were made up to the length desired by butting the standard 8.25-in.-long grains end to end, clamping them in a special fixture, and wrapping them with the standard restriction of Selectron resin and glass tape. The disassembled unit, exposing the propellant grain, is shown in Figure 139.

e. The assembled unit is shown in Figure 140. Here, the steam was piped to a turbo-supercharger dynamometer, where the power generated in the turbine was absorbed by the direct-coupled supercharger. By varying the total nozzle area and throttling the air output, a variety of power outputs and speeds were attainable. With this setup, the output of the steam generator was put to work. Measurements were made of the rpm and torque, as well as of pressures and temperatures. Measurements were made of bulk water temperature, steam temperature (in the tee), chamber pressure, and steam pressure (in the tee). These data were recorded on a multichannel oscillograph using iron-constantan thermocouples and reluctance-type pressure pickups. The oscillograph also provided a duration-of-run record. The heights of water before and after the run were recorded on a data sheet, as well as the water temperature, air temperature, and data concerning the unit and the propellant.

f. A total of 16 successful test runs were made with this unit without the turbo-supercharger dynamometer. Because of the short duration of most of the tests, steady-state operation was not achieved, and the performance data seem to be scattered. The more reliable data fall within the spread of data obtained with the Alclo hydroduct motor, and it can be reasonably assumed that, for any given set of operating conditions, the performance of the two units will be similar.

g. A total of seven test runs were made with the turbo-supercharger dynamometer. The power output was varied over a limited range. Performance data for these runs are listed in Table 19. In these tests no attempt was made to obtain the maximum efficiency from the turbine; the equipment on hand was used. Therefore, the performance figures do not represent the maximum attainable under any given set of operating conditions. Performance data for the short-duration runs appear somewhat scattered because the transient conditions which exist in starting make exact calculations difficult.

h. The unit operated stably in all tests. Only slight irregularities were evident as the burning passed the butt joints where the individual propellant grains were joined. A plot of the performance data vs time for Run No. 7 is shown in Figure 141.

i. The effect of the solid products in the steam was investigated in detail. It was found that 38% of the solids was deposited in the various passages before reaching the turbine wheel, and that less than 1% collected on the wheel itself (only a fraction of this in the turbine blades). The remaining 61% was assumed to have passed through the turbine and exhausted. Visual inspection showed that the thin film of powdery residue on the turbine blade was no worse after 43-sec (Run No. 7) of continuous operation than it was at the end of a short-duration run, indicating that an equilibrium was established in the extent of the coating. In the 43 sec of operation, residue deposited in the nozzle throat increased the area-ratio from 6.98 to 7.3.

j. Although the solids did not appear to cause difficulty in these tests, there are applications for which absolutely clean steam is necessary. Several types of commercial steam separators are available, and would be used when necessary.

k. A complete report on the testing of the VSG Mk III is included in References 44 and 45.

C. ALCLO-FUELED SUBMARINE POWER PLANT

1. Introduction

a. Alclo, a propellant that requires no external source of supply of oxygen, and which upon combustion leaves substantially no gaseous products, appears to be well suited as a source of power for submarine propulsion. The absence of a gaseous intake and exhaust will permit the submarine to operate submerged for extended periods of time.

b. The power plant is envisioned as consisting of a specially designed steam generator that utilizes the heat of combustion of this propellant and suitable conventional steam propulsion equipment. The full description of the principal features is given in "Proposal for the Development of Alclo Submarine," submitted to the office of Naval Research on 21 July 1950, and is illustrated in the schematic diagram of Figure 142.

c. As a result of this proposal, development was initiated, the objective of which was to build a small experimental steam generator using Alclo as the source of heat, and capable of operating in a closed cycle similar to the intended full-scale application. Extensive testing of this miniature power plant would bring out the problems that would be encountered, such as optimum methods of burning of Alclo for this application, ash removal, deleterious effects of the high Alclo-flame temperatures, etc.

2. Design and Selection of Test Equipment

The test equipment consisted principally of a boiler capable of 500 lb/hr evaporation at 150 psig and a 700°F total steam temperature, and the necessary auxiliary equipment. The arrangement of this equipment is shown in Figures 143 and 144. The boiler pressure parts (boiler, feed pump, safety valve) were acquired from local manufacturers. The furnace was built from refractory brick, the choice dictated by the relatively small size of the unit and for simplicity of construction. The air (or an inert gas) enclosed within the volume of the steam generator was recirculated by means of a fan. This air does not take part in Alclo combustion, but is used to carry the heat of combustion to portions of the boiler not directly exposed to the radiant heat of the flame. The air also carries the powdery products of combustion to a dust collector for removal from the closed gas cycle. The refractory furnace provided a simple means of admitting this recirculated air around the flame, thus absorbing large portions of the released heat. The low-temperature melting constituent of the products of combustion (KCl) was slagged in the furnace and allowed to flow into a water-filled tank.

3. Preliminary Performance Calculations

Preliminary performance figures and a heat balance of the complete test unit were calculated to serve as a guide for the selection of test equipment and for future operation. The heat release rate of 268,000 Btu/hr/eprs (effective projected radiant surface) is well within normal for a unit of this size. The temperature of the recirculated air entering the furnace is approximately 590°F, which does not appear excessive. Because the unit operates in a closed cycle, there are no stack losses and the calculated efficiency for the test unit is 92.6%, though this figure can be increased by reducing the wall-radiation losses by increased insulation.

4. Testing

a. The major portion of test work was devoted to the development of methods and equipment for burning of Alclo. Because the burning of fuel directly combined with an oxidizer is new to the steam generating field, utilization of a propellant in a furnace called for exploration of methods of handling and combustion unlike those for conventional fuels. This combustion testing was carried out most of the time within the test furnace.

b. Burning of Alclo in suspension, similarly to pulverized coal, was tried in several ways. A portion of the recirculated air was used to blow the powdered propellant into the furnace (see Figures 145 and 146). The fuel and oxidizer were kept separated and the two streams were mixed either inside of the barrel of an internally-mixing burner or mixed directly in the flame. A butane torch was used for lighting off, and removed after ignition was obtained. The internally mixing burner (Figure 147) was subject to occasional flash-back because of irregular material feeding. The externally mixing burner (Figure 148), though more reliable, permitted unmixed and unburned material to get past the flame. Both types of burners were capable of burning a complete container of propellant (about 50 lb) during a test run, maintaining their own flames for periods of more than one-half hour. Yet, because of the possibility of unpredictable failure the cycle of the test unit was not closed when these burners were used.

c. Restricted solid grains of Alclo were burned in successive trains and also were fired successfully in the closed cycle (Figure 149). Problems of maintaining ignition from grain to grain were being overcome at the conclusion of the project. The total time of firing in a closed cycle amounted to more than one-half hour.

5. Results of Investigation

a. The successful operation of the closed cycle of the steam generator was demonstrated.

b. The boiler performed well with no ill effects due to the high Alclo flame temperature.

c. Several hours of Alclo burning in the test furnace showed no damage to the refractory brick from the high heat concentrations, and the method of using recirculating air to control furnace temperatures appeared satisfactory.

d. The removal of products of combustion was not very troublesome. KCl slagged within the furnace without signs of being carried into the boiler. The other constituent (powder Al_2O_3) was removed by the dust collector and the layers collected on the various surfaces were easily re-suspended by means of short air blasts.

e. The burning of the propellant was sufficiently controlled to permit closed-cycle operation of the test unit.

f. Complete results of this investigation are given in References 12, 13, 41, 42, 44, and 45.

XI. ALCLO HYDRODUCTOR

A. INTRODUCTION

1. An underwater missile such as the Alclo hydroduct is propelled by a jet of high-velocity steam exhausting through a De Laval nozzle. However, as the missile achieves greater depth and the back pressure increases, the steam velocity decreases and the thrust of the system deteriorates until the power plant becomes inoperative. This phenomenon imposes a limitation on the missile and restricts its maximum service depth to a value governed by the pressure in the combustion chamber. By condensing the exhaust with a steam-jet condenser, a low back-pressure on the steam nozzle can be maintained, and the performance of the missile can be increased and made relatively insensitive to depth. Since the exhaust of the Alclo hydroduct consists of steam and solid reaction products, and is therefore completely condensable, a direct-contact condenser can be applied to the system. When the steam-jet condenser is applied to the hydroduct, the device is termed a hydroductor.

2. The steam-jet condenser design is such that sufficient quantities of seawater to condense the exhaust steam are ducted into the chamber through external scoops. The design of the seawater inlet orifices in the scoop is such that the total pressure head, equal to the sum of ram- and static-pressure heads, is totally converted to velocity head. The pressure within

the mixing chamber is the vapor pressure of the condensed mixture, which amounts to only a few pounds per square inch absolute. This condition results in an extremely high steam-exhaust velocity, by permitting expansion from the initial conditions down to a very low enthalpy level. A schematic diagram of the hydroductor is shown in Figure 150.

3. Through impact, and by an exchange of momentum between the steam and water particles, the resultant mixture achieves a high velocity at the end of the condensing chamber. After leaving the condensing chamber, the high-velocity mixture passes through a diffuser, where a portion of the velocity is converted into pressure head, matching the ambient conditions of the particular depth where operation is taking place. The reaction products at operating temperatures will be solids, and the steam will be totally condensed within the mixing chamber, thereby giving a vehicle with no gaseous wake.

B. DEVELOPMENT OF THE HYDRODUCTOR MOTOR

1. Small-Scale Steam-Jet Condenser Study

a. To ascertain the feasibility of the steam-jet condenser as applied to missile propulsion, a small-scale steam-jet condenser unit was built and tested. A complete report of this work, as well as of the results obtained, is given in Reference 48. Pictures of the equipment are shown in Figures 151 and 152.

b. Various condenser shapes were studied, and the effect of flow-passage area and geometry was investigated. The results, which were presented as a set of dimensionless curves, showed what kind of a chamber would have to be constructed for proper operation of a 4.5-in.-dia hydroductor test vehicle.

2. Short Combustion Chamber for the Alclo Hydroduct

a. From the results of the small-scale steam-jet condenser tests it was found that the combustion chamber of the Alclo motor would have to be radically reduced in length so that the test missile would not be too large. Whereas the combustion chamber of the Alclo hydroduct motor was 13.75 in. long, the chamber of the Alclo hydroductor motor could only be 3.50 in. long. The development of this chamber was carried on in the static test facility described in Reference 12.

b. Various types of turbulating devices were tried in order to obtain adequate mixing between the steam and the hot solid-reaction products. It soon became obvious that some type of flow deflector in the form of a "button" turbulator would be needed to accomplish this. The problem was then reduced to one of finding a material that could resist the high chamber temperatures. Carbon was finally selected, and the chamber configuration shown in Figure 153 operated very successfully.

3. Full-Scale Steam-Jet Condenser Study

a. With the combustion chamber for the Alclo hydroductor fully developed, a study of full-scale steam-jet condensers was undertaken. Data from the small-scale studies were used, and the static-test facility was enlarged to provide the water for the condensing processes. A schematic diagram of the installation is shown in Figure 154, a diagram of the motor in Figure 155 and a picture of the installation in Figure 156. The installation is fully described in Reference 12.

b. Various geometric and flow parameters were investigated on this test installation. The starting sequence, which was found to be critical on the small-scale work, was investigated and found to be very important for proper condenser operation. The performance data from two typical test runs are compared in Figure 157.

c. An attempt was made to install a back-pressure system to allow for testing the hydroductor at simulated deep-launching conditions. A schematic diagram of this system is shown in Figure 158 and a photograph of the test installation is shown in Figure 159. The flow of water through this system is very large, so that the pressure drop through the back-pressure valve was relatively high. It was, therefore, impossible to maintain a simulated depth operation of less than about 300 ft. Furthermore, the back-pressure system, because of its size, hindered the measurement of thrust, so that only qualitative results were obtained. These, however, did show that hydroductor operation was possible at great depth, i.e., the condensing chamber pressure was low and the thrust produced should be adequate for the free-running hydroductor test missile (see Figure 160 and Reference 49).

d. Several free-running tests have been made of the 4.5-in.-dia Alclo hydroductor test missile (see Figure 161) under sponsorship of the Armament Branch, Office of Naval Research, Contract Nonr 1002(00). Performance of the free-running test missile has not been completely successful, as there is apparently excessive drag of the test-missile configuration. Results of these tests have been reported in References 50 through 53.

C. HYDRODUCTOR INVESTIGATIONS ON THE ROTATING BOOM

1. During the motor development program in the static-test pit, it was decided to initiate a hydroductor program on the rotating-boom test facility in an effort to determine the hydrodynamic characteristics, with particular reference to the water scoop, as well as to obtain additional information on motor performance. Accordingly, a steam-delivery system was designed for application to the rotating boom, to supply saturated steam at approximately 200 psi absolute to the simulated combustion chamber of a hydroductor model. This system is shown schematically in Figure 162. Work was also started on the fabrication of a simulated hydroductor model, shown in Figure 163. The steam nozzle and scoop details for this model are shown in Figure 164. A

simulated hydroduct model was also fabricated, making use of the same nose and center section, for comparative purposes. This model is shown in Figure 165. To determine the performance of the hydroductor motor, a complete instrumentation program was instituted to provide measurements of the simulated combustion-chamber pressure, the condensing-section pressure, and a mixed-velocity stagnation pressure taken at the exit of the condensing-water scoop. Drag measurements were obtained from a three-component hydrodynamic balance which had been fabricated and used on a previous program.

2. One of the first important contributions of the rotating-boom program was to point out the extreme importance of a proper sequence of operation. The initial tests were conducted with the condensing section of the hydroductor freely flooded. It was expected that the application of steam to the condensing chamber would purge the latter of water, enabling proper condensing operation to begin. This proved to be impractical, as it was not possible to obtain condensing operation with a freely flooded system. This led to the development of several scoop-closure designs to permit delivery of steam to the combustion chamber prior to the addition of condensing water through the scoops. With the development of a satisfactory sealing arrangement, condensing operation was achieved. As soon as proper motor operation was obtained, an intensive photographic study of the hydroductor in action was undertaken, using Microflash techniques. The early photographs indicated a large amount of cavitation from the leading edges of the condensing-water scoop. Careful checking of the condensing section showed that the scoop design had not been followed closely enough during fabrication. The scoop passage converged from entrance to exit section, which caused pre-diffusion of the external flow, and external cavitation at the lip of the scoop. An attempt was made to modify the scoop passage and some improvement was noted, but the existing design could not be changed sufficiently to completely eliminate cavitation. A scoop-modification program was then started, with emphasis on a new design that would have a gradually increasing cross-sectional area in each condensing-water passage. The increasing-area scoop was proposed to provide for boundary-layer growth in the scoop passage, and also, to eliminate any further possibility of pre-diffusion. Several new scoop sections were fabricated in accordance with the new design, and subsequent Microflash photographs indicated a substantial improvement in performance. Cavitation from the leading edge of the scoop lip was virtually eliminated. Scoop details for the increasing-area scoops are shown in Figure 166 and the improvement in the cavitation picture is illustrated in Figures 167, 168, 169, and 170. Sample performance curves for the simulated hydroductor power plant are given in Figures 171 through 174. One additional condensing section was tested in an attempt to apply the Ramus step principle (see Section XV) to the internal walls of the condensing section in an effort to minimize frictional resistance. The internally stepped afterbody is shown in Figure 175. No particular improvement in performance was obtained from this configuration. Table 20 presents a compilation of tabulated data for many of the model hydroduct and hydroductor runs on the rotating boom, indicating the differences in performance obtained from the various configurations.

XII. SOLID-PROPELLANT GAS-TURBINE TORPEDO POWER PLANT

A. OBJECTIVE

As a result of Aerojet Proposal PW-3205, dated 8 July 1953, to the Bureau of Ordnance, regarding development of a solid-propellant turbine power plant applicable to the EX-2 torpedo, a great deal of interest was shown in this new type of torpedo power plant. The proposed unit was an extremely simple power plant, as well as one that would be practical and reliable under all service operating conditions. A net power of 28.3 hp for 2 min at a maximum operating depth of 1000 ft was required. Proposal PW-3205 was not accepted but the Office of Naval Research authorized the Aerojet-General Corporation to conduct a development program to prove the feasibility of this unit.

B. DESCRIPTION OF WORK

1. Turbine

a. In order that an operating power plant might be obtained in the shortest length of time and at minimum cost, components developed under other programs were utilized whenever possible. A single-stage impulse turbine of 4 in. pitch dia, designed for another program that required a 40,000 rpm wheel, was modified to operate at 63,000 rpm. The turbine wheel was an integrally cast one-piece unit of Stellite No. 31. A turbine bonnet, containing the single 0.096-in.-dia nozzle, was bolted to the wheel casing. The turbine shaft was welded to the turbine wheel and supported by a ballbearing at one end, and by a sleeve-type, water-cooled carbon bearing at the other end, adjacent to the turbine wheel. Water served as a lubricant for the carbon bearing, removed excess heat from the bearing area, and, in conjunction with a slinger, sealed out the high-pressure exhaust gases resulting from operation at a depth of 1000 ft. In addition to causing a sealing problem, the high back pressure created a thrust load on the turbine ballbearing. This thrust load caused some bearing difficulties when operating at 63,000 rpm, but by dividing the load between the turbine ballbearing and a bearing in the gearbox, satisfactory operation was attained.

b. A study of several run records where bearing malfunctions occurred showed that the critical speed of the turbine shaft was 60,000 rpm. Since this turbine was originally designed for 40,000 rpm and the experimental critical speed was 60,000 rpm, it was decided that subsequent testing would be at either 63,000 rpm where operation was satisfactory or at the 40,000-rpm design speed of the turbine. As a result of continued testing, the turbine bearing arrangement was changed, to eliminate the carbon bearing at the wheel root and to provide shaft support by means of 3 ballbearings. A pair of duplex radial-thrust bearings at the end of the turbine shaft absorbed thrust loads.

2. Gas Generator

Two gas generators were designed and fabricated for use in the test pit with 5.75-in.-dia propellant grains. Both were fabricated of seamless steel tubing; one accommodated 6-in.-long grains for tests of 1-min duration, and the other was designed to handle 12-in.-long grains for 2-min tests. The chambers were uncooled, and in the tests were used without wall insulation other than that afforded by the 0.125-in.-thick grain restriction. The outlet end of the chamber was insulated with an 0.25-in.-thick laminate of glass and melamine, covered by a carbon disk. This combination has been used many times. The outlet tube and nozzle were lined with pure molybdenum. Neither erosion in the tube nor any nozzle enlargement occurred. The igniter screwed into the center of the outlet end of the chamber, and a pressure-tight seal was maintained through use of an O-ring.

3. Igniter

An igniter previously developed for another solid-propellant unit was adapted to the torpedo-engine gas generator. This igniter was one of the three-element type, consisting of a black-powder initiator, a mixture of Alclo and black powder, and a charge of either JPN ballistite or AN-581 propellant. This igniter proved adequate for the size of grain and the chamber configuration.

4. Speed Regulator

a. This specific torpedo power plant required a turbine speed-regulating device to maintain the turbine speed constant within very close limits (and consequently, the alternator speed) for all load conditions with operating depths varying from sea level to 1000 ft. Considerable thought was devoted to the solution of this problem, for this device required thorough reliability in order to maintain the inherently high reliability of a solid-propellant power plant.

b. Consideration of several types of systems led to the selection of a chamber-pressure bleed system as the most desirable. This system consists of a bleed valve in which a spring-loaded pintle is balanced by the chamber pressure, exhaust pressure, and pump pressure (the latter being a function of shaft speed). At sea level, the regulator is open to such an extent that the chamber pressure is approximately 1700 psia. As the torpedo descends, the closing of the controller causes an increase in chamber pressure down to a depth of 1000 ft, where the regulator is completely closed. Chamber pressure is less than the design value of 2300 psia at any depth less than 1000 ft. The propellant burning rate, which is a function of pressure, is therefore decreased, and this will result in a greater run duration. The control system is effectively a variable-chamber-pressure system.

c. Figure 176 shows the elements comprising the speed control valve. The spring is adjusted to create the desired balance position. Cavities for exhaust pressure, chamber pressure, and pump pressure (the speed signal) are located in the regulator body. The complete dynamic torpedo system was set up on the electronic analog computer operated by Aerojet. The results indicated that the proposed system was stable, and that the response time was satisfactory. The simulator showed that, at the worst condition, when the propellant grain is almost consumed, a 10% step-change in load resulted in less than a 5% change in the turbine speed.

5. Propellant

a. For initial testing, the ammonium nitrate solid propellant designated AN-2011 was utilized. However, continuing propellant developments by Aerojet have made available an improved formulation of similar constituents that has been designated AN-2091AX. This propellant was employed for all recent testing of the gas-turbine power plant. AN-2091AX is one of the formulations of the Aeroplex propellant systems originally developed by Aerojet in 1945 for the Armed Forces. Since the original development of the Aeroplex propellant system, continued research and development has produced a whole family of closely related formulations that now constitute one of the most versatile propellant systems available.

b. The AN-2091AX propellant is characterized by a slow burning rate and a low flame temperature, both necessary requirements for a long-duration, turbine-powered torpedo. AN-2091AX propellant may be described as a castable, composite propellant containing a crystalline oxidant of ammonium nitrate that is dispersed in a fuel system consisting of an unsaturated polyester (Glenpol A-20 resin) copolymerized with styrene and methyl acrylate (GSMA). The composition of the propellant and the thermodynamic properties of the propellant gases are presented in Table 21. For a more detailed description of the Aeroplex propellant system, with the emphasis directed toward the AN-2000 series of propellants, see Reference 54.

C. RESULTS

1. Propellant

a. Only a small number of gas-generator tests were conducted, because ignition and propellant performance were quite satisfactory. Good reproducibility was attained with grains cast from several different batches. Propellant for this program was initially cast in laboratory batches, but in order to provide data more nearly representative of that which would be attained in production units, propellant was taken from large production batches being mixed for another Aerojet solid-propellant motor. Grains from numerous batches were tested, with substantially no difference in performance among them.

b. Figure 177 is a pressure-time plot for a 2-min gas-generator test. It may be seen that the variation in chamber pressure is only ± 3.5% for the full 2-min duration. The weight-flow parameter, C_W, for this test was 0.00836 lb/sec-lb, compared with a theoretical C_W of 0.00810 lb/sec-lb. The parameter, C_W, is important in solid-propellant study; it is equal to the reciprocal of the commonly used specific impulse divided by C_F, the nozzle thrust coefficient. This parameter gives an indication of the fraction of the available chemical energy that is delivered to the nozzle. It is defined as

$$C_w = \frac{\text{Propellant-wt flow rate}}{\text{Chamber press. x nozzle throat area}}$$

c. AN-2091AX propellant has demonstrated exceptionally good handling characteristics. No unusual techniques are necessary. Ignition is prompt, and has caused no difficulty; no propellant malfunctions have occurred. The only tests stopped prematurely were those having mechanical malfunctions in the turbine or gearbox.

2. Turbine

Most of the tests conducted have been with the combined turbine, gas generator, and gearbox. All tests were with 6-in.-long grains that provided a run duration of approximately 60 sec. Numerous tests were carried to completion with no malfunction in any of the rotating mechanisms, even though an operating speed of 62,000 rpm was maintained. Output from the gearbox as high as 27 hp was attained. Figure 178 is a plot of data from one of the turbine tests. It may be seen that approximately 25 hp was measured at a shaft speed of nearly 63,000 rpm. All the turbine tests were conducted at a full back pressure of 460 psia (equivalent to a 1000-ft depth).

D. PROGRAM CHANGE OF SCOPE

1. The program up to August 1954 had pursued the development of a test engine of sufficient power to be adaptable to the EX-2 torpedo. However, at this time, with the engine feasibility clearly demonstrated, the objective of the program was shifted to compliment another program, Contract NOrd 14993. Under NOrd 14993, a similar solid-propellant turbine power plant, to operate at an 80-hp level for 4 min at a 1000 ft depth, was to be developed for testing in the Mk 41 torpedo shell. The turbine configuration for the new development was to be nearly identical with the previous one; the primary change being that the propellant grain diameter was increased to 12 in. and the length to 22 in.

2. The extent of the complimentary assistance to Contract NOrd 14993 through Contract N6ori-10, was limited to development of the speed-control valve in its final form suitable for use with the Mk 41 power plant.

E. TURBINE SPEED-CONTROLLER DEVELOPMENT

1. The required modifications of the earlier speed-control valve to suit the needs of the 80-hp engine are summarized below:

a. Eliminated the heat exchanger, as it was no longer feasible with the larger volume of gas to be handled.

b. Added a small water cooling jet at the pintle seat to compensate for the lack of the heat exchanger.

c. Replaced the valve pintle of 4130 steel with one of Kentanium to minimize erosion and increase service life.

d. Increased the size of the overboard-discharge ports and lines to minimize exhaust restrictions to the control valve when bleeding at a maximum rate.

2. Having arrived at the above changes, partly through known requirements and partly from the results of initial testing, the overall performance of the control valve was again examined by means of an analog computer simulation capable of testing the valve at operating limits beyond the scope of test-pit trials. The results of this examination indicated that the control valve had adequate capacity to handle the relatively great increases in the propellant burning rate (i.e., a 50% excess burning rate without significant changes in speed or power). Under normal ambient-temperature conditions (100°F or less) the burning rate could not approach the 50% figure. However, at the extreme upper service-temperature limit of 130°F, it is expected that the full capacity of the control valve will be required when the torpedo is surface-running at a low back pressure. The analog computer simulation further pointed up the marginal characteristics of the water pump used with the system. Subsequently, the water pump design was modified to achieve operation with a more conservative margin, but the altered pump design has not yet been tested.

3. The speed-control valve operates to control the turbine speed by bleeding gas from the gas generator when the power plant is operating at below-maximum loads. This gas bleeding reduces the mass flow of gas to the turbine, as well as the power output of the turbine. A secondary benefit is realized by the reduction of the operating chamber pressure. This reduction results in a lower burning rate of the propellant, thus extending the duration. Calculations made of the performance show that, with this type of control, the range of a torpedo (when operating at sea level) would be 25% greater than when operating at a depth of 1000 ft.

4. Figure 179 shows schematically the control system for a torpedo engine. This control system consists of a centrifugal water pump driven by the turbine and the control valve. The control valve is a spring-loaded, piston-and-pintle valve, in which the pump pressure acts to open the valve, and the spring acts to close the valve. The combustion gases are directed into the valve so that the chamber pressure also tends to open the valve. The spring cavity is vented to the ambient pressure to make the controller depth-insensitive. The water is piped to the valve-actuating piston to provide the reference pressure. The centrifugal water pump supplies the fluid for operation of the system, and it also supplies cooling water to the turbine. The characteristics of the pump are dictated by the volume of water required and the pressure requirements of the control valve. The discharge pressure of the pump is the sensing signal of the speed controller. If the speed is too high, the pump pressure is high, causing the control valve to open. This allows gas from the chamber to bleed out, reducing the chamber pressure, which reduces the mass rate of gas generation. Consequently, the mass flow of gas to the turbine is reduced, and the speed of the turbine decreases. If the speed is too low, the converse occurs. Figure 176 shows the actual valve parts that are used.

5. At present, 30 tests of the Mk 41 engine have been run with the control valve in use. In the majority of these tests, the speed-control valve functioned satisfactorily, maintaining the speed constant within ± 1.5%, at back pressures varying from 50 to 460 psi. The lack of proper speed control in the several irregular runs was attributed in each case to external malfunctions which adversely affected control-valve operation (i.e., failure of water pressure, or improper adjustment of the control-valve balance spring, etc).

F. CONCLUSIONS AND RECOMMENDATIONS

1. Solid-Propellant Gas-Turbine Torpedo Power Plant

Development of the solid-propellant turbine engine applicable to the EX-2 torpedo was carried to a state of development that clearly demonstrated its feasibility. In view of the simplicity and reliability of the unit, such a propulsion system deserves consideration in meeting the propulsion requirements of future torpedoes. The primary deterrent in its use is the presently unavoidable wake left by solid-propellant combustion products, which affects only concealed-attack situations. Worthy of special attention is the feasibility of operating a solid-propellant turbine-drive system at any power level from 5 to 700 hp within a 21 in. diameter torpedo envelope, while retaining adequate volume for controls and warhead.

2. Speed-Control Valve

a. In its present configuration, the gas-bleed speed-control valve closely meets the needs of the Mk 41 torpedo engine. Figure 180 is a plot of a test run for the full 4-min duration of the Mk 41 engine, with speed control entirely by automatic valve action.

b. Based on data obtained in the analog computer evaluation of the control valve, the way is now clear to design pressure-bleed speed-control valves operating on this principle, or with some modifications that will control the much-higher-burning-rate propellants with possibly closer speed regulation than the present valve provides, should the needs of future applications require.

c. Continued application of the gas-bleed speed controller is recommended for future solid-propellant propulsion systems in view of the following advantages:

(1) Total duration is extended as much as 25% under shallow-depth running conditions.

(2) High sensitivity to speed is obtained by employing the pump discharge pressure as the actuating signal to the valve. This pressure varies as the square of pump/turbine speed.

(3) Ultra-safe gas-generator operation is obtained by using a gas-bleed of sufficient capacity to act as a speed controller under normal conditions, and as a safety-vent valve under unusually adverse conditions.

XIII. HIGH-SPEED LONG-RANGE TORPEDO DESIGN STUDY

A. OBJECTIVE

1. Pursuant to Contract N6ori-10, Task Order I, Amendment No. 16, dated 26 August 1954, a design study was conducted to determine the feasibility of a power plant (the fuel was not specified) applicable to a 21-in.-dia torpedo capable of running at a speed of 75 knots for approximately 30,000 yd.

2. The secondary objectives that were imposed were:

a. The stored length was to be 123 in., in order to double the storage capacity of present submarine torpedo racks.

b. The warhead weight was to be not less than 600 lb.

c. The power plant was to be designed for normal running at a depth of 25 ft, but operable, at reduced performance, at a depth of 1000 ft.

d. The overall specifications were to be generally comparable to those for the modern anti-ship torpedo (Mast) presented in NOTS TM No. 1256 and prepared under Task Assignment NOTS - Re6a-280-13-53.

3. A complete report covering this study will be found in Reference 22.

B. SUMMARY

1. Propellant

a. The selection of a solid-propellant fuel was based on the experience gained in adapting that fuel for use in a similar turbine drive applicable to the Mk 41 torpedo. This earlier work demonstrated the practicability of the system, and in addition to high performance, three important additional benefits were provided, reliability, simplicity, and safety.

b. Type AN-2091AX solid propellant, with one of the highest specific impulses among the solid propellants available for turbine operation, was chosen for maximum power and range. Once assembled in the gas generator, the solid propellant has an almost unlimited shelf life, and it remains readily available without further servicing for use over a wide range of operating conditions. Table 21 describes the characteristics of AN-2091AX propellant.

c. It is the nature of the solid-propellant system to operate at virtually any required power level; however, run duration will be reduced at higher power levels. Increases in horsepower are made by decreasing turbine nozzle size in order to achieve a higher chamber pressure, which in turn, promotes faster burning of the solid propellant. This more-rapid combustion produces a higher mass flow to the turbine, resulting directly in a horsepower increase. The most practical propellant grain configuration is a cylinder in which burning is started at one end and allowed to progress along the length, in a manner similar to that of a cigarette. The area of the end of the grain bears a relationship to the horsepower output desired, and the length of the grain, in conjunction with burning rate, determines the run duration. In the proposed design, the grain cross-sectional area has been raised to the maximum possible within a 21-in.-dia shell, thus providing the required horsepower at a minimum burning rate of 0.08 in./sec, at a chamber pressure of 1500 psi. Expressed in terms of range, at 70 knots this burning rate propels the torpedo 493 yd per lineal inch of propellant grain. The grain length in a 123-in. torpedo can be made no greater than 42 in. without hampering other components, or increasing the hull drag excessively. Accordingly, a range of 20,000 yd at 70 knots must be accepted as optimum for this type of power plant in this half-length torpedo application. Increasing the torpedo length to more than 123 in., to provide for a longer propellant grain, would increase the range, but the required horsepower would also increase because of the increase in shell surface.

d. Table 21 shows propellant ballistic data, and in Figure 181 the gas-generator design may be seen.

2. Propulsion Machinery

a. Propulsion is achieved by means of a high-speed, single-stage impulse turbine driving a single-stage, rear-mounted external pump jet. The turbine develops 675 hp at the turbine shaft, with a rotational speed of 45,900 rpm. The turbine efficiency is 61.7%, and the pressure ratio across the nozzle (P_c/P_e) is 60 at the depth for which the unit was designed. Tables 22 and 23 are provided to briefly summarize the more salient propulsion and turbine design data of the torpedo.

b. The torpedo hull form is similar to that of the NOTS Mast torpedoes, in that it has a modified, ellipsoidal forward section with a flat nose, a central cylindrical section, and a tail section of Lyon "A" form, with a fineness ratio of 5:1. A snap-on tail extension, with a large cutoff diameter for the exhaust exit, is fitted just prior to firing.

c. The performance requirements demand the greatest possible length and diameter of propellant grain that are commensurate with a low-drag hull contour. The drag analysis of the hull indicates a value of 2515 lb at the 70-knot design speed. The range available at this speed will be 20,000 yd.

d. The auxiliary equipment for the turbine consists of one water pump requiring approximately 5 hp, one oil pump with a negligible power requirement, a chamber-pressure control valve to hold the turbine speed constant, and two alternators.

e. A key feature of the turbine-wheel design is the use of Kentanium, a relatively light-weight, heat-resistant, titanium-nickel sintered carbide for the complete wheel and shaft. This material retains a high percentage of its cold strength at temperatures as high as 1500°F, and by virtue of its low density in comparison to more conventional materials, reduces wheel stresses by about one-third. Fabrication of the turbine wheel in more conventional material (such as Haynes Stellite No. 31) would limit rotational speed to 40,000 rpm, due to the high wheel stresses. However, a speed of 67 knots with a range of 19,000 yards could be achieved with a power plant using the Stellite turbine. The propulsion machinery arrangement is shown in Figure 182.

C. CONCLUSIONS AND RECOMMENDATIONS

In view of the established engineering feasibility of a 70-knot torpedo with a range of 20,000 yd, as demonstrated by this design study, it is recommended that preliminary design and evaluation be conducted for three propulsion components, prior to extensive torpedo-component development.

1. Kentanium turbine wheels should be fabricated to determine the capabilities and limitations involved in the fabrication process. Important factors to be checked would include the minimum practicable blade-leading-edge thickness, the smoothness of the surface finish, and dimensional tolerances. The buckets could then be checked for durability and strength by conducting trial runs at rated speed and reduced horsepower level, but with temperature conditions simulated by a hot-gas source.

2. Detail design of a dual jackshaft-drive helical gearbox should be undertaken.

3. Design and manufacture of 20-in.-dia propellant grains should be initiated, and proof-testing should be conducted to establish the most effective propellant-restriction material. Subsequent to the initial development of the components mentioned above, the fabrication and testing of experimental models of the complete torpedo should be considered, and actively supported.

XIV. EIGHTY-FT ROTATING TEST BOOM AND RING CHANNEL TEST FACILITY

A. OBJECTIVE

1. The development of underwater propulsion systems at the Azusa, California plant of the Aerojet-General Corporation had demonstrated, as early as 1946, the need for a more elaborate underwater testing facility, capable of continuous submerged operation. Variable test speeds up to 100 knots were required for research shapes as large as 21 in. in dia and 10 ft long, to run at 2-1/2 diameters submergence. It was intended that the new facility would not only serve the underwater research work being carried out at Aerojet, but would be flexible enough in application to accommodate related work of other agencies desiring to use the facility.

2. In determining the type of configuration for the facility best suiting the needs, much practical experience was drawn from previous operation of a small circular test channel at Aerojet. This small channel consisted of an annular-ring tank equipped with a rotating boom 40 feet in diameter, which is shown in Figure 183. In operation at moderate velocities, the small channel had proved satisfactory in principle, limited only by the speed, power, and size of the test unit that it could accommodate. Consequently, the most feasible and economical approach to the new facility took the form of a generally scaled-up version of the small channel.

3. Negotiations for the construction of the facility were opened by Aerojet on 28 August 1946, and on 19 March 1947, Amendment No. 2, Task Order No. 1 of Contract N6ori-10 was issued by the Office of Naval Research authorizing construction of the proposed facilities. Construction commenced in April 1947 under cognizance of a Resident Officer in Charge appointed by the Bureau of Yards and Docks, at the request of the Office of Naval Research, and was completed in June 1948.

B. SUMMARY

1. In its final form, the test facility now known as the Ring Channel has the following physical dimensions and capacities:

Inside Diameter of Ring Channel	70 ft
Outside Diameter of Ring Channel	110 ft
Average Depth	11.5 ft
Main Boom Diameter	80 ft
Maximum Boom Diameter (with extension)	100 ft
Maximum Velocity at 50-ft Radius	100 knots
Maximum Model Weight at 40-ft Radius	10,000 lb
Contained Water, Volume	466,000 gal
Freeboard at outer wall	18 in.
Power Capacity (Single Electric Induction Motor)	250 hp
Boom Speed at 100 knots	32.2 rpm

2. The following associated major equipment is fitted to the ring channel:

a. A built-in steel cab, provided at the center of the boom, houses electrical and hydraulic systems.

b. An "ashore" control building, remotely located, houses the main control equipment, and serves as a shielded observation station.

c. Underwater ports and lighting are provided at both the inner and outer tank circumference for observation and photography.

d. Box-shaped wave dampers of the swash-plate type are mounted on the outer circumference of the tank to limit surface disturbances.

e. The rotating boom is equipped to provide a multitude of electronic data pickups, hydraulic pickups, and compressed air and steam service for the vehicle under test.

3. A detailed discussion of the ring channel may be found in Reference 55. Figure 184 illustrates the ring channel in its finished form. Note that the boom extension is assembled. Building 73 in the background is the "ashore" control station. In Figure 27 the direct hydropulse is shown under test at 56.5 knots.

C. CONCLUSIONS AND RECOMMENDATIONS

1. The employment of the Ring Channel in underwater research has been entirely satisfactory within its designed limits. Testing at speeds of 100 knots has been possible. An example of work with larger bodies is the Mk 40 torpedo, a 21-in.-dia, 123-in.-long, self-powered vehicle which was tested at 65 knots actual speed, with good results. Virtually all of the development programs for underwater devices undertaken by Aerojet-General subsequent to the completion of the Ring Channel have benefited from this test facility. A few of many developments that have been tested are the following:

a. Hydropulse (chemical and gasoline-air)

b. Hydroturbojet

c. Hydroduct

d. Vortex-Ring Generator

e. Low-Frequency Sound Generators

f. Pumpjets

g. Hydroductor

h. Underwater Swimmer Propulsion Devices

i. Singing Vanes

j. Hydrodynamic Models

k. Mine-Sweeping Devices

l. Recoilless-Gun Launcher

2. Normally, the hydrodynamic test data from the Ring Channel is available in reasonably refined form; but when necessary, slight adjustments to readings obtained may be easily applied to compensate for variations in flow patterns peculiar to the circular track. A major refinement for measuring the drag of smaller shapes consists of an "Internal Balance" system fitted inside the model which provides strain gauge readings through electrical pickups for recording. This system proved necessary for the smaller shapes, while for large shapes the earlier thrust-plate deformation system is still used.

3. Because of its unique configuration and capabilities, the Ring Channel provides the means to conduct underwater research quickly and inexpensively in a manner unlike that of any other test facility in the United States. That such a facility has been made available for underwater research on its premises is taken as a matter of company pride within the Aerojet-General Corporation.

XV. HYDRODYNAMICS STUDIES

A. EXTERNALLY STEPPED MISSILE BODY

In an attempt to reduce the skin friction of high-speed underwater bodies, an investigation was carried out on the externally stepped missile configuration shown in Figures 185 and 186. This form was evolved by applying the Ramus step design to a body of revolution, with the intention of substituting a low-resistance layer of gas at the skin of the body for the high-resistance layer of liquid. Gas released at the leading step was swept along the surface, collecting in the successive steps to form a layer or ring of gas behind each step along the length of the body. This model was tested on the 80-ft rotating boom with and without air discharge from the leading step, and the drag results were compared with those for a smooth body with the same volume and fineness ratio. These results, shown in Figure 187, indicated higher drag for the stepped body at low speeds, with a marked decrease in the rise of the drag curve above 57 knots. Extrapolating the data, the stepped-body principle appears very promising for a missile of this type at velocities above 100 knots.

B. SINGING VANES

1. Investigations were made of the phenomenon of the vibration (singing) of thin, submerged struts or vanes from the action of hydrodynamic forces. Measurements of sound frequency and strut forward velocity were used in conjunction with Microflash photography to aid in the analysis, and to define the cause. It was concluded that the singing was caused by the shedding of a Karman vortex strut. A definite correlation was made between the strut trailing-edge thickness and the spacing of the vortices. It was found that singing was entirely suppressed when the ratio of trailing edge thickness (measured in inches) to chord length (in feet) was reduced to 0.007 - 0.015. This was called the limiting edge-thickness fraction.

2. A complete report on this study was submitted to the Office of Naval Research (see Reference 56).

C. DYNAMIC RECOVERY OF THRUST EFFECT

During the early phase of the hydroduct program, attention was attracted to the possibility of a "thrust-recovery" effect which might obviate the need for a variable-exit-area exhaust nozzle, to compensate for operations at varying depths. It was felt that effective expansion of the exhaust jet to ambient pressure could be achieved outside the nozzle with the aid of the dynamic flow of water around the jet, without sacrificing thrust. This is illustrated in Figure 188. The external expansion would permit the utilization of a simple, critical pressure nozzle without sacrificing thrust. However, one important requirement for this situation is that the ratio of ram pressure to the pressure difference between nozzle throat and ambient conditions should be greater than unity. A test program verified the existence of the external expansion by means of Microflash photographs, as shown in Figure 189. Performance measurements on models having either fully expanded or critical-flow nozzles showed no loss in thrust for the latter (see Table 4).

REFERENCES

1. Research and Development on the Hydropulse and Related Jet Propulsion Devices, Aerojet Engineering Corporation Report No. R-55, 20 September 1945 (Confidential).

2. Research and Development on the Hydropulse and Related Jet Propulsion Devices, Aerojet Engineering Corporation Report No. R-60, 15 March 1946 (Confidential).

3. Research and Development on the Hydropulse, Aerojet Engineering Corporation Report No. R-77, 30 June 1947 (Confidential).

4. Research, Development and Testing of Underwater Propulsion Devices, Aerojet Engineering Corporation Report No. 387, 7 September 1949 (Confidential).

5. Research, Development and Testing of Underwater Propulsion Devices, Aerojet Engineering Corporation Report No. R-97, 3 September 1948 (Confidential).

6. Research and Development on the Hydropulse, Aerojet Engineering Corporation Report No. R-86, 31 December 1947 (Confidential).

7. Leonard Bairstow, Applied Aerodynamics, 2nd Edition, Longmans, Green and Co., London, 1939.

8. Study of Internal Hydropulse Action, Aerojet Engineering Corporation, Technical Memorandum No. RTM-27, 2 October 1946.

9. Research, Development and Testing of Underwater Propulsion Devices, Aerojet Engineering Corporation Report No. 357, 18 February 1949 (Confidential).

10. U. S. Naval Ordnance Test Station Technical Memorandum No. 5042-2, Noise Measurement and Analysis of Aerojet Hydropulse, 1 April 1949.

11. Research and Development on the Hydropulse, Aerojet Engineering Corporation Report No. R-68, 30 July 1946 (Confidential).

12. Research, Development and Testing of Underwater Propulsion Devices, Aerojet Engineering Corporation Report No. 791, 26 February 1954 (Confidential).

13. Research, Development and Testing of Underwater Propulsion Devices, Aerojet Engineering Corporation Report No. 725, 5 August 1953 (Confidential).

REFERENCES (cont.)

14. Research and Development on the Hydropulse, Aerojet Engineering Corporation Report No. R-69, 31 December 1946 (Confidential).

15. Hydrofuels for Torpedo Propulsion, Aerojet Report No. 727, 30 July 1953 (Confidential).

16. Design and Development of a Lithium Hydroturbojet, Aerojet Report No. 633, 16 September 1952 (Confidential).

17. Design and Development of a Lithium Hydroturbojet, Aerojet Engineering Corporation Report No. R-99, 20 August 1948 (Confidential).

18. Design and Development of a Lithium Hydroturbojet, Aerojet Engineering Corporation Report No. 380, 10 May 1949 (Confidential).

19. Design and Development of a Lithium Hydroturbojet, Aerojet Engineering Corporation Report No. 412, 31 October 1949 (Confidential).

20. Design and Development of a Lithium Hydroturbojet, Aerojet Engineering Corporation Report No. 448, 24 April 1950 (Confidential).

21. Design and Development of a Lithium Hydroturbojet, Aerojet Engineering Corporation Report No. 534, 8 August 1951 (Confidential).

22. Design Study for a High-Speed Long-Range Torpedo Power Plant, Aerojet Report No. 1071, 24 February 1956 (Confidential).

23. Development of a Hydroduct, California Institute of Technology Report by R. G. Anderson, C. W. Rush and T. R. McClellan, 1947 (Confidential).

24. H. M. Lyon, The Effect of Turbulence on the Drag of Airship Models, ARC, RM 1511, 1932 (Unclassified).

25. The Alclo Hydroductor and the Alclo Hydroduct as Underwater Missiles, Aerojet Report No. 528, 16 July 1951 (Confidential).

26. Free-Running Underwater Launchings of the 4.5-in. Alclo Hydroduct Test Missile, Harold C. Yost, USNOTS, TM No. 661, 27 June 1952 (Secret).

27. An Evaluation of Existing Instrumentation for Testing the 4.5-in. Alclo Hydroduct at Morris Dam, T. W. Layton, USNOTS, TM No. 679, 24 September 1952 (Secret).

28. Range Testing of the 4.5-in. Alclo Hydroduct, Aerojet Report No. L2815-1, 12 May 1953 (Secret).

REFERENCES (cont.)

29. Range Testing of the 4.5-in. Alclo Hydroduct, Aerojet Report No. L2815-2, 2 June 1953 (Secret).

30. Range Testing of the 4.5-in. Alclo Hydroduct, Aerojet Report No. L2815-3, 29 June 1953 (Secret).

31. Range Testing of the 4.5-in. Alclo Hydroduct, Aerojet Report No. L2815-4, 31 July 1953 (Secret).

32. Underwater Performance of the 4.5-in. Alclo Hydroduct Test Missile, NavOrd-NOTS Report 3510, Robert H. Hornidge, 6 June 1955 (Secret).

33. The Hydroduct Missile, Aerojet Special Report No. 671, January 1953 (Secret).

34. Preparation of Ethyl Aluminum Sesquihydride, Aerojet Engineering Corporation Report RTM - 33, 2 June 1947 (Confidential).

35. Investigation of Liquid Rocket Propellants, Aerojet Report No. 367, 11 March 1949 (Confidential).

36. Investigation of Liquid Rocket Propellants, Aerojet Report No. 401, 7 September 1949 (Confidential).

37. Investigation of Liquid Rocket Propellants, Aerojet Report No. 420, 26 January 1950 (Confidential).

38. Literature Survey of Water-Reactive Materials, USNOTS, Pasadena, California Memo, 15 March 1950 (Confidential).

39. Research, Development and Testing of Underwater Propulsion Devices, Aerojet Engineering Corporation Report No. 464, 31 July 1950 (Confidential).

40. Research, Development and Testing of Underwater Propulsion Devices, Aerojet Engineering Corporation Report No. 495, 12 February 1951 (Confidential).

41. Research, Development and Testing of Underwater Propulsion Devices, Aerojet Engineering Corporation Report No. 533, 15 August 1951 (Confidential).

42. Research, Development and Testing of Underwater Propulsion Devices, Aerojet Engineering Corporation Report No. 579, 7 February 1952 (Confidential).

REFERENCES (cont.)

43. Research, Development and Testing of Underwater Propulsion Devices, Aerojet Engineering Corporation Report No. 419, 17 February 1950 (Confidential).

44. Research, Development and Testing of Underwater Propulsion Devices, Aerojet Engineering Corporation Report No. 631, 12 August 1952 (Confidential).

45. Research, Development and Testing of Underwater Propulsion Devices, Aerojet Engineering Corporation Report No. 675, 9 February 1953 (Confidential).

46. Research, Development and Testing of Underwater Propulsion Devices, Aerojet Report No. 859, 16 August 1954 (Confidential).

47. Research, Development and Testing of Underwater Propulsion Devices, Aerojet Report No. 938, 17 February 1955 (Confidential).

48. Steam-Jet Condenser for Hydroductor Propulsion System, Aerojet Report No. 707, 25 May 1953 (Confidential).

49. Research, Development and Testing of Underwater Propulsion Devices, Aerojet Report No. 1008, 27 September 1955 (Confidential).

50. Range Testing of the 4.5-in. Alclo Hydroduct, Aerojet Report No. L2815-9, 14 January 1954 (Confidential).

51. Range Testing of the 4.5-in. Alclo Hydroduct, Aerojet Report No. L2815-27, 7 July 1955 (Secret).

52. Range Testing of the 4.5-in. Alclo Hydroduct, Aerojet Report No. L2815-35, 20 March 1956 (Secret).

53. Range Testing of the 4.5-in. Alclo Hydroduct, Aerojet Report No. L2815-36, 2 April 1956 (Confidential).

54. Application of Aeroplex Propellant to a Torpedo of Advanced Design, Aerojet Report No. 751, September 1953 (Confidential).

55. The 80-Foot Rotating Test Boom and Circular Water Channel Test Facility, Aerojet Engineering Corporation Research Technical Memorandum No. 44, 18 February 1949 (Confidential).

56. A Study of Vanes Singing in Water, Aerojet Research Technical Memorandum No. 76, 3 May 1951 (Confidential).

TABLE 1

SUMMARY OF DIRECT HYDROPULSE TEST DATA
MOLTEN LITHIUM FUEL

Run No.	Date of Run, 1949	Motor No.	Drag Coefficient C_D lb Drag/in. H_2O Vel. Hd.	Frequency f cycles/sec	Velocity V ft/sec	Velocity V knots	Thrust F lb	Specific Impulse I_{sp} sec	Specific Power $I_{sp} \times V$ ft	Specific Fuel Cons. W_f lb-fuel/ thrust hp-hr
12	1-5	25	.34	10.0	72.3	42.8	347	1985	143,600	13.8
13	1-28	25	.49	9.4	75.0	44.5	510	2490	187,000	10.6
14	2-1	25	.34	9.5	74.4	44.0	183	4000	298,000	6.65
15	2-8	25	.37	10.2	75.2	44.5	370	1910	143,500	13.8
16	2-10	25	.37	10.2	76.0	45.0	430	1760	133,800	14.8
17	2-15	25	.37	10.0	76.0	45.0	530	1360	103,300	19.2
18	3-14	25	.43	10.2	78.0	46.2	269	1563	122,000	16.2
19	3-17	25	.52	10.2	74.9	4[illegible].5	620	2980	223,000	8.9
20	3-25	25	.52	10.4	70.0	41.0	249	2630	184,000	10.8
21	3-30	25	.52	10.4	No Run					
22	3-31	25	.52	11.1	79.6	47.1	790	3080	245,000	8.1
23	4-8	25	.55	11.1	74.4	44.0	480	2275	169,000	11.7
24	5-5	25	.50	11.1	86.9	51.4	780	3540	307,500	6.4
25	5-11	25	.50	13.0	92.5	54.7	915	3040	281,000	7.0
26	5-13	25	.50	13.0	95.4	56.5	825	2750	262,000	7.6
27	5-25	25	.50	12.2	No Run					
28	5-27	25	.50	15.0	97.1	57.5	920	No Data		
29	6-1	25	.50	15.0	103.0	61.0	1380	3300	340,000	5.8
30	6-3	25	.50	13.0	74.4	44.0	548	3960	295,000	6.7
31	6-13	25	.50	14.3	91.2	54.0	905	3530	322,000	6.2
32	6-22	25	.50	15.0	102.3	60.5	1185	3660	375,000	5.3
33	6-28	25	.50	14.0	102.3	60.5	1150	3180	326,000	6.1
34	7-7	26	.325	13.0	93.0	55.0	870	3320	309,000	6.4
35	9-28	26	.33	11.7	108.2	64.0	830	3190	347,000	5.7
36	10-24	25	.50	13.0	95.5	57.5	740	4060	388,000	5.1

TABLE 2

EFFECT OF VARIOUS INJECTION CHARACTERISTICS ON DIRECT HYDROPULSE PERFORMANCE WITH MOLTEN LITHIUM FUEL

Run No.	Spray Mechanism	Dia. of Orifice, in.	Fuel Press. lb	Injection & Reaction Duration, Millisec	Thrust lb	Speed knots	W_f Lb Li /thrust hp-hr
4	Deflector Plate, Fan Shaped Spray	0.128	1500	Over 33	530	34.8	28.9
5	Twin Tangential Passage, 24° Solid Cone, Hard Spray	0.128	1500	23	453	36.2	9.8
7	Twin Tangential Passage, 24° Solid Cone, Hard Spray	0.128	1500	20	482	39.4	15.8
9	Twin Tangential Passage, 50° Solid Cone, Soft Spray	0.128	1500		396	36.5	6.0
11	Twin Tangential Passage, 50° Solid Cone, Soft Spray	0.157	1500		387	41.6	6.8
13	Spiral Pintle, 50° Solid Cone, Soft Spray	0.157	1500		510	44.5	10.6
14	No. 10 Sprayco Vane, 50° Solid Cone, Soft Spray	0.157	1500		183	44.0	6.6
17	Twin No. 10 Sprayco Vanes, Soft Spray	2 Holes 0.157	1500	18	530	45.0	19.2
19	Twin No. 10 Sprayco Vanes, Soft Spray	2 Holes 0.157	1500	17	620	44.5	8.9
20	65 Diverging Jets, Needle-like Spray	65 Holes 0.028	1500		249	41.0	10.8
23	37 Impinging Jets, 60° Solid Cone, Soft Spray	37 Holes 0.047	1650		480	44.0	11.7
24	No. 15 Sprayco Vane, 50° Solid Cone, Soft Spray	0.182	1500	16	780	51.4	6.4
25	No. 15 Sprayco Vane, 50° Solid Cone, Soft Spray	0.182	1650		915	54.7	7.0
26	No. 15 Sprayco Vane, 50° Solid Cone, Soft Spray	0.182	2000		825	56.5	7.6
28	Spiral Spray Vane, 50° Solid Cone, Soft Spray	0.219	2200	10	920	57.5	-
29	Rein. No. 15 Sprayco Vane, 60° Solid Cone, Soft Spray	0.219	2200	10	1380	61.0	5.8
32	Rein. No. 15 Sprayco Vane, 60° Solid Cone, Soft Spray	0.219	2200		1185	60.5	5.3
33	Rein. No. 15 Sprayco Vane, 60° Solid Cone, Soft Spray	0.219	2200	8	1150	60.5	6.1

TABLE III

SUMMARY OF HYDRODUCT STATIC-TEST DATA

Run No.	Date of Run, 1950	Static Thrust, lb	Lithium Flow, lb/sec	Water Flow, lb/sec	β $\frac{w_{Li}}{w_{Li}+w_{H_2O}}$	Chamber Pressure, psig	Duration of Run, sec	Specific Impulse, sec	C_F	c^* ft/sec	c ft/sec	Δp, Water Injector, psi	Turbu-lator
63	1-16	445	.445	9.0	.034	155	17.1	980	1.22	1245	1520	50	SAE 4130
64	1-20	380	.346	8.9	.037	120	21.8	1100	1.31	1010	1320	60	SAE 4130
66	1-30	380	.332	8.9	.036	120	45.4	1145	1.31	1010	1325	60	SAE 4130
67	2-3	400	.337	8.6	.038	120	46.4	1190	1.38	1440	1040	70	SAE 4130
68	2-28	400	.336	8.9	.036	120	23	1190	1.36	1395	1025	70	Molyb-denum

TABLE 4

SUMMARY OF TEST-FIRING DATA FOR LITHIUM HYDRODUCT

Run No.	Date, 1951	Speed knots	Duration of Run sec	Lithium Flow Rate lb/sec	Thrust lb	Specific Impulse, lb-sec/lb	Ram Press. psig	Chamber Press. psig	Δp Water Inj. psi	C_F	Type Turbulator	Exhaust Nozzle
90	1-9	90.8	29.7	.340	340	1000	160	100	60	1.50	4H	de Laval
91	2-12	95.5	24.2	.388	300	775	172	100	72	1.36	4H	↓
92	2-15	95.8	28.8	.322	270	840	175	95	80	1.31	4H	↓
93	2-20	95.5	28.5	.331	300	905	172	90	82	1.50	4H	↓
94	2-33	95.5	26.9	.329	320	975	170	105	65	1.38	4H	↓
96	3-16	95.5	20.0	.465	340	875	170	110	60	1.39	4H	Critical Pressure
97	3-21	94.5	--	--	325	--	170	110	60	1.33	4H	↓
98	3-26	94.7	22.0	.357	295	825	170	100	70	1.30	4H	↓
99	3-28	95.5	25.3	.369	295	800	170	100	70	1.34	4H	↓
100	4-3	94.8	21.0	.447	285	590	160	100	60	1.15	Double Enzian Ring	de Laval
101	4-5	94.8	25.0	.364	255	700	165	75	90	1.32	Double Enzian Ring	↓
102	4-9	95.5	27.2	.350	320	915	170	100	70	1.30	Double Enzian Ring	↓
104	6-12	95.0	34.3	.321	320	995	165	100	65	1.30	Double Enzian Ring	Critical Pressure
105	6-15	95.4	34.0	.364	370	1015	165	110	55	1.4	Double Enzian Ring	↓
106	6-22	94.7	32.3	.353	325	920	165	110	55	1.3	Double Enzian Ring	↓
107	7-3	96.1	45.7	0.346	330	954	170	117	53	1.2	↓	↓
108	7-17	95.5	32.0	0.500	565	1130	170	120	50	1.3	↓	↓
109	7-24	95.9	35.7	0.469	480	1025	168	108	60	1.2	↓	↓
110	7-30	95.3	34.7	0.486	600	1235	170	128	42	1.3	↓	↓

TABLE 5

HEATS OF HYDROLYSIS

Element	Melting Point °C	Heat of Hydrolysis kcal/cc	Reaction Compound Formed
Be	1280 ± 40	14.3	$Be(OH)_2$*
Al	660 ± 0.1	9.6	Al_2O_3
U	1850	9.5	UO_2
Th	1800 ± 150	9.4	ThO_2
V	1735 ± 50	8.3	V_2O_3
Ti	1800 ± 100	8.12	TiO_2
B	2300 ± 300	7.9	B_2O_3
La	826 ± 5	5.58	La_2O
Mg	650 ± 2	5.55	MgO
Nd	840 ± 40	5.5	Nd_2O_3
Si	1430 ± 20	5.09	SiO_2
Pr	940 ± 50	4.9, 3.6	Pr_2O_3 - PrO_2
Ce	600 ± 50	4.7 to 4.83	CeO_2
Li	186 ± 5	3.69	LiOH
Ca	850 ± 20	3.25	CaO
Zr	1750 ± 700	2.97	ZrO_2
Mn	1260 ± 20	2.93, 1.43	MnO - Mn_2O_3
Sr	770 ± 10	2.14	SrO
Na	97.7 ± 0.2	1.84	NaOH
Ba	704 ± 20	1.81	BaO
Zn	419.5 ± 0.1	1.74	ZnO
K	63 ± 1	0.94	KOH
Rb	39 ± 1	0.8	RbOH
Cs	28 ± 2	0.68	CsOH

TABLE 5 (cont.)

Element	Melting Point °C	Heat of Hydrolysis kcal/cc	Reaction Compound Formed
Sn	231.9 ± 0.1	0.07	SnO or SnO_2
Cd	320.9 ± 0.1	-0.24	CdO
Pb	327.4 ± 0.1	-0.3, -1.14	Pb_2O - Pb_3O_4
As	814 ±	-1.4 to -0.5	As_2O_3
Mo	2525 ± 50	-0.6	MoO_2
Fe	1539 ± 3	-0.6, - 1.02	FeO - Fe_2O_3
Tl	300 ± 3	-0.86	Tl_2O
Sb	630.5 ± 0.1	-1.09	Sb_2O_3
W	3410 ± 20	-1.1, -1.6	WO_2 - W_2O_5
Bi	271.3 ± 0.1	-1.6	Bi_2O_3
Ni	1455 ± 1	-1.6	NiO
Co	1490 ± 20	-1.6	CoO
Hg	-38.87 ± 0.02	-1.6, -3.2	Hg_2O, HgO
Ta	3000 ± 100	-1.9	Ta_2O_5
Cu	1083.2 ± 0.1	-2.0, 4.7	Cu_2O - CuO
I	114 ± 1	-2.9	I_2O_5
Pd	1554 ± 1	-5.3	PdO
Pt	1773.5	-5.4	$Pt(OH)_2$*
In	156.4 ± 0.1	-5.8	In_2O_3
Ru	2500 ± 100	-7.1 to -9.5	RuO_2

*Hydroxide given only as a relative value. Oxide rather than hydroxide would be expected.

TABLE 6

ALUMINUM-BASE ALLOYS

Composition	Specific Gravity	Melting Point, °F	Reaction with Water	Remarks
62% Al 32% Mg 6% Li	1.97	898	Slow	Extremely brittle
92% Al 8% Li	2.04	1115	Partial	Viscous when molten
92% Al 8% Ca	2.55	1137	Slow	Very viscous even at 1700°F
85.2% Al 7.4% Ca 7.4% Li	1.98	1100	Slow	Viscous when molten
90.9% Al 9.1% Hg	2.73	1215	Slow	
98% Al 2% Na		1212		
96% Al 4% Na		1210	Slow	
1.85 Al/Mg 15% Li	1.523	972 (mushy)		Very hard and brittle
1.85 Al/Mg 30% Li	1.148	858		
1.85 Al/Mg 45% Li	0.919	762		
1.85 Al/Mg 60% Li	0.770	Approx. 510		
1.85 Al/Mg 75% Li	0.662	403 mushy to 520		

TABLE 7

MAGNESIUM-BASE ALLOYS

Composition	Specific Gravity	Melting Point, °F	Comparison with Lithium Weight Basis, %	Comparison with Lithium Volume Basis, %	Remarks
66.7% Mg 33.3% Al	2.04	836			No reaction at 1485°F
2.84 Mg/Al 2.0% Li	1.79	807			Slow reaction
2.84 Mg/Al 4% Li	1.76	797			Slow reaction
2.84 Mg/Al 8% Li	1.63	818	35	108	
81% Mg 19% Ca	1.72	983			Slow reaction
77% Mg 18% Ca 5% Li	1.52	940	49	137	
98% Mg 2% Na	1.71	1175			Partial explosion, prolonged reaction
96% Mg 4% Li	1.60	1132	46	135	
92% Mg 8% Li	1.44	1113	73	195	

TABLE 7 (cont.)

Composition	Specific Gravity	Melting Point °F	Comparison with Lithium Weight Basis, %	Comparison with Lithium Volume Basis, %	Remarks
88% Mg 12% Li		1094			
84% Mg 16% Li		1055	68	161	
68.5% Mg 25.0% Al 4.5% Li 2.0% Na		795			Partial explosion, prolonged reaction.
1.0 Mg/Zn 6% Li	2.24	793	27	112	
1.0 Mg/Zn 12% Li		730	37	126	

TABLE 8

CALCIUM-BASE ALLOYS

Composition	Specific Gravity	Melting Point, °F	Comparison with Lithium: Weight Basis, %	Comparison with Lithium: Volume Basis, %	Remarks
90% Ca 10% Na	1.46	1290			Partial explosion, prolonged reaction
3.7 Ca/Mg 10% Na	1.49	853			Sodium did not alloy
3.7 Ca/Mg 5.5% Li	1.43	685			Fair explosion, prolonged reaction
3.7 Ca/Mg 10% Li		650	45	109	Brittle
3.7 Ca/Mg 5% Zn 5% Li	1.50	648	40	111	
3.7 Ca/Mg 10% Zn 5% Li	1.56	590	50	144	
3.7 Ca/Mg 20% Zn 4% Li	1.72	538			Low order explosion, prolonged reaction
3.7 Ca/Mg 19% Zn 10% Li		Mushy at 660			Fair explosion, prolonged reaction, shatters like glass
3.7 Ca/Mg 5% Zn 10% Li	1.38	667 (not sharp)			Fair explosion, prolonged reaction, extremely brittle

TABLE 8 (cont.)

Composition	Specific Gravity	Melting Point, °F	Comparison with Lithium: Weight Basis, %	Comparison with Lithium: Volume Basis, %	Remarks
3.7 Ca/Mg 5% Zn 5% Li 5% Na	1.46	665 (Not sharp)			Fair explosion, prolonged reaction
53% Ca 42% Zn 5% Li	2.02	Indefinite, thick mush at 460			Prolonged reaction
71% Ca 24% Al 5% Li	1.56	923			Prolonged reaction, very brittle
37% Ca 29% Mg 29% Zn 5% Li	1.85	Indefinite, softens at 810	33	111	Brittle
3.76 Ca/Mg	1.587	833			
+25% Li	1.062	668 Mushy to 710			
+40% Li	0.888	353 Mushy to 475			
+55% Li	0.761	331 Mushy to 400			
+70% Li	0.668	333 Mushy to 350			
+85% Li	0.594	347			

TABLE 9

ALLOYS OF MAGNESIUM, CALCIUM, ZINC, AND LITHIUM

Alloy No.	Composition, %				Melting Point, °F
	Mg	Ca	Zn	Li	
28	18	67	10	5	590
182	15	40	40	5	683
183	10	50	35	5	705 to 775
184	0	60	35	5	425 to 470
185	5	60	30	5	506 to 540
186	0	70	25	5	525 to 540
187	45	20	30	5	706 to 721
188	35	20	40	5	707 to 717
189	35	40	20	5	916 to 1005
190	25	50	20	5	793 to 873
191	25	60	10	5	815 to 892
192	10	70	15	5	516 to 575
193	65	20	10	5	870 to 888
194	65	10	20	5	782 to 787
195	55	10	30	5	710 to 724
196	45	10	40	5	733
197	55	30	10	5	864 to 877
198	50	25	20	5	807 to 818

TABLE 10

LITHIUM-CALCIUM ALLOYS

Composition	Specific Gravity	Melting Point, °F	Comparison with Lithium: Weight Basis, %	Comparison with Lithium: Volume Basis, %	Remarks
3.7 Ca/Mg 90.6% Li	0.58	368	86	92	
88% Li 7% Ca 5% Na	0.58	343	105	110	
95% Li 5% Ca	0.56	352	84	87	
92% Li 8% Ca	0.57	350			
88% Li 12% Ca		344			
83.3% Li 16.7% Ca	0.61	330	75	85	
80% Li 20% Ca		323			
70% Li 30% Ca		297			
65% Li 35% Ca	0.70	295			
63% Li 37% Ca	0.71	295			

TABLE 10 (cont.)

Composition	Specific Gravity	Melting Point, °F	Comparison with Lithium Weight Basis, %	Comparison with Lithium Volume Basis, %	Remarks
60% Li 40% Ca	0.73	295	72	97	
56% Li 44% Ca	0.76	292			
54% Li 46% Ca	0.77	294.5			
50% Li 50% Ca	0.80	341			
1.17 Li/Ca 5% Na	0.78	286			
2.12 Li/Ca 5% Na	0.69	285			
1.50 Li/Ca 5% Na	0.74	285	90	123	
1.50 Li/Ca 10% Na	0.743	286			Fair explosion, prolonged reaction
1.50 Li/Ca 15% Na	0.776	286 Mushy to 310			Fair explosion, prolonged reaction
1.50 Li/Ca 5% K	0.717	294			Fair explosion, prolonged reaction
1.50 Li/Ca 10% K	0.713	294			All K did not alloy

TABLE 10 (cont.)

Composition	Specific Gravity	Melting Point, °F	Comparison with Lithium Weight Basis, %	Comparison with Lithium Volume Basis, %	Remarks
1.50 Li/Ca 5% Na 5% K	0.734	286			NaK did not alloy
1.50 Li/Ca 5% Na 5% Zn	0.764	277			Fair explosion, prolonged reaction
1.50 Li/Ca 5% Na 10% Mg	0.800	Indefinite Mushy to 405			Fair explosion, prolonged reaction
1.50 Li/Ca 5% Na 2.5% Al	0.744	279 Mushy to 295			Fair explosion, prolonged reaction
1.50 Li/Ca 5% Na 5% Al	0.758	280			
1.50 Li/Ca 5% Na 7.5% Al	.773	285			
1.50 Li/Ca 5% Na 10% Al	0.792	286	87	130	
1.50 Li/Ca 5% Na 20% Al	0.856	Indefinite Mushy to 670			Fair explosion, prolonged reaction.
1.50 Li/Ca 5% Na 30% Al	0.936	Indefinite Mushy to 650			Low order explosion, prolonged reaction.

TABLE 10 (cont.)

Composition	Specific Gravity	Melting Point, °F	Comparison with Lithium: Weight Basis, %	Comparison with Lithium: Volume Basis, %	Remarks
60% Li 40% Ca	0.73	295			
56% Li 44% Ca	0.76	292			
50% Li 50% Ca	0.80	341			
1.17 Li/Ca 5% Na	0.78	286			
2.12 Li/Ca 5% Na	0.69	285			
1.50 Li/Ca 5% Na	0.74	285			
1.50 Li/Ca 10% Na	0.743	286			Fair explosion, prolonged reaction
1.50 Li/Ca 15% Na	0.776	286 Mushy to 310			Fair explosion, prolonged reaction
1.50 Li/Ca 5% K	0.717	294			Fair explosion, prolonged reaction
1.50 Li/Ca 10% K	0.713	294			All K did not alloy
1.50 Li/Ca 5% Na 5% K	0.734	286			NaK did not alloy

TABLE 10 (cont)

Composition	Specific Gravity	Melting Point, °F	Comparison with Lithium Weight Basis, %	Comparison with Lithium Volume Basis, %	Remarks
1.50 Li/Ca 5% Na 40% Al	1.037	Indefinite Mushy to 740			Low-order explosion, prolonged reaction
1.50 Li/Ca 5% Na 50% Al	1.159	898 Mushy to 960			
1.50 Li/Ca 5% Na 5% Si	.760	285			
1.50 Li/Ca 5% Na 10% Si	.788	311	82	121	
1.50 Li/Ca	.820	319 Mushy to 375			
1.50 Li/Ca 5% Na 5% Al 5% Si	.790	305 Mushy to 380			
1.50 Li/Ca 5% Na 10% Al 5% Si	.824	Indefinite Mushy to 455			

TABLE 11

LITHIUM-ALUMINUM-SODIUM-CALCIUM ALLOYS

Alloy No.	Composition, % Li	Al	Na	Ca	Specific Gravity	Melting Point, °F	Comparison with Lithium: Weight Basis %	Volume Basis %
109	66.4	16.6	7.0	10.0	.692	343	120	155
112	62.4	15.6	7.0	15.0	.717	331	90	120
111	58.4	14.6	7.0	20.0	.742	327 to 420		
158	62.2	20.8	7.0	10.0	.725	342		
160	58.1	24.9	7.0	10.0	.759	343	77	110
162	55.4	27.6	7.0	10.0	.784	340		
159	56.2	18.8	10.0	15.0	.756	321		
161	52.5	22.5	10.0	15.0	.790	329		
163	50.0	25.0	10.0	15.0	.820	345		

TABLE 12

LITHIUM-SILICON ALLOYS

Composition	Specific Gravity	Melting Point, °F	Comparison with Lithium	
			Weight Basis, %	Volume Basis, %
95% Li 5% Si	0.552	360	96	99
90% Li 10% Si	0.575	360	100	108
80% Li 20% Si	0.628	590 Mushy to 730	134	158

TABLE 13

TERNARY ALLOYS OF LITHIUM-CALCIUM-STRONTIUM

Alloy No.	Alloy Composition %	Melting Point °F
131	20 Li, 20 Ca, 60 Sr	352
132	20 Li, 40 Ca, 40 Sr	397
133	20 Li, 60 Ca, 20 Sr	430
134	40 Li, 20 Ca, 40 Sr	265
135	40 Li, 40 Ca, 20 Sr	275 to 337
136	60 Li, 20 Ca, 20 Sr	276
137	80 Li, 10 Ca, 10 Sr	324
138	65 Li, 10 Ca, 25 Sr	259 to 280
142	50 Li, 25 Ca, 25 Sr	270
143	40 Li, 30 Ca, 30 Sr	287
139	65 Li, 25 Ca, 10 Sr	282
140	55 Li, 15 Ca, 30 Sr	264
141	55 Li, 30 Ca, 15 Sr	280
144	30 Li, 35 Ca, 35 Sr	346 to 392

TABLE 14

TERNARY ALLOYS OF LITHIUM-CALCIUM-BARIUM

Alloy No.	Alloy Composition %	Melting Point °F
146	55 Li, 15 Ca, 30 Ba	255 to 300
147	55 Li, 25 Ca, 20 Ba	285
148	55 Li, 35 Ca, 10 Ba	286 to 325
145	53 Li, 30 Ca, 17 Ba	280
152	50 Li, 10 Ca, 40 Ba	252 to 265
153	50 Li, 20 Ca, 30 Ba	250 to 263
149	45 Li, 20 Ca, 35 Ba	271 to 286
150	45 Li, 30 Ca, 25 Ba	275
151	45 Li, 40 Ca, 15 Ba	279
154	51 Li, 7 Ca, 42 Ba	251
155	53 Li, 10 Ca, 37 Ba	257
156	49 Li, 13 Ca, 38 Ba	261 to 275
157	47 Li, 10 Ca, 43 Ba	251 to 272

TABLE 15

QUATERNARY ALLOYS OF LITHIUM-CALCIUM-BARIUM-STRONTIUM

Alloy No.	Alloy Composition %	Melting Point °F
164	Li 45, Ca 9, Ba 36, Sr 10	258
165	Li 40, Ca 8, Ba 32, Sr 20	256
166	Li 35, Ca 7, Ba 28, Sr 30	267
167	Li 45, Ca 18, Ba 27, Sr 10	259
168	Li 36, Ca 22.5, Ba 31.5, Sr 10	260
169	Li 36, Ca 13.5, Ba 40.5, Sr 10	255
170	Li 40, Ca 16, Ba 24, Sr 20	260
171	Li 32, Ca 12, Ba 36, Sr 20	257
172	Li 32, Ca 20, Ba 28, Sr 20	260 to 266
173	Li 35, Ca 14, Ba 21, Sr 30	250 to 260
174	Li 28, Ca 10.5, Ba 31.5, Sr 30	254 to 266
175	Li 28, Ca 17.5, Ba 24.5, Sr 30	257 to 283
176	Li 27, Ca 13.5, Ba 49.5, Sr 30	258
177	Li 24, Ca 12, Ba 44, Sr 20	258 to 277
178	Li 21, Ca 10.5, Ba 38.5, Sr 30	280
179	Li 27, Ca 22.5, Ba 40.5, Sr 10	272
180	Li 24, Ca 20, Ba 36, Sr 20	282
181	Li 21, Ca 17.5, Ba 31.5, Sr 30	288

TABLE 16

COMPOSITION OF MATERIALS OF CONSTRUCTION

Name of Material	Percentage Composition							Miscellaneous
	Tungsten	Molybdenum	Iron	Nickel	Cobalt	Chromium	Carbon	
Stellite 31	8	—	2	10	53.5	26	0.5	
Stellite Star J	17	—	—	—	48.6	32	2.4	
Inconel	—	—	6.5	78	—	14	0.08	0.25 Si, 0.2 Cu, 0.25 Mn.
Hastelloy B	—	20	20	60	—	—	—	
Hastelloy C	—	17	8	60	—	15	—	Boron 2.75 to 4.75%
Colmonoy No. 6	—	—	—	70	—	15	—	Fe + Si + C = 10% max.
Armco Iron	—	—	99.9	—	—	—	0.08	
Kennametal K-6	—	—	—	—	Balance	—	—	Tungsten carbide (WC) and other carbides
Kennametal K-3H	—	—	—	—	Balance	—	—	Tungsten titanium carbide (WT_iC_2) and other carbides
Kennametal K-138	—	—	—	—	20	—	—	80% Titanium carbide
Kennametal K-151-A	—	—	—	20	—	—	—	80% Titanium carbide

Molybdenum	Commercially pure
Titanium	Commercially pure
Vanadium	Commercially pure
Beryllium	Commercially pure
Sapphire	Aluminum oxide (Al_2O_3)
Norbide	Boron carbide (B_6C)

TABLE 17

A SUMMARY OF ALCLO PROPELLANT MIXTURES

Mixture	Equation in Pressure Range		Rate at 150 psia	Energy - Density kcal/cc	Methods of Test*
Alclo (Stoichiometric)	$r = .004\ p^{1.08}$	100-900	0.59	6.1	CB
Alclo + 10% $(NH_4)Cr_2O_7$	$r = .105\ p^{.52}$	15-200	1.45		VSG
Alclo + 10% $Ca(PO_4)_3$ + 1% Fe_2O_3	$r = .021\ p^{.76}$	15-200	0.95		CB
Alclo + 10% $Ca(PO_4)_3$	$r = .043\ p^{.64}$	15-350	1.05		CB
Alclo + 10% Cr_2O_7	$r = .223\ p^{.25}$	15-150	0.79		VSG
Alclo + 10% $CoCr_2O_3$	$r = .069\ p^{.46}$	40-100	0.96		VSG
Alclo + 5% CoO_2 + 5% Fe_2O_3	$r = .345\ p^{.16}$	15-100	0.78		VSG
Alclo + 10% Fe_2O_3	$r = .196\ p^{.34}$	15-150	1.08		VSG
Alclo + 10% Ferro-Vanadium	$r = .276\ p^{.18}$	15-150	0.68		VSG
Alclo + 5% Pb + 5% $(NH_4)_2Cr_2O_7$	$r = .178\ p^{.34}$	15-150	0.98		VSG
Alclo + 13% Pb	$r = .039\ p^{.66}$	100-600	1.08	6.1	CB, HD, VSG
Alclo + 5% Pb + 1% Fe_2O_3	$r = .145\ p^{.39}$	50-300	1.02		VSG
Alclo + 5% Pb + 5% Fe_2O_3	$r = .227\ p^{.33}$	15-200	1.16		VSG
Alclo + 5% Pb + 5% NiO	$r = .153\ p^{.38}$	15-200	0.98		VSG
Alclo + 10% PbO	$r = .175\ p^{.30}$	15-150	0.79		VSG
Alclo + 10% MnO_2	$r = .111\ p^{.45}$	15-150	1.07		VSG
Alclo + 6% Sn	$r = .041\ p^{.67}$	80-300	1.20	6.0	CB
Alclo + 10% $Ca(PO_4)_3$ + 1% Fe_2O_3	$r = .021\ p^{.755}$	15-215	.95		CB
Alclo + 5% Carbon Black	$r = .092\ p^{.163}$	25-240	.21		VSG
	$r = .0156\ p^{.76}$	240-440			
Alclo + 10% Cobalt	$r = .087\ p^{.50}$	15-300	1.06		VSG
Alclo + 10% Cobaltic Oxide	$r = .0472\ p^{.65}$	55-300	.94		VSG
Alclo + 5% Cobaltic Oxide + 5% Ferric Oxide	$r = .345\ p^{.16}$	15-75	.78		VSG
Alclo + 10% Copper	$r = .078\ p^{.49}$	15-100	.91		VSG
Alclo + 5% Pb + 5% $(NH_4)_2Cr_2O_7$	$r = .178\ p^{.34}$	15-150	.98		VSG
Alclo + 30% Pb	$r = .152\ p^{.435}$	15-210	1.28	5.9	VSG
Alclo + 13.96% Pb	$r = .487\ p^{.412}$	115-240	1.03		VSG
Alclo + 5% Pb + 10% KBr	$r = .341\ p^{.30}$	37-480	1.30		VSG
Alclo + 5% Pb + 5% NiO	$r = .153\ p^{.38}$	15-200	.99		VSG

* CB Crawford bomb
VSG vertical steam generator
HD 2-in. hydroduct test chamber

TABLE 18

SOME PHYSICAL PROPERTIES OF ALCLO

PROPERTY	Alclo +12.8% Pb	Stoichiometric Alclo
Sp Gr (theoretical)	2.87	2.58
Sp Gr (actual)	2.80	2.45
Density (actual) lb. ft^{-3}	175	153
Heat of combustion 10^3 cal. gm^{-1}	2.17	2.49
Heat of combustion Btu lb^{-1}	3920	4500
Energy density 10^3 cal cc^{-1}	6.1	6.1
Energy density Btu ft^{-3}	683,000	683,000
Ignition temperature, ^oF	850	1050
Flame Temperature, ^oF	—	7150
Shear strength, psi	122	74
Compressive strength, psi	5530	4650
Porosity $in.^3$ $hr.^{-1}$ $in^{-2}(\Delta p/in.)^{-1}$ helium diffusion	0.0086	0.0286
Coeff. of thermal expansion (axial)	.0000845	.0000585
Coeff. of thermal expansion (radial)	.0000315	.0000275
Specific heat Btu. lb^{-1} $^oF^{-1}$(at 100^oF)	0.176	0.198
Thermal Conductivity, k, at 200^oF Btu hr^{-1} $ft^{-2}(^oF/ft)^{-1}$		3.7
Thermal diffusivity $k\rho^{-1}Cp^{-1}$ ft^2 hr^{-1}		.122
Electrical resistivity	- - very high - - - - - -	
Trauzl expansion, cc	25	25
Impact sensitivity, cm drop with 2kg wt	35	35
Friction sensitivity, cm drop of pendulum	17	—
Detonation velocity	detonation does not propagate	

Table 18

TABLE 19

DATA FOR TURBO-SUPERCHARGER DYNAMOMETER TESTS ON VERTICAL STEAM GENERATOR, MK III

Run No.	Duration sec	Grain Length in.	Grain Weight lb	Area Ratio $\frac{A_p}{AA_t}$	Wt H_2O Evap. lb	Equilib. Steam Press. psig	Equilib. Steam Temp. ^oF	Equilib. Steam Rate lb/hr	Equilib. Power Output hp	S_s $\frac{lb}{hp\text{-}hr}$	S_p $\frac{lb}{hp\text{-}hr}$	Equilib. Turbine Speed rpm
1	9.1	8.23	9.06	7.4	16.3	230	370	16,000	250	29.6	11.0	19,500
2	8.6	8.25	9.06	7.5	17.3	235	410	11,100	490	22.6	11.8	25,000
3	-	16.45	18.12	7.5	-	225	375	-	450	-	-	25,000
4	21.1	24.64	27.18	7.5	64.0	280	690	15,500	660	23.6	10.0	26,500
5	18.6	24.65	27.18	7.5	64.0	310	410	16,900	630	26.9	11.3	26,500
6	9.5	8.22	9.06	6.98	20.6	250	500	11,100	360	30.8	17.2	25,000
7	43.3	49.20	54.35	6.98	154.0	175	375	13,100	370	35.4	12.1	23,000

S_s = Specific steam consumption.

S_p = Specific propellant consumption.

TABLE 20

HYDRODUCTOR TESTING ON THE ROTATING BOOM

Tabulated Data for P_c = 190 psig

Group	Run No.	Scoop Ht. (in.)	"A" Ratio	Ref. Drag (lb) (P_c = 50 psig)	Thrust (lb) (P_c = 190 psig)	P_{mv} (psig)	P_{cv} (in. Hg)	Remarks
I	108	0.080	0.7	380	65	63	12.2	Fully instrumented
	109	0.080	0.7	372	54	64	13.2	
	110	0.080	0.7	381	65	65	17.5	
	111	0.080	0.7	380	72	67	16.9	
		Av value		378	64	65	15	
II	112	0.090	0.7	363	64	67	-	Fully instrumented
	113	0.090	0.7	373	77	71	18.2	
	114	0.090	0.7	374	58	67	18.2	
	115	0.090	0.7	370	67	70	19.9	
	127	0.090	0.7	390	60	73	17.8	
	128	0.090	0.7	363	60	70	12.6	
	129	0.090	0.7	367	69	69	14.3	
	130	0.090	0.7	386	54	70	13.7	
	131	0.090	0.7	350	70	69	13.8	
	132	0.090	0.7	356	67	69	11.0	
		Av value		369	65	70	16	

Notes:
1. "A" ratio of water-scoop exit area to condensing-section diffuser area.
2. P_{mv} is ram pressure of the water at the exit of the condensing-water scoop.
3. P_{cv} is pressure in the condensing section.

TABLE 20 (cont.)

Group	Run No.	Scoop Ht. (in.)	"A" Ratio	Ref. Drag (lb) (P_c = 50 psig)	Thrust (lb) (P_c = 190 psig)	P_{mv} (psig)	P_{cv} (in. Hg)	
III	122	0.090	0.7	379	80	--	--	No internal instrumentation →
	123	0.090	0.7	383	83	--	--	
	124	0.090	0.7	383	79	--	--	
	125	0.090	0.7	375	75	--	--	
	126	0.090	0.7	373	84	--	--	
		Av value		379	80	--	--	
IV	133	0.090	0.7	363	64	70	--	Fully instrumented (partially stepped afterbody) (Poor vacuum gage response)
	134	0.090	0.7	351	60	69	--	
	136	0.090	0.7	358	66	69	--	
	137	0.090	0.7	356	66	68	--	
		Av value		357	64	69	--	
V	100	0.100	0.7	383	59	73	22.0	Fully instrumented →
	101	0.100	0.7	365	58	75	16.0	
	102	0.100	0.7	355	52	69	23.0	
	103	0.100	0.7	342	41	74	23.0	
	104	0.100	0.7	355	58	71	21.0	
	105	0.100	0.7	358	54	75	23.6	
	106	0.100	0.7	363	58	70	20.9	
	107	0.100	0.7	354	48	71	17.1	
		Av value		359	54	72	21	
VI	116	0.100	0.7	364	70	59	18.9	Fully instrumented (Stepped afterbody) →
	117	0.100	0.7	367	57	62	22.5	
	118	0.100	0.7	350	66	62	20.3	
		Av value		360	64	[illegible]	[illegible]	

TABLE 20 (cont.)

Group	Run No.	Scoop Ht. (in.)	"A" Ratio	Ref. Drag (lb) (P_c = 50 psig)	Thrust (lb) (P_c = 190 psig)	P_{mv} (psig)	P_{cv} (in. Hg)	Remarks
VII	119	0.100	0.7	365	87	--	--	No internal instrumentation (stepped afterbody)
	120	0.100	0.7	367	79	--	--	
	121	0.100	0.7	354	79	--	--	
		Av value		362	82	--	--	
VIII	146	--	---	392	112	--	--	Hydroduct
	147	--	---	405	108	--	--	
	148	--	---	373	105	--	--	
		Av value		390	108	--	--	
IX	149	0.090	0.6	318	70	--	22.0	Modified instrumentation
	150	0.090	0.6	304	71	--	14.0	
	151	0.090	0.6	360	74	--	14.5	
	152	0.090	0.6	386	80	--	18.0	
		Av value		342	74	--	17	
X	153	0.090	0.5	415	81	--	18.0	
	154	0.090	0.5	409	88	--	18.0	
	155	0.090	0.5	378	77	--	21.0	
	156	0.090	0.5	389	82	--	23.0	
	157	0.090	0.5	375	73	--	20.0	
		Av value		393	80	--	20	

TABLE 20 (cont.)

Group	Run No.	Scoop Ht. (in.)	"A" Ratio	Ref. Drag (lb) (P_c = 50 psig)	Thrust (lb) (P_c = 190 psig)	P_{mv} (psig)	P_{cv} (in. Hg)	Remarks
XI	158	0.090	0.7	360	77	--	21.0	Fully stepped afterbody, revised instrumentation ↓
	159	0.090	0.7	-	—	--	--	
	160	0.090	0.7	381	79	--	20.0	
	161	0.090	0.7	366	72	--	19.0	
	162	0.090	0.7	365	77	--	20.0	
	163	0.090	0.7	376	78	--	19.0	
	164	0.090	0.7	389	87	--	16.0	
		Av value		373	78	--	19	

TABLE 21

BALLISTIC PROPERTIES OF AN-2091AX PROPELLANT

Formulation	wt%	Gas Composition at Adiabatic Flame Temperature mole %	
Ammonium nitrate	75.00	CO_2	8.7
Ammonium dichromate	2.00	CO	15.4
Styrene	2.98	H_2O	20.5
A-20 resin	7.24	H_2	35.6
Methyl acrylate	11.08	N_2	19.8
Methyl ethyl ketone peroxide	0.40		
Cobalt (1% in styrene)	as required		
Lecithin (10% in styrene)	0.80		
Calcium phosphate	0.50		
Density of solid propellant, lbm in.$^{-3}$	0.055		

Thermodynamic Properties

Theoretical I_{sp}, lbf sec lbm^{-1} (at 1000 psia)	190
Theoretical C_w, lbm lbf^{-1} sec^{-1}	0.00813
Molecular Weight of gases, M	20.89
Effective k = C_p/C_v	1.276
Theoretical Flame Temperature, $^{\circ}$F	2388

Ballistic Parameters

Below 60°F

$$r = 0.00297\ e^{0.00136(T-60)}\ p^{.44}$$
$$K = 49.8\ e^{-0.00134(T-60)}\ p^{.56}$$
$$\pi_r = 0.00238$$
$$\pi_p = 0.00238$$

Above 60°F

$$r = 0.00297\ e^{0.00181(T-60)}\ p^{.44}$$
$$K = 49.8\ e^{0.00183(T-60)}\ p^{.56}$$
$$\pi_r = 0.00325$$
$$\pi_p = 0.00325$$

TABLE 21 (cont.)

where

r = Burning rate, in. sec^{-1}

K = Area ratio, propellant burning area to nozzle throat area

π_p = Temperature coefficient of pressure at constant K ratio, $^oF^{-1}$

π_r = Temperature coefficient of burning rate at constant K ratio, $^oF^{-1}$

p = Chamber pressure, psia

T = Initial grain temperature, ^oF

Report No. 1106

OVERALL SUBJECT INDEX FOR ALL CONTRACT REPORTS

OVERALL SUBJECT INDEX FOR ALL CONTRACT REPORTS (cont.)

Report No. 1106

DISTRIBUTION LIST

	No. of Copies
Chief of Naval Research Department of the Navy Washington 25, D. C. Attn: Code 429 VIA: Bureau of Aeronautics Representative/Azusa	5
Chief of Naval Research Department of the Navy Washington 25, D. C. Attn: Code 463	1
Chief of Naval Research Department of the Navy Washington 25, D. C. Attn: Code 465	1
Chief of Naval Research Department of the Navy Washington 25, D. C. Attn: Code 466	1
Director Office of Naval Research Branch Office 1030 E. Green Street Pasadena 1, California	2
Bureau of Aeronautics Representative Aerojet-General Corporation 6352 N. Irwindale Azusa, California	1
U. S. Naval Underwater Ordnance Station Newport, Rhode Island	1
Director Office of Naval Research Branch Office 150 Causeway Street Boston, Massachusetts	1
Director Office of Naval Research Branch Office 844 North Rush Street Chicago 11, Illinois	1

DISTRIBUTION LIST (cont.)

	No. of Copies
Director Office of Naval Research Branch Office 346 Broadway New York 13, New York	1
Director Office of Naval Research Branch Office 1000 Geary Street San Francisco 9, California	1
Officer in Charge Office of Naval Research Navy No. 100 Fleet Post Office New York, New York	1
Chief of Naval Research c/o Navy Research Section Library of Congress Washington 25, D. C. Attn: Mr. J. H. Heald	10
Officer-in-Charge U.S. Naval Ordnance Experimental Unit c/o National Bureau of Standards Connecticut Avenue and Van Ness St., N. W. Washington 25, D. C.	1
Commander U. S. Naval Air Missile Test Center Point Mugu, California	1
U. S. Naval Engineering Experiment Station Annapolis, Maryland	2
Chief, Bureau of Ordnance Navy Department Washington 25, D. C.	
Attn: Re2	1
Re3	1
Re9	1
Re6	1
Rexc	1

DISTRIBUTION LIST (cont.)

	No. of Copies
Commander U. S. Naval Ordnance Test Station Inyokern P.O. China Lake, California Attn: Reports Unit	4
Commanding Officer Naval Research Laboratory Washington 25, D. C. Attn: Code 2021	1
Commander Naval Ordnance Laboratory, White Oak Silver Spring - 19, Maryland Attn: The Library, Room 1-333	1
Chief of Naval Operations Department of the Navy Washington 25, D. C. Attn: Op 316	1
Chief, Bureau of Aeronautics Department of the Navy Washington 25, D. C. Attn: TD-4	1
Library Branch, Information Office Research and Development Board Room 3E 1065, The Pentagon Washington 25, D. C. Attn: Mr. C. R. Flagg	1
Dr. J. E. Henderson Director Applied Physics Lab. University of Washington VIA: Inspector of Naval Material 2300 Eleventh Ave, S. W. Seattle 4, Washington	1
Commander Naval Ordnance Test Station Pasadena Annex 3202 East Foothill Blvd. Pasadena 8, California Attn: Dr. N. A. Renzetti	1

DISTRIBUTION LIST (cont.)

	No. of Copies
Commanding Officer and Director U. S. Navy Electronics Laboratory San Diego 52, California	1
Commanding Officer U. S. Naval Torpedo Station Newport, Rhode Island	1
Committee on Guided Missiles Research and Development Board Room 3D-125, The Pentagon Washington 25, D. C.	1
Department of the Army Office, Chief of Ordnance Washington 25, D. C. Attn: ORDTU	1
Chief, Bureau of Ships Navy Department Washington 25, D. C.	
Attn: Code 519D	1
Code 430	1
Chief, Research and Engineering Division Office, Chief of Chemical Corps Army Chemical Center, Maryland	1
Corona Laboratory National Bureau of Standards Corona, California Attn: Chief, Missile Development Division	1
Classified Technical Library Atomic Energy Commission 1901 Constitution Avenue Washington 25, D. C.	2
Director Hydrodynamics Laboratory California Institute of Technology 1204 East California Street Pasadena 4, California VIA: Office of Naval Research Branch Office 1030 E. Green Street Pasadena 1, California	1

DISTRIBUTION LIST (cont.)

	No. of Copies
Applied Physics Laboratory Johns Hopkins University Silver Spring, Maryland VIA: Naval Inspector of Ordnance Applied Physics Laboratory Johns Hopkins University 8621 Georgia Avenue Silver Spring, Maryland	1
The Kellex Corporation Silver Spring Laboratory 936 Wayne Avenue Silver Spring, Maryland VIA: Naval Inspector of Ordnance Applied Physics Laboratory Johns Hopkins University 8621 Georgia Avenue Silver Spring, Maryland	1
Head of Ordnance and Gunnery U. S. Naval Academy Annapolis, Maryland	1
U. S. Naval Post Graduate School Monterey, California	1
Commanding Officer Diamond Ordnance Fuze Laboratories Connecticut Ave and Van Ness St., N. W. Washington 25, D. C.	1
Central Intelligence Agency 2430 E. Street, N. W. Washington 25, D. C. Attn: Liaison Division, OCD	1
Commanding General Redstone Arsenal Huntsville, Alabama Attn: Technical Library	1
Chief, Armed Forces Special Weapons Project P. O. Box 2610 Washington 25, D. C. Attn: Development Division	1

DISTRIBUTION LIST (cont.)

	No. of Copies
Explosive Ordnance Disposal School Naval Powder Factory Indianhead, Maryland	1
Commanding Officer David W. Taylor Model Basin Washington 7, D. C.	1
Executive Secretary Committee on Undersea Warfare National Research Council 2101 Constitution Avenue, N. W. Washington 25, D. C.	1
Fairchild Engine and Airplane Corp. Fairchild Engine Division Farmingdale, Long Island, New York VIA: Representative in Charge, BuAer Fairchild Engine and Airplane Corp. Guided Missiles Division Farmingdale, Long Island, New York	1
M. W. Kellogg Company Foot of Danforth Avenue Jersey City 3, New Jersey Attn: E. M. Hedley VIA: Inspector of Naval Material Naval Industrial Reserve Shipyard Building 24, Port Newark Newark 5, New Jersey	1
Reaction Motors, Inc. Stickle Avenue and Elm Street Rockaway, New Jersey VIA: Bureau of Aeronautics Representative Reaction Motors, Inc. Stickle Avenue and Elm Street Rockaway, New Jersey	1

DISTRIBUTION LIST (cont.)

	No. of Copies
Propulsion Research Corporation 309 E. Regent Street Inglewood 1, California VIA: Director Office of Naval Research Branch Office 1030 East Green Street Pasadena 1, California	1